FEDERAL UNIVERSITY OF TECHNOLOGY - PARANÁ
DAELN - ACADEMIC DEPARTMENT OF ELECTRONICS
BACHELOR'S IN ELECTRONIC ENGINEERING

ANDERSON VALENGA GUIMARÃES

ANALYSIS OF GLASS TILTING DYNAMIC ON DOORS WITH SINGLE-GUIDED WINDOW REGULATORS AND THE IMPACT OF TRAPPING FORCE MEASURING METHODS ON ANTI-TRAPPING BEHAVIOR

BACHELOR THESIS

CURITIBA
2019

ANDERSON VALENGA GUIMARÃES

ANALYSIS OF GLASS TILTING DYNAMIC ON DOORS WITH SINGLE-GUIDED WINDOW REGULATORS AND THE IMPACT OF TRAPPING FORCE MEASURING METHODS ON ANTI-TRAPPING BEHAVIOR

Bachelor Thesis presented to the program of Bachelor's in Electronic Engineering at Federal University of Technology - Paraná, as partial requirement to obtain the title of Bachelor.

Supervisor: Paulo Roberto Brero de Campos
Universidade Tecnológica Federal do Paraná

CURITIBA
2019

ANDERSON VALENGA GUIMARÃES

ANALYSIS OF GLASS TILTING DYNAMIC ON DOORS WITH SINGLE-GUIDED WINDOW REGULATORS AND THE IMPACT OF TRAPPING FORCE MEASURING METHODS ON ANTI-TRAPPING BEHAVIOR

Este Trabalho de Conclusão de Curso de Graduação foi apresentado como requisito parcial para obtenção do título de Engenheiro Eletrônico, do curso de Engenharia Eletrônica do Departamento Acadêmico de Eletrônica (DAELN) outorgado pela Universidade Tecnológica Federal do Paraná (UTFPR). O aluno Anderson Valenga Guimarães foi arguido pela Banca Examinadora composta pelos professores abaixo assinados. Após deliberação, a Banca Examinadora considerou o trabalho aprovado.

Curitiba, 13 de Setembro de 2019.

_____

Prof. Dr. Robinson Vida Noronha
Coordenador de Curso
Engenharia Eletrônica

_____

Profª. Drª. Carmen Caroline Rasera
Responsável pelos Trabalhos de Conclusão de Curso
de Engenharia Eletrônica do DAELN

BANCA EXAMINADORA

_____

Prof. Dr. Paulo Roberto Brero de Campos
Universidade Tecnológica Federal do Paraná
Orientador

_____

Prof. Me. Ricardo Umbria Pedroni
Universidade Tecnológica Federal do Paraná

_____

Prof. Dr. Rubens Alexandre de Faria
Universidade Tecnológica Federal do Paraná

A folha de aprovação assinada encontra-se na Coordenação do Curso de Engenharia Eletrônica.

This dissertation is dedicated to all who supported me and guided me to success through my life.

To mom and dad, who took me to the library.

To my love, Thayenne, who was always my best friend and confident.

To my friends from all over the world, whom I wish I could still meet everyday.

To caffeine and sugar, without whom this thesis and graduation would have been impossible.

ACKNOWLEDGEMENTS

First of all, my special thanks to Sergio Boppre, who saw my potential and had me embark on a journey, with an engineering internship in Germany and, soon, a job in Japan. Your guiding, knowledge and support through this process have been unfathomable.

To Brose and Roland Kalb for the opportunity to develop this work and ingress into the automotive industry.

To Franck Desaindes, who was of big help throughout this project with his vast knowledge and also a great friend.

To Prof. Paulo Roberto Brero de Campos, who supervised not only this thesis and internship, but also my work while in Brazil.

To the Federal University of Technology of Paraná and all of its teachers, who somehow supported me and gave me the opportunity to grow as a Electronic Engineer, professionally and personally.

The Road goes ever on and on
Down from the door where it began.
Now far ahead the Road has gone,
And I must follow, if I can,
Pursuing it with weary feet,
Until it joins some larger way,
Where many paths and errands meet.
And whither then? I cannot say.
(TOLKIEN, J.R.R., 1954)

ABSTRACT

VALENGA GUIMARÃES, Anderson. Analysis of glass tilting dynamic on doors with single-guided window regulators and the impact of trapping force measuring methods on anti-trapping behavior. 2019. 93 f. Bachelor Thesis – Bachelor's in Electronic Engineering, Federal University of Technology - Paraná. Curitiba, 2019.

For the past few decades, the automation of vehicles has been gradually changing the user overall experience when on the road. While some functionalities improve the reliability on several car systems, new security concerns are also raised. This is the case for window regulators with automatic-up function, which can lead, with a single button press, to accidents like the trapping of passenger arms, fingers and subsequent injuries. These particular concerns are handled by the presence of a reversal algorithm on the electronic of the system, which prevents the window from closing after it detects an obstacle. To validate this function, various measurements are done during product development in order to keep the trapping force under the values specified by law. However, some elements can interfere on the anti-trapping behavior, such as the glass tilting, which was identified on past projects and will be explored during this work. Several tests will be done through a design of experiments matrix and a set of different sensors to analyze the most important factors related to the phenomenon. The purpose is to aggregate enough data in order confirm that a new method of trapping force measurement is necessary, to simulate real-life situations better during window regulator project development.

Keywords: Window regulators. Anti-trapping. Glass tilting. Trapping force measurement. Design of experiments. Automotive industry.

RESUMO

VALENGA GUIMARÃES, Anderson. Analysis of glass tilting dynamic on doors with single-guided window regulators and the impact of trapping force measuring methods on anti-trapping behavior. 2019. 93 f. Bachelor Thesis – Bachelor's in Electronic Engineering, Federal University of Technology - Paraná. Curitiba, 2019.

Nas últimas décadas, a automação de veículos vem mudando gradualmente a experiência geral do usuário em trânsito. Embora algumas funcionalidades melhorem a confiabilidade em vários sistemas automotivos, também são levantadas novas questões de segurança. É o caso de reguladores de janela com função de elevação automática, que podem levar, com o pressionar de um único botão, a acidentes como aprisionamento (*trapping*) de braços e dedos dos passageiros e ferimentos subseqüentes. Essas preocupações particulares são tratadas pela presença de um algoritmo de reversão no sistema eletrônico do sistema, que impede que a janela se feche após detectar um obstáculo. Para validar esta função, várias medições são feitas durante o desenvolvimento do produto, a fim de manter a força de *trapping* sob os valores especificados por lei. No entanto, alguns elementos podem interferir no comportamento do sistema anti-trapping, como o *glass-tilting*, que foi identificado em projetos anteriores e será explorada durante este trabalho. Vários testes serão realizados através de uma matriz de experimentos (DOE) e um conjunto de diferentes sensores para analisar os fatores mais importantes relacionados ao fenômeno. O objetivo é agregar dados suficientes para confirmar a necessidade um novo método de medição da força de *trapping*, para simular melhor as situações da vida real durante o desenvolvimento de projetos de reguladores de janela.

Palavras-chave: Reguladores de vidro. Anti-esmagamento. Tombamento de vidro. Medição de forças de esmagamento. Design de experimentos. Indústria automotiva.

List of Figures

List of Tables

List of abbreviations and acronyms

ASIC	Application Specific Integrated Circuit
AT	Anti-trap
CAN	Controller Area Network
CP	Center Point
DC	Direct current
DCU	Door Control Unit
DOE	Design of experiments
ECU	Electronic Control Unit
EMF	Electromotive force
ISO	International Standards Organization
LIN	Local Interconnect Network
OFAT	One-factor-at-a-time
OSI	Open System Interconnection
WR	Window Regulator
WRD	Window Regulator Drive

SUMMARY

1 INTRODUCTION

This thesis will address the effects of glass tilting movement on window regulator systems, a mechanism that is part of most vehicles all around the world, and its relation with trapping force measuring methods. The work was developed at Brose Fahrzeugteile GmbH & Co. KG, multinational manufacturer of mechatronic systems for vehicles based on the city of Bamberg, Germany. It was part of an internship work by the author at the Electronic Applications for Door Systems department, from February 2019 until July 2019.

1.1 BROSE FAHRZEUGTEILE GMBH & CO. KG

Founded in 1908 by Max Brose, the company Brose Fahrzeugteile GmbH & Co. KG is still family owned to this day. Since its inception, Brose has been a supplier to the automotive industry, offering system components and complete solutions for doors and tailgates, front and rear seat adjustment systems, powertrain, chassis and thermal management (Figure 1). However, the main business are still the door components of the side doors, which includes the window lift drive with integrated electronics, the cable window regulator and the door control unit.

The company now employs 26,000 people in 23 countries at 62 locations and generates up to 6.3 billion annually. By investing 8% of its sales in research and development, Brose is at the forefront of automotive suppliers worldwide and stands for innovation and creativity, as evidenced by the large number of existing patents.

In its products, Brose combines the areas of mechanics, electronics and sensor technology into complete mechatronic systems, which are found in one of every two new vehicles

Figure 1 – Brose product range

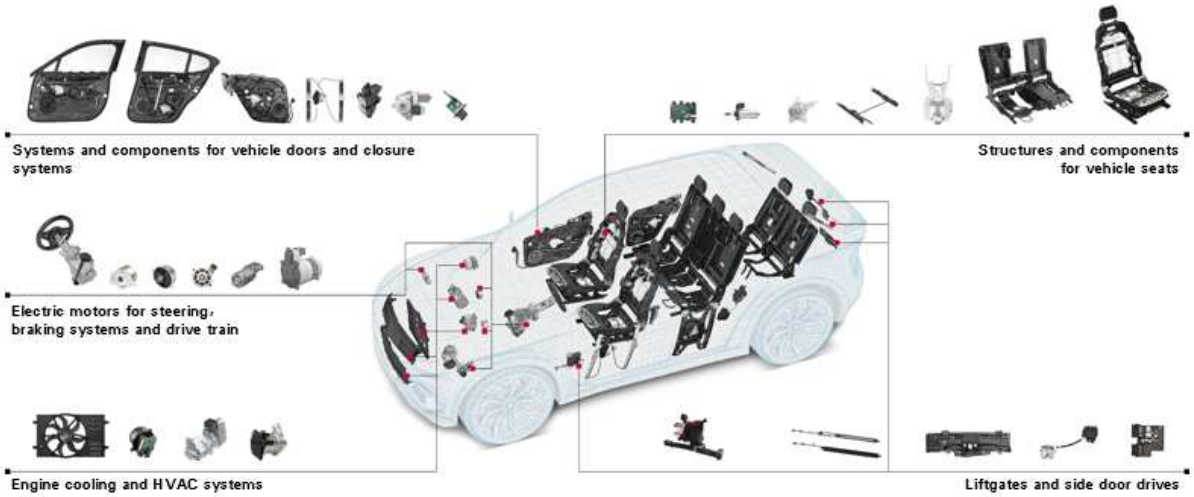

Source: Brose internal document

assembled worldwide. Due to the high degree of standardization of the mechatronic systems, automobile manufacturers have the opportunity to put together the components required for them in the same way, so there is a high degree of flexibility on the offered and demanded products for both sides.

1.2 SYSTEM OVERVIEW AND PROBLEM RECOGNITION

An electric powered window regulator is one of the main systems implemented on vehicle doors and is responsible for opening and closing the window according to user's commands. It operates in an up/down direction, with manual or automatic operation. Brose is one of the global leaders on developing those systems, producing more than 52 million WR per year and supplying manufacturers such as Toyota, Renault-Nissan, BMW and many others.

While on automatic mode, the systems produced worldwide are obliged to have a reversal function on the motor gear that triggers in case of an obstacle (mainly during up direction), to avoid injuries like bruises, bone breaks and even asphyxiation of the user. The test specifications vary by region: in Europe, the trapping force must not go above 100 N, measuring with a $10\,\mathrm{N\,mm^{-1}}$ spring rate device; in the US the spring rates are 20 and $65\,\mathrm{N\,mm^{-1}}$. A load gauge fixed on the window, with adjustable contact distance and springs, measures this trapping force. This condition is one of the main factors analyzed throughout product development.

To activate the reversal function, the electronic uses an indirect method. After calculating the window speed and position, if a speed drop occurs beyond a set limit, the power given to the actuator is inverted so it changes its direction of rotation, freeing the enclosed object. Some door frames, however, have a geometric singularity: because of some gaps on both sides of the door sealing and the single window slider clipping the glass, a tilting behavior may occur while trapping an object. In the case of figure 2, the measurement gauge acts as a lever, rotating the glass around the slider when it hits the upper sealing. The result of this behavior is a re-acceleration of the motor because of the window horizontal movement. Since all the electronic sees is the motor speed, the algorithm may decide that the stiffness of the object is still low or even that there's no real obstruction.

Earlier studies made within the company, especially by Petkun (2018) and Feyh (2019), confirm that, while the current measuring method certainly has an impact on how the glass ends up rotating and leaning to one of the columns, real-life situations like the trapping of a finger don't have the same behaviour. Actually, the behavior is more similar to when the measuring device is held against the door frame instead of clamped on the glass. However, while the impact on the placement of the gauge was already studied in individual cases, a more general scientific method, characterizing and comparing this effect with other system variables was yet to be done.

As such, the first objective of this project is to analyze and compare the effects of several door factors on glass movement while measuring trapping forces, focusing on the position of the current measuring device. This will be first done on a single design, the Renault

Figure 2 – Glass tilting on up direction

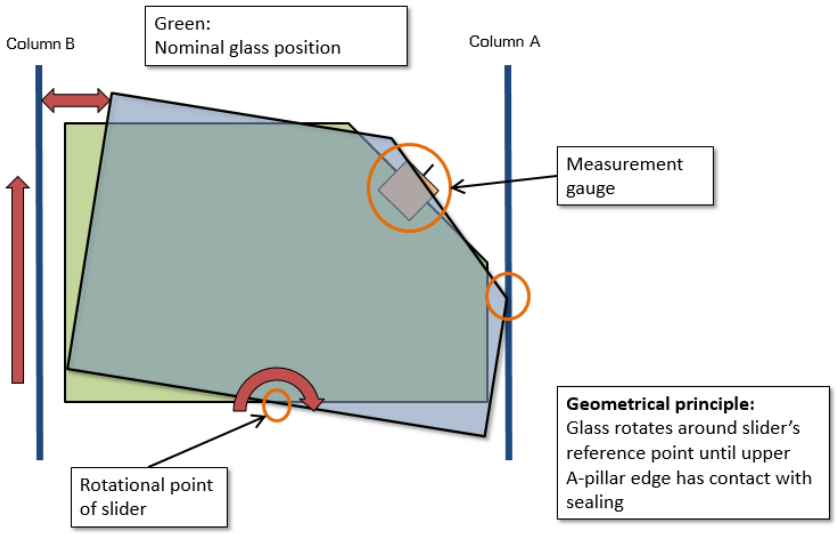

Source: Own elaboration

Kadjar driver door, through an statistical method that aims to minimize system variability between each test measurement. Having all the main factors outlined, alternatives to the current test procedure will be tested, in an effort to get results more tangible to real-life situations. Finally, all the results should be confirmed on a different door type, guaranteeing that this analysis can be extended to other configurations.

Since most automakers have been using the same method of force measurement for decades, the overall aim of this work is to gather enough data through reliable and reproducible experiment methods, in order to argue for alternatives that will guarantee a better development process and more safety to the final user.

1.3 MOTIVATION

Even though vehicle crashes are the main cause of injuries during traffic incidents, non-crash accidents also have a substantial impact on population's safety and health. According to the latest studies by the NHTSA (2015), during 2011 and 2012, it's estimated that 647.000 people were injured annually in non-crash incidents involving motor vehicles in the United States alone. Of this number, 2.000 were caused by closing the window of a car, in which more than half were kids and three each year resulted in death. For a wider scope, more than 50 children have died in incidents involving power windows since 1990, in the US. According to the website Estradas (2005), in Santa Catarina, Brazil, Renault had to make a recall of 22.130 vehicles after a boy died strangulated by a power window regulator in 2005.

To regulate these products and avoid more injuries caused by them, governments around the world proposed different legislation about the necessity of anti-trapping mechanisms on powered window regulators. The K.T. Safety Act of 2007, implemented in the United States the following year, requires "power windows and panels on motor vehicles to automatically

reverse direction when such power windows and panels detect an obstruction to prevent children and others from being trapped, injured, or killed (SCHAKOWSKY, 2008)". This was later regulated by the standard FMVSS 118, which states that:

> S5.1.While closing, the power-operated window, partition, or roof panel shall stop and reverse direction either before contacting a test rod with properties described in S8.2 or S8.3, or before exerting a squeezing force of 100 Newton (N) or more on a semi-rigid cylindrical test rod with the properties described in S8.1, when such test rod is placed through the window, partition, or roof panel opening at any location in the manner described in the applicable test under S7 (NHTSA, 2008, p. 2).

Similar documentations were drafted for other regions, such as Brazil:

> "[. . .] the device must reverse the movement before exerting a jamming force greater than 100N within an opening of 4mm to 200mm above the end of the power window, divider panel or in front of the front end of a sunroof in the sliding function and the position of opening of a sunroof in the tiltable function (CONTRAN, 2013)."

A full table comparing the legislations of all regions is available in this document as appendix.

Through this background, the importance of maintaining the trapping force within the specifications is highlighted. Guaranteeing these conformities is one of the main jobs within the creation of a window regulator electronic and the assessment of the forces generated by the mechanism is done throughout the whole development process. Since the glass tilting seems to have a significant impact on the reversal algorithm and on the measurement results, the outcome of this work can help maintain the robustness of the concerning projects and avoid situations that can significantly impact Brose's reliability as a supplier.

1.4 OBJECTIVES

As mentioned on the problem overview, the main objective of this work is to analyze and compare the main factors that contribute to the glass tilting effect on single-guided window regulators during anti-trap force measurements. Having the main factors established, other measurement methods should be explored in order to approximate the window behavior to real-life situations. Finally, with a properly planned scientific method and the results that follow, structure the data as an argument to convince automakers to adopt a different approach to the future window regulator developments and validation tests.

The specific objectives are the following:

- Use an statistical experimental method that aims to minimize system variability between each measurement, such as door sealing settling and equipment setup.
- Acquire reliable data regarding the glass tilting mechanical behavior for analysis in different situations and environments.
- Simulate all measurements through software and generate a report with all the necessary system responses automatically.

- Analyze if there's a direct correlation between transmission stiffness seen by the motor and the glass tilting movement itself.
- Try-out of other methods that may minimize the glass tilting effects.
- Confirmation of results in another door system.

1.5 DOCUMENT STRUCTURE

Throughout this thesis, the glass tilting will be evaluated by several different method and all of them will be explained for a better understanding of the project.

Chapter 2 starts with all the theory, materials and background that were necessary to conduct the experiments and understand what they implicated. It covers topics such as: what are window regulator systems and how they operate, what is the glass tilting effect and why is it a problem for the product development, as well as what sensors and statistical methods were used for its analysis.

After that, Chapter 3 shows the methodology applied and how the work was effectively done. This goes through the integration of all the devices used for the glass tilting analysis, how and which tests were planned and finally how all data was collected and interpreted.

The results section on Chapter 4 has all the statistical and individual analysis of the data assembled, showing what factors in the door system have the most overall impact on the tilting effect through statistical methods. It also interprets individual and groups measurements that can be considered as important to better understand and minimize the phenomenon.

Chapter 5 concludes the thesis and summarizes the results obtained, as well as the problems encountered through its development and suggestions for future works on the subject. Finally, the last sections present all the references used for this project and any additional material of interest as annex or appendix.

1.6 COSTS

The project implicated in no costs to the author. All the costs of having a working space, computer and software were sponsored by Brose, as well as all the sensors, car doors and other hardware used during the internship.

1.7 PROJECT SCHEDULE

The worksheet presented by Figure 3 briefly details how this project was developed, mostly at the first semester of 2019. Since it had to be developed simultaneously with other activities from the internship job, it was not until the end of April/2019 that it got a bigger focus. At the same time, when these other activities turned again with a bigger priority, the project was stopped or delayed at some points. However, the overall progress went smoothly over time and had a satisfiable completion rate.

Methodology and the analysis of the results were supervised with weekly meetings and questions about the window regulator systems were solved on a daily basis with the department's supervisors and colleagues. More specific subjects for the work, like the study of a statistical background as well as the design of experiments planning were self-researched.

Figure 3 – Project schedule

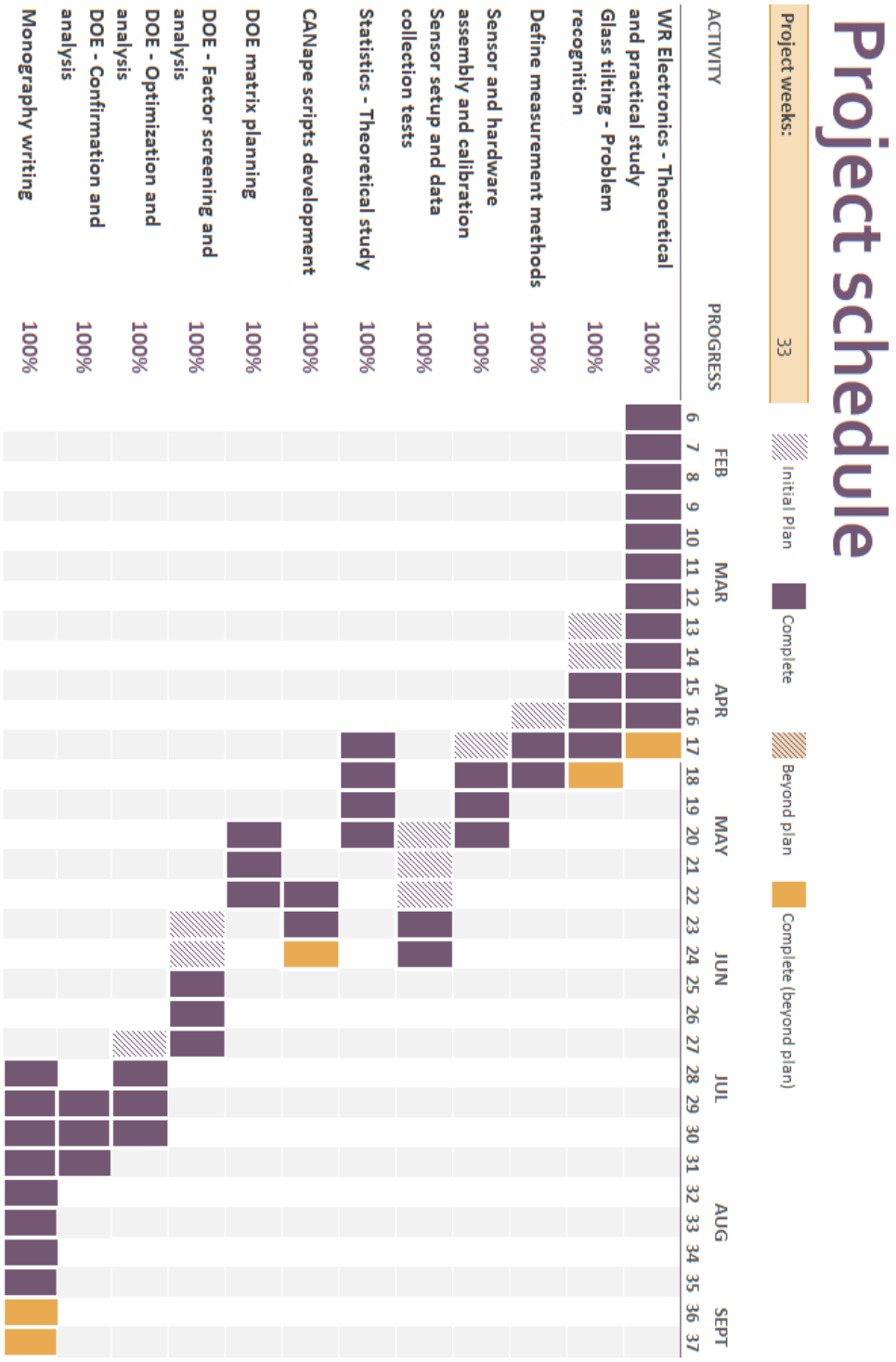

Source: Own elaboration

2 BACKGROUND

The aim of this chapter is to present the main theoretical bases of the project and the tools used during the development. Starting with how window regulators and its electronics work, the main problem of glass tilting and the experimental method used for its analysis will also be explained. Not every topic will be presented in full detail but deep enough to understand this work's methodology and final results.

2.1 STATE-OF-THE-ART - WINDOW REGULATORS

Since its origin at the end of the 19th century, the automobile industry always aims in improving the driver's experience at each technological innovation. With the emergence of automatization, every part of the vehicle is being improved in order to work with as little effort and as much safety as possible. This includes the opening and closing of the car's doors through a specific mechanism.

While manual window regulators were first introduced in 1926 by Max Brose, it wasn't until the 1960's that they started being powered electrically by a DC motor, and only by the 1980's, with the growing development of semiconductors, an electronic took over as the operation center for the system, allowing automatic window movement and other functionalities. Nowadays, most cars have at least the driver's door in possession of an electronic window regulator and the trend is that it keeps growing even more.

Currently there are two main variants of WR spread on vehicles all over the world: cable guided WR and arm guided WR. This thesis will only focus on the former, since it's the system in which the problem of glass tilting mainly occurs and it's the most widespread mechanism nowadays (around 98% of Brose's WR production). Glass tilting also happens at on single-arm WRs, but arm-guided WR are less and less in use.

2.1.1 Single-guided Cable Window Regulator

A single-guided cable WR is a mechatronic mechanism responsible for lowering or raising the vehicle's window as desired by the user (Figure 4). It's composed of a drive, manual or electric, attached to a cable drum house, which stores part of the cable responsible for the window movement. The drive, when electrial, can be then commanded by an attached electronic or by an external DCU (Door Control unit). The torque applied by the actuator makes the cable run loosely through a single metal or plastic guiding rail and a pair of pulleys that dictate it's movement. Finally, the force is transmitted to the glass through its clamping or fixing on a rail slider connected to the cable.

Evidenced by its name, a single-guided WR has only one guiding rail and, consequently, only one fixation point on the glass. The choice of this design is influenced by many factors,

Figure 4 – Single-guided cable WR

Source: Brose internal document

such as size and weight of the glass, geometry of the door, range of glass movement and also production and material costs.

2.1.2 Double-guided Cable Window Regulator

While the concept of this design is similar to the single-guided, the main difference is the amount of support the glass has during movement. Figure 5 shows that a pair of rails allows more stability for the window, ensuring that the force is transmitted and preventing the glass to tilt inside the frame. Therefore, double-guided WRs are more suitable for doors with limited glass guidance (front doors).

Figure 5 – Double-guided cable WR

Source: Brose internal document

2.2 WINDOW REGULATOR ACTUATORS

The actuator of a window regulator is the main part of the system, both in importance and in component cost. Manual actuators were the first step to this technology, using a rotating lever and cranks as means to move the glass up and down. However, nowadays most users look for an easier, more comfortable and more secure way to adjust their windows, so electrical powered motors started being used. While the future holds a place for the more advanced brush-less motors, most actuators are still brushed DC motors (Figure 6), transforming current into mechanical torque through a direct pair of contacts or an electronic interface, either attached to the motor itself or separated as a DCU.

Figure 6 – Window regulator DC Motor

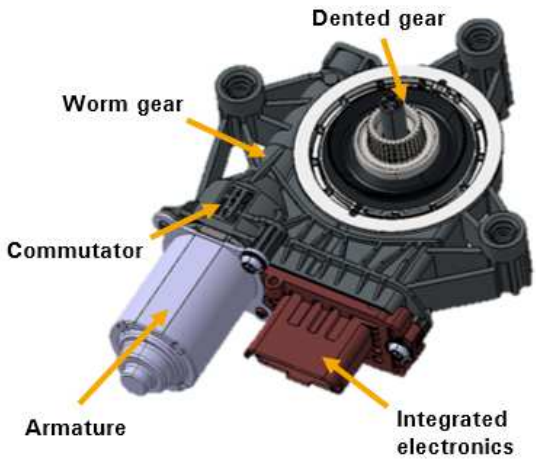

Source: Brose internal document

2.2.1 DC Motors

Actuators for a myriad of mechatronic devices, the direct current (DC) motors are widely used in the automotive industry, from window regulator systems to side-door drives and power lift gates. They can be structured in multiple different ways: the magnetic field required to start the rotation can be generated either by coils excited by an electric current or by permanent magnets, placed inside the stator.

The later group, which includes most WRDs and especially the ones used in this project, have magnetic fields supplied by permanent magnets that create two or more poles in the armature by passing magnetic flux through it. Inside the magnetic field of the stator, a rotor is placed, with an armature enveloped by copper wires supplied with electric current. those wires are connected directly to a circular commutator placed along the rotor axis, excited by the conducting brushes that receive external energy from the connector. Then, the magnetic flux causes the current-carrying armature conductors to create a torque. This flux remains

basically constant at all motor speeds — the speed-torque and current-torque curves are linear (FINK; BEATY, 2006).

Knowing that the force on a moving charge q, with speed $\vec{v}$, inside a magnetic field $\vec{B}$ is given by Lorentz law:

$$\vec{F} = q\vec{v} \times \vec{B} \tag{1}$$

when applied to a current-carrying wire, it translates into

$$\vec{F} = \vec{I}L \times \vec{B} \tag{2}$$

where $\vec{I}$ is the current in Ampere and L the length of the conductor perpendicular to the magnetic flux, in meters. This force generates torque in a rotary motor, with a r average winding radius and Z number of conductors, proportional to:

$$T = B \cdot I \cdot L \cdot r \cdot Z \tag{3}$$

Developing it further, using

$$I = \frac{I_a}{A} \quad \text{and} \quad B = \frac{\phi}{a} = \frac{\phi}{\left(\frac{2\pi rL}{P}\right)} \tag{4}$$

where I_a is the armature current, A the number of parallel paths, a the cross-sectional area of flux path per pole, ϕ the magnetic flux per pole and P the total number of poles. Also, as the back EMF (electromotive force) E_b is defined by:

$$E_b = \frac{P\phi ZN}{60A} \tag{5}$$

where N is the rotational speed of the motor in rpm. Putting together equations 4 and 5 on 3 and using π as $3{,}14$, we finally get the torque of the rotor:

$$T = 0.159\phi I_a Z\frac{P}{A} \quad \longrightarrow \quad T = 9.55\frac{E_b I_a}{N} \tag{6}$$

as $E_b I_a$ being the power supplied by the source to the armature.

The linear correlation shows how the torque is directly related to the current supplied and also the resulting rotational speed. Every motor then has a characteristic performance curve like the one in Figure 7, from a WR actuator. While the dotted lines establish the overall torque and current limits for the project, the blue lines create a much more strict limit on the region of operation of the WRD that has to be followed for its correct performance.

Both motors analyzed during this project, the BM2010 and the WR19, have a region of operation around 3 N m to 5 N m, with a 1:80 ratio between the rotor worm gear and the external dented gear that has interface with the WR system.

Figure 7 – DC motor performance curve

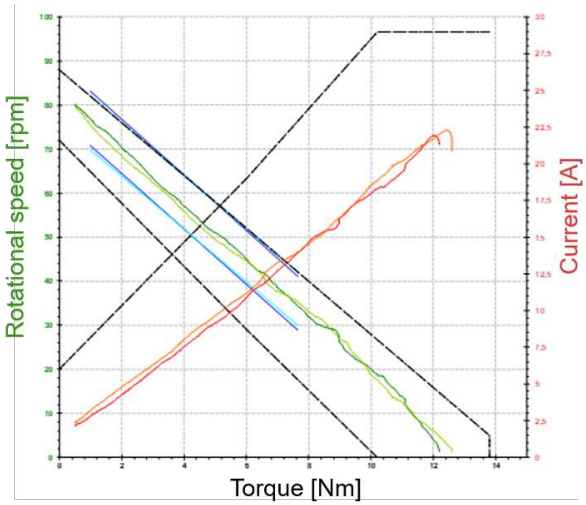

Source: Brose internal document

2.2.2 Motor electronics

As mentioned at the start of this section, a WR that uses automatic function should have a electronic component to monitor and manage the WRD performance during operation. This is mostly done by integrating a hardware that acts as a interface between the car switch and the actuator itself, as seen on Figure 8. Its inputs are: the power given by the car's switch and battery, a single or a couple of Hall sensors, placed near the commutator to monitor the rotation of the motor axis, and a LIN serial interface, which is a protocol used for communication between components inside a vehicle. All the signals are processed by a microcontroller, which calculates the WRD speed and position and also controls the system operation. Finally, the output to the actuator is then delivered through the activation of a relay or a MOSFET.

The software embedded on the electronic is developed as a general template for a whole range of vehicles from the same automaker's platform. This encompasses how the motor

Figure 8 – WR motor integrated electronics

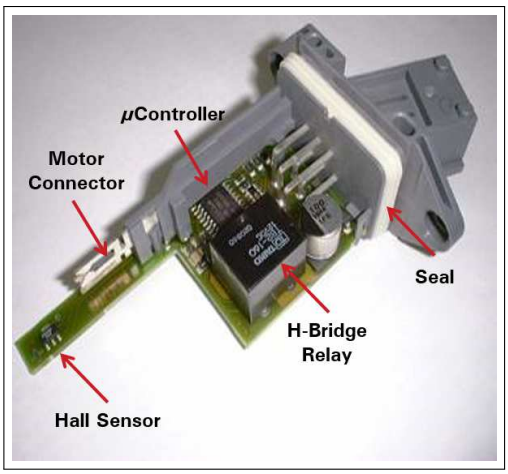

Source: Brose internal document

Figure 9 – Signal processing by Hall sensors

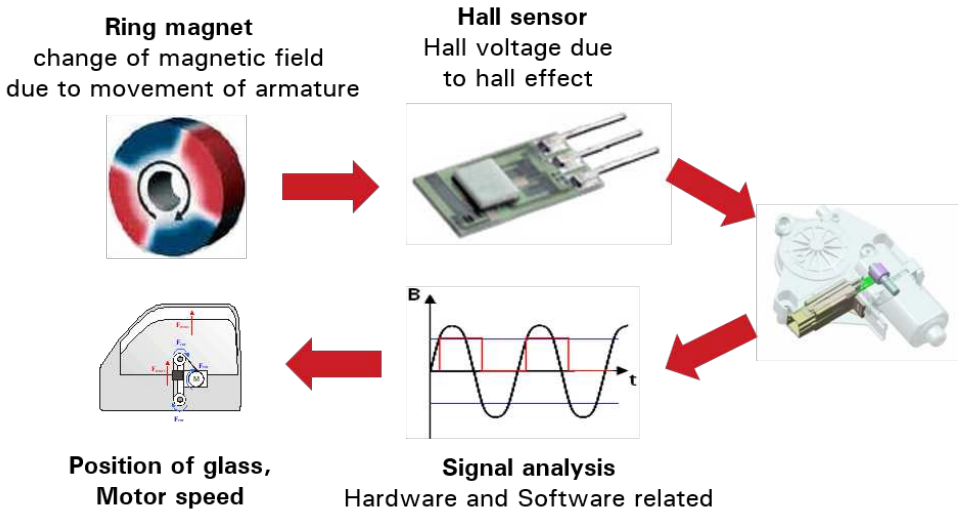

Source: Own elaboration

should behave regarding many factors, such as range of movement, protection against high temperatures, soft-stop near the limits of the frame and anti-trap functionalities (Figure 9). However, the parameters which limit and govern each function are set separately for each individual car project to adequate the electronic to that specific environment, since there are many physical differences inside the same vehicle platform, size and geometry of glass for example. This work has a big importance as it guarantees the safe and robust operation of a window regulator according to law and customer specifications.

Instead of using Hall sensors to monitor the rotation speed and glass position, some more specific applications calculate it through the analysis of the ripple signal caused by the brush commutations. Also, for cars in which the manufacturer needs to concentrate all the functions of the door system in one place instead of a integrated hardware for each component, a DCU (Door Control Unit) is developed, managing not only the window regulator but also side door drives, latches and automated rear view mirrors.

2.3 COMMUNICATION PROTOCOLS

To establish communication between multiple devices in a electronically connected environment, some network protocols were established. Defining rules, syntax and synchronization methods, these protocols guarantee the robustness in the operation of window regulator systems. This section briefly deals with two main protocols used on the automotive industry, the Controller Area Network (CAN) and the Local Interconnect Network (LIN), and further presents the tools used to test these communications and calibrate ECUs.

2.3.1 Controller Area Network

After decades of improvements in automotive technology, the development of a high-integrity bus system that connected all the different electronic devices in a vehicle was a real necessity. At the beginning, this was done purely by point-to-point wiring, relying on heavy and bulky copper wires and harnesses that kept growing in number and weight with each new electronic added.

First introduced by Robert Bosch GmbH in 1985, the Controller Area Network, known as CAN, still is to this day the standard for in-vehicle network, lowering costs and providing a durable way to multiplex all the signals required for serial communications from different ECUs. Every message is broadcasted to all the devices connected, leaving each one of them to filter which messages are relevant or not.

Currently defined by the ISO 11898, the CAN architecture is divided into two layers from the OSI model: data link and physical. As shown by Figure 10, the data link layer is implemented by a CAN controller, usually an ASIC embedded in a microcontroller, responsible for receiving and transmitting each message, handling re-synchronizations, error signaling, data encapsulation, frame coding and filtering of messages. The physical layer is handled by a CAN transceiver, supporting high-speed (up to 1 Mbit/s) or low-speed/fault-tolerant (up to 125 kbit/s) transmissions, structured in a two-pin layout. Since the transmission is differential voltage based, to eliminate the interference from motors and other types of nodes, the bus consists of a high and a low line, terminated by resistors to prevent signal reflections.

Figure 10 – CAN node communication

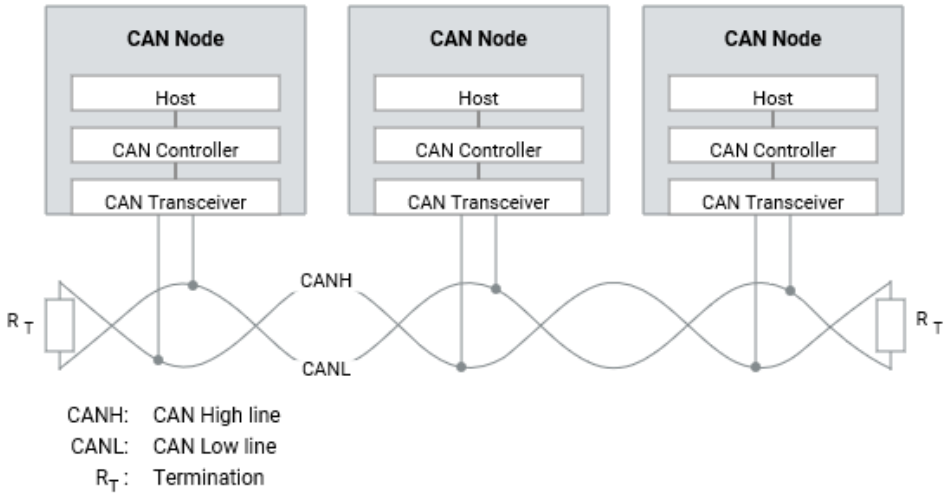

Source: Vector Informatik GmbH

The framing of data is done in a maximum payload of 8 bytes (Figure 11). It includes, besides the data itself, mainly the message identification address, data length code, checksum and a field for the receiver acknowledgement, as the figure describes. Besides the frame to transmit data, the CAN protocol also establishes: the remote frame, used to request the

Figure 11 – CAN frame structure

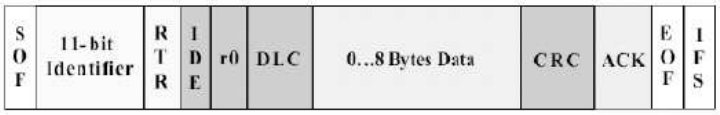

Source: Brose internal document

transmission of data (rarely used in automotive networks); the error frame, for error detection by nodes; overload frame, to add a delay between data and request frames.

2.3.2 Local Interconnect Network

While the CAN protocol simplified the vehicle network as whole, it was too expensive to implement for every mechatronic component. To achieve a cheaper and common standard for these applications, in 2002 a consortium of BMW, Volkswagen, Audi, Volvo and Mercedes-Benz published the first version of the Local Interconnect Network. The main objective of LIN is creating smaller networks, comprised of 16 nodes maximum, in which one master node initiates the communication with all the other slaves through a single wire. Being comparably simpler than a CAN bus, the LIN one has no bus arbitration and collision detection and has a guaranteed latency with data transmissions of up to 20 kbit/s.

Figure 12 – LIN bus communication

Source: <https://www.csselectronics.com/screen/page/lin-bus-protocol-intro-basics/language/en>

The master node loops through each one of the slave nodes in its cluster, requesting information through a header frame, for which the slaves reply with a response frame of 2, 4 or 8 bytes of data (Figure 12). For window regulator applications, this means that the driver's door, for example, can act as the main ECU of the car, controlling all the other window movements through a central switch.

2.3.3 CAN and LIN analysis

During the development process of a window regulator project, several tools are used to configure the electronics and also monitor its operation during measurements and simulations. The VN1640a hardware interface, shown at Figure 13, by the company Vector Informatik GmbH, acts as a FPGA based CAN/LIN transceiver, providing access to these networks through

Figure 13 – Vector products - Left: VN1600 interface family; Right: CANape software

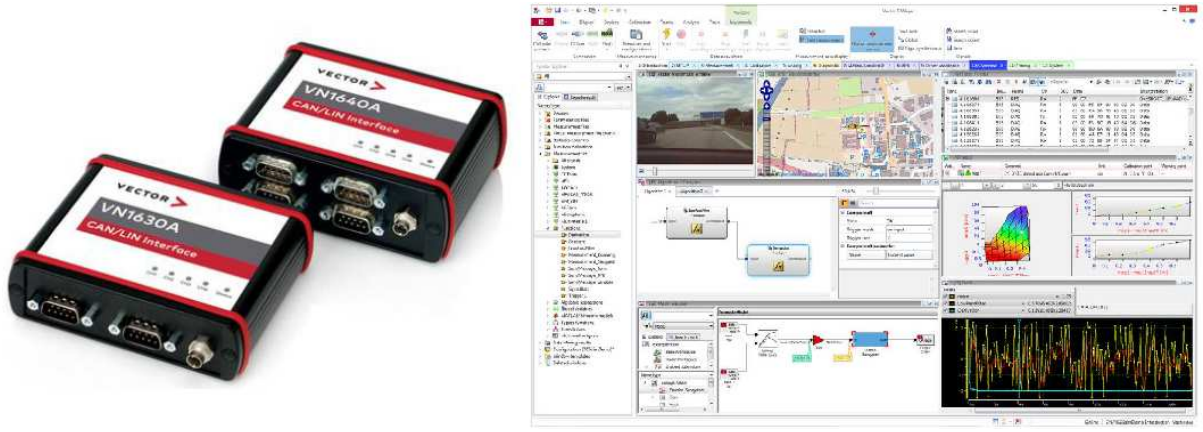

Source: Vector Electronik GmbH

4 different channels. Connected to a computer via USB cable, it can send and receive CAN/LIN messages via its own software, CANape, also from Vector.

CANape is a platform mainly designed for the calibration of ECUs. Through a customizable user interface, it's possible not only to directly configure the parameters inside a window regulator electronic, but also direclty access its memory, plot and data mine bus signals during operation and even simulate already saved measurements on a different set of parameters for analysis.

In order to use these interfaces on its own electronic products, Brose developed in-house an auxiliary hardware for LIN signal analysis, called Robel Steuer Gerät (RSG), translated as Robel Controlling Device. Both devices were used in conjunction during this project.

2.4 ANTI-TRAP FUNCTION

Along with several processes that an electronic provides to a window regulator unit, one of the most important is the anti-trap function. Amidst an automatic raising of the window, the mechanism has to be able to reverse in case the glass encounters an obstacle, avoiding any accidents on the user side and preserving the integrity of the system itself. This section aims to describe the anti-trap general principles, how it's evaluated and the effect that the glass tilting has on it.

2.4.1 Anti-trap Detection

When a WR initiates its movement in automatic mode, raising the glass along the door frame with a single press on the switch, the motor electronic is entirely in charge of the operation. For devices containing Hall sensors on the hardware, as the gear and commutator rotate, a stable quadratic pulse is delivered to the microcontroller. With this signal is possible not only to compute the current WRD speed but also the position of the window on the door structure, having its lower and upper limits as range reference.

Figure 14 – Example of anti-trap event

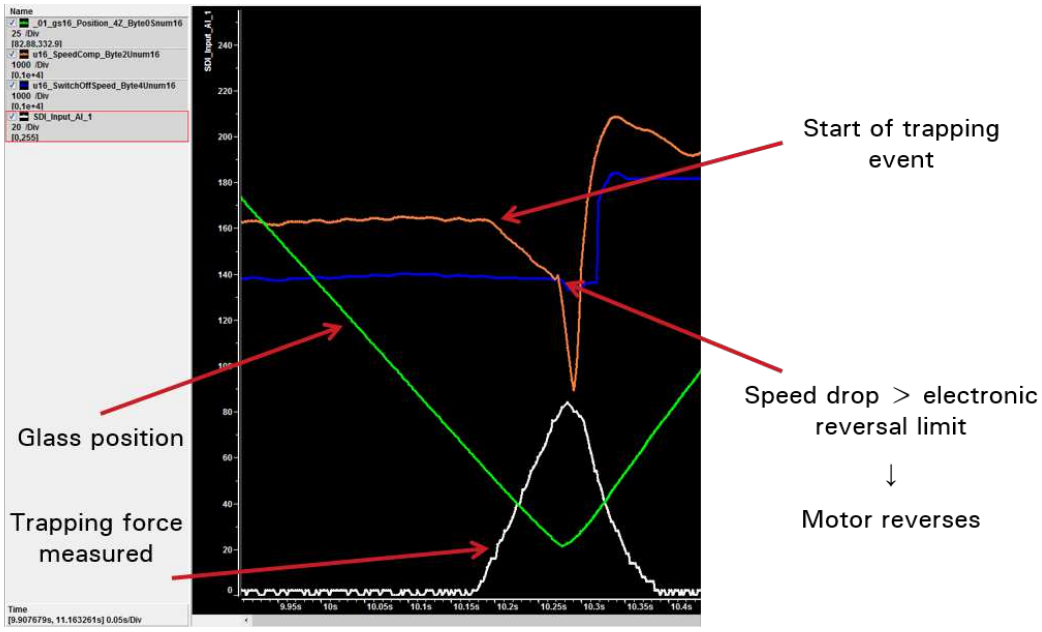

Source: Own elaboration

As a general rule, while the glass follows along the Z-axis (the full vehicle coordinate system is presented in Annex A), from the first point it reaches the door upper sealing/frame, there must be a safety range from 4 mm to 200 mm in which the system must reverse in case of obstruction.

To achieve a quick response and avoid accidents, the difference between the last motor speed values is continuously compared to a tracking limit and a switch-off signal, which is essentially the speed signal with a negative offset. When there's a speed drop quick enough so the difference between the last recorded values crosses the tracking limit, the switch-off signal is frozen on the same value until the speed difference lowers again below the threshold. If the rotational speed keeps dropping, after some time it will be lower than the switch-off signal, indicating a reversal event, as shown in Figure 14. From this moment, the polarity of the actuator terminals is switched and it starts revolving in the opposite direction.

While many factors influence the complex AT algorithm, most of them are not necessary to understand the objectives of this project. The essential aspect is that a constant drop on the motor speed is the optimal situation. Since the system also accounts for other factors to avoid miss-reversing the window, such as vehicle vibrations on rough-road situations, if in a stable environment the WRD speed already fluctuates during a trapping event, it's much harder to develop its parameters to achieve an acceptable robustness.

Summarising, the main signals evaluated by the window regulator during anti-trapping events are:

- Position: value displaying in which section of the complete range of motion the motor gear and, consequently, the glass currently is. This value is given by the motor electronic and incremented at each Hall sensor pulse.

- Motor Speed: rotational speed calculated by the electronic from the Hall sensors attached to the DC motor.
- Diff. speed: the difference between the last few speed values calculated by the electronic; positive values mean that the WRD is accelerating and negative values mean that the WRD is decelerating.
- Tracking threshold: parameter defined to evaluate if a trapping event is starting to occur. If the diff. speed signal gets above this limit, the switch-off signal is frozen on its last value.
- Switch-off threshold: calculated from the speed signal with an adjustable negative offset. If the actuator speed drops below this value, the window starts to reverse. In case the diff. speed signal drops below the tracking threshold before the reversing, the switch-off value is updated by the electronic and is no longer frozen.

2.4.2 Trapping Force Measuring Method

As mentioned on chapter 1, the pinching force generated between glass and door sealing has to respect some critical limits. While 100 N is the standard maximum value, throughout development an average point of 60 N is intended, considering that a low enough force can cause situations in which the WR reverses with no actual obstructions, amidst vehicle vibrations on rough roads, as mentioned before. The tests are conducted in many environments, between high and low temperatures (-30 $\sim$ 80 °C), according to each customer specification.

Figure 15 – SDI force gauge fixed on the window

Source: Own elaboration

The current device used by most automakers and suppliers to measure those trapping forces is the SDI Model 10293 (Figure 15), from HITEC Sensor Developments. This hands-free sensor is attached directly on the glass edge, from which a metal arm is connected to a pair of springs and placed perpendicular to the direction of movement, between window and frame. It has the following features:

- Weight of 0,75 kg
- Pairs of springs with different spring rates, mainly 5, 10, 20 and 65 N mm^{-1}
- Adjustable measuring height
- Maximum load of 200 N
- Output of 2 mV/V
- Operating temperature of -65 $\sim$ 250 °C

The calculation of the force applied follows Hooke's law:

$$F_S = kx \tag{7}$$

where k is the spring rate and x the total displacement of the spring in meters. The analog signal is sent from the SDI to a processing device, PMAC 3000, through a serial cable on a rate of 10 000 samples/s. The device has a digital display, to configure value limits and show peak or current force values, and a ± 5 or ± 10 V analog output.

2.4.3 Glass Tilting Effect

On single-guided WRs, the up-movement on the Z-axis works as an bi-stable inverted pendulum. In this arrangement, the center of mass is above the pivot point which is being pushed, oscillating back and forward between the X-axis according to the door architecture. Some designs have more stability (mainly rear doors), by operating lighter windows and having them more tightly adjusted to the side columns of the frame, while others allow the glass to rotate a lot more around the pivot (mainly front doors), by having a heavier total mass and less or no guiding rail at all in one of the columns. When measuring trapping forces on systems from the later case and with the SDI placed outside the WR rail axis, the measuring device helps with this rotational movement.

The moment it hits the upper sealing, it creates a second rotation point on the system, generating a momentum that is presented in Figure 16. When F_{gauge} in applied on the window by the A-column side, a R_x movement component is created, pushing the glass away from the B-column and thus reducing $F^B_{friction}$. While this movement also increases $F^A_{friction}$, the area of contact between glass and sealing on that side is lower, which in turn re-accelerates the WR motor for a brief period.

This change on the speed drop rate is seen by the electronic, as shown on the comparison made in Figure 17. Figure 17a shows an ideal AT detection, with the speed lowering on a constant rate from the moment the obstacle hits the window, increasing the force on the measuring device and the torque generated by the actuator also on a linear basis. During a tilting situation however, if the speed re-acceleration shown at Figure 17b gets the diff. speed value below the tracking threshold, explained at the subsection 2.4.1, the electronic will update the switch-off limit, essentially delaying the trapping detection. While this happens, the force on the SDI and the torque given by the motor will keep increasing and the window will end

Figure 16 – Glass tilting to the A-column

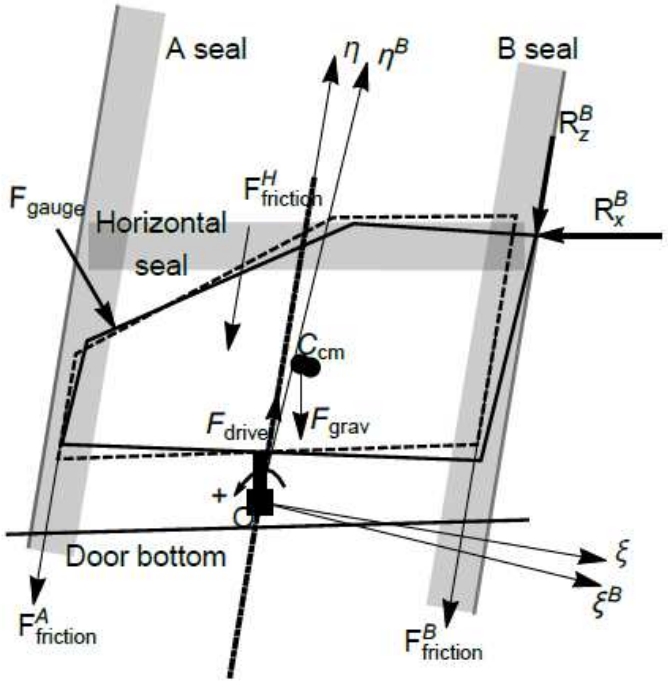

Source: Petkun (2018)

Figure 17 – Speed drops detected by the electronic

(a) Standard AT event

(b) Tilting AT event

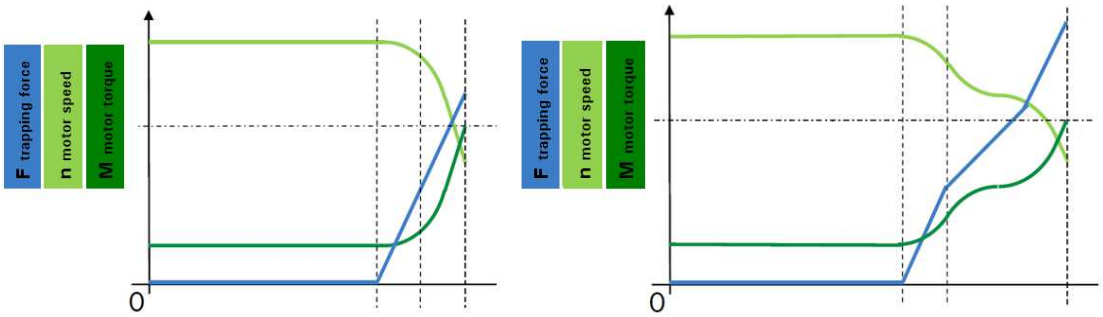

Source: Own elaboration

up reversing moments later, effectively raising the overall trapping force detected on the test, sometimes above 100 N.

In real life situations, the trapping of a finger, for example, generates little tilting movement, in contrast to the dynamic observed during validation tests. According to Feyh (2019), this difference can be explained by some mechanical factors on the system composition:

- The SDI has a constant stiffness throughout the trapping event; a real finger has variable levels of stiffness because of the different tissues composing it.
- Surface of contact is lower on the SDI arm than on a real finger, penetrating more into the rubber of the sealing and increasing the rotational effect on the contact point.
- The weight of the SDI attached to the glass (0,75 kg) changes its center of mass in the direction of the A-column, already displacing the glass away from the B-column rail.

For these reasons, already explored in preliminary works at Brose, the influence of the measuring device on the tilting seems evident. However, the magnitude of its effect among other system variables wasn't yet evaluated, which is one of the objectives of this thesis.

2.5 DATA ACQUISITION

In an effort to analyze the window regulator behavior during the experiments, several devices were used. This section will briefly present the main components used, including sensors and signal converters, showing primarily their technical specifications. The whole setup and how the devices were used will be shown on Chapter 3.

2.5.1 Torque Sensor

Besides the rotational speed calculated by the electronic, the other main variable to be analyzed from the DC motor is the torque it creates to operate the WR system. To measure it, a linear torque sensor with a rotating measuring shaft was chosen: model 5413-1200/20-S (Figure 18), from Kistler Instrumente GmbH.

Figure 18 – Torque sensor 5413-1200/20-S

Source: Kistler Instrumente GmbH.

This type of device operates according to a strain gauge principle, in which a sensor, supplied by an external power supply, varies its resistance according to the force applied between both ends of the axis that trespasses it and generating an analog output signal in mV/V. Also, an incremental disk is present for angle of rotation measurement, delivering a two-phase shifted signal, according to the direction of rotation.

The model used on this project has the following main characteristics (complete specification present on the component datasheet from Kistler Instrumente GmbH (2017)):

- Nominal torque: 20 N m, with 20% maximum overload
- Nominal characteristic value: 2 mV/V
- Nominal supply voltage: 5 V
- Nominal temperature range: 10 °C to 40 °C
- Maximum permitted axial force: 400 N
- Maximum rotational speed: 1500 rpm
- Angle increments per revolution: 360

The cage for the placement of the sensor between the motor and the window regulator drum house, as well as the couplings for the connections of the axis were developed internally at Brose by the Tests Department, according to the technical drawings from the 5413-1200/20-S datasheet.

2.5.2 Amplifier

Amplifiers are electronic circuits and devices used to increase the magnitude of a input signal. For this project, a 8B family module from Dataforth Corporation was chosen, specifically the 8B40-02 voltage input module, built together with the 8BP02-01 analog I/O backpanel and a 8BPWR-2 power converter inside a small metal box, as seen on Figure 19.

The 8B40-02 module not only amplifies the voltage input, but also isolates and filters the signal, providing 100 dB of common-mode rejection (CMR) and per decade of normal-mode

Figure 19 – Amplifier box built with 8B40 module

Source: Own elaboration

rejection (NMR) above 1 kHz. Other main characteristics are as follows (complete specification present on the component datasheet from Dataforth Corporation (2017a)):

- Input range: -50 mV to 50 mV
- Output range: -5 V to 5 V
- ANSI/IEEE C37.90.1 Transient Protection
- Input Protection to 240VAC Continuous
- 1 kHz Signal Bandwidth
- $\pm 0{,}05\%$ Accuracy
- $\pm 0{,}02\%$ Linearity
- Operational temperature range from $-40\,^{\circ}$C to $85\,^{\circ}$C

The 8BPWR-2 power supply module used together with the amplifier encapsulates a 7 V to 34 VDC, providing a stable 5 VDC supply for the 8B40-02 amplifier. The full specifications are also available on datasheet from Dataforth Corporation (2017b).

2.5.3 Potentiometric Displacement Sensor

Used to measure small distances between objects with high precision, the potentiometric displacement sensor family 8712 (Figure 20), from Burster Praezisionsmesstechnik GmbH, consists of a spring attached to a rod that slides by the measurement object. The rod is guided by a low friction sliding bearing, providing high durability and measuring quality, while the pre-stressed spring presses the sensor tip against the measurement object, eliminating the need of coupling between them. The main areas of application are evaluating the displacement of electromagnets, hydraulic cylinders, switches and buttons; measurements of deformation in general, bending, press-fits and feed-strokes.

As for the important technical points for the 8712-25 sensor used on this project (full specifications are also available on datasheet from Burster Praezisionsmesstechnik GmbH & CO KG (2018)):

- Measuring range: 25 mm
- Resolution: 0,01 mm

Figure 20 – Potentiometric displacement sensor 8712-25

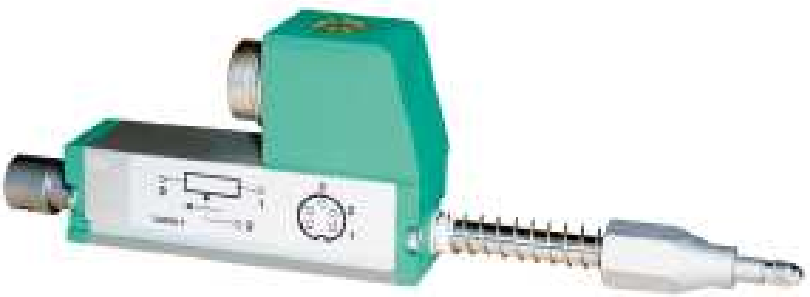

Source: Burster Praezisionsmesstechnik GmbH

- $\pm 0{,}2\%$ Non-linearity
- Max. operating voltage: 25 V
- Recommended current in slider circuit: $<$0,1 µA
- Total mass: 75 g
- Operational temperature range from $-30\,^{\circ}$C to $100\,^{\circ}$C

Finally, an adaptor was necessary to clip the sensor to the glass. For this, a small and light metal clipping device was adapted for it, with a small mass to interfere in the least possible way on the system's dynamic and the center of mass position.

2.5.4 AD Converter Module

Developed by CSM GmbH, the AD-Scan MiniModul (Figure 21a) is a analog/digital converter module developed for the automotive industry, resistant to extreme temperatures and environmental conditions, besides being very compact and ideal for test benches. The four galvanically isolated voltage inputs can be adjusted to measure signals from $\pm$100 mV to $\pm$60 V and up to 10 kHz, modulating and delivering a single CAN signal as output. The module also has high-precision bipolar sensor excitation, adjustable per channel, allowing the connected devices to be supplied and deliver their signals through a single cable.

Additional technical data (also available on document from CSM GmbH (2018)):

- Measurement ranges: $\pm$100 mV, $\pm$200 mV, $\pm$500 mV, $\pm$10 V, $\pm$20 V, $\pm$60 V
- Resolution: 16 bit
- Internal sampling rate per channel: 10 kHz
- HW input filter: low-pass filter 3rd order, approx. 2,5 kHz
- SW input filter: switchable 6th order Butterworth filter, 0,1 Hz to 2000 Hz
- Gain error at 25 °C: max. $\pm 0{,}05\,\%$
- Sensor excitation: $\pm$5 V to $\pm$15 VDC, max. $\pm$30 mA per channel

Figure 21 – CSM MiniModul hardware and software set

(a) CSM AD-Scan MiniModul

(b) CSMconfig software

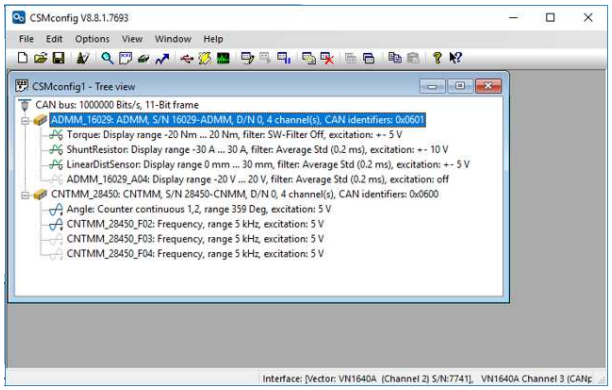

Source: CSM GmbH

- CAN 2.0B (active), High Speed (ISO 11898-2.2016), 125 kBit/s to max. 1 MBit/s, up to 2 MBit/s with CSMcan Interface, data transfer free running
- Operational temperature range from $-40\,^{\circ}C$ to $125\,^{\circ}C$

To configure the module, the supplier's software CSMconfig (Figure 21b) is used to define each sensor's physical conversion rate, signal offset and range, as well as its excitation supply. It has an automated detection of all connected CSM modules and many sensors, allowing the the configuration of the CAN bus parameters, like frame size and bit rate. The software can also be integrated into the CANape application, giving the possibility of adjusting the CAN network directly from the measurement window.

2.6 STATISTICS AND EXPERIMENTAL DESIGN

In the engineering field, to understand a system or process while its operating, it's not enough to only observe it. Changing the inputs in a controlled way and analyzing how the outputs behave with each change can help understanding cause-and-effect relationships, followed by the crafting of theories and hypotheses about what makes the system work. In order to achieve this, experiments need to be done on the system.

A experiment is a test or series of runs in which purposeful changes are made to the input variables of a process or system so it's possible to observe and identify the reasons for changes that may be detected in the output response (MONTGOMERY, 2006). Experimentation is a vital part of the scientific method. While mechanistic models, such as mathematical ones, can be used for ideal situations in which the phenomenons are completely understood, in most engineering cases this elucidation must be done through empirical models.

Much more than just collecting raw data, a well-design experiment is important to not only show the effects of the factor changes in the experimented system responses, but also to check for patterns and achieve higher repeatability and reproducibility of the tests. The general approach to planning and conducting a experiment is called strategy of experimentation. Among many strategies used nowadays in the industry, three of them stand out: best-guess approach, one-factor-at-a-time (OFAT) and factorial experiments.

Considering a system composed of several changeable inputs, the best-guess strategy is frequently used by engineers and scientists, who use practical and theoretical knowledge (often called "know-how") to guess the optimal factor levels to achieve a desired process response. In this approach, the variables are continuously switched according to the previous test results until they are acceptable. However, this leads to some problems: the experiments can continue for a long and not definite time, without guarantee of success; and even if it seems that success was achieved, there's no guarantee it was the best solution possible.

Based on this, the OFAT approach establishes a baseline set of levels for each factor and successively changes them in a planned way over their range, one at a time. After the experiments are finished, it's possible to identify the impact of each one of the changes while

all the other variables are held constant. This is know as a factor individual effect. Since that switch occurs individually, it's not possible to consider any factor interactions with this method, as in what would happen if two factors changed at the same time. For example, if a certain variable A has a X effect while it changes its level from low to high and a factor B is set to low, it's possible that X doesn't happen if B is set to high. Another problem is the possible propagation of errors between each setup, considering the variables remain all the same except for the one being changed.

Finally, the correct approach to dealing with several factors is to conduct a factorial design of experiments, in which the factors are varied together, instead of one at a time. This method will be the main one covered on this section, as well as some of the techniques to analyze the results generated by it.

2.6.1 Design of Experiments (DOE)

Statistical design of experiments refers to the process of planning the experiment so that appropriate data will be collected and analyzed by statistical methods, resulting in valid and objective conclusions. When the problem involves data that are subject to experimental errors, statistical methods are the only objective approach to analysis (MONTGOMERY, 2006). In order to achieve a better understanding of the analyzed system, the DOE is based on three main principles: randomization, replication and blocking.

Randomization is the cornerstone of a well-design DOE: it means that both the order in which the runs are conducted as well as the allocation of the experimental samples are completely randomized. This satisfies the statistical requirement of independence of observations and ensures that any noise and extraneous effects are minimized between each experimental run. For example, in case the force gauge is fixed incorrectly on the glass during a single run of a window regulator force measurement test, this error won't be propagated to subsequent runs, since the setup will be remade and checked before them. It means that, after a run, each factor has to be re-normalized: to a middle value inside its range, if it's a continuous-level factor (i.e. motor voltage), or completely re-done, if it's a discrete-level factor (i.e. attachment of the force gauge). In the situation exemplified before, the force gauge would have to be re-attached to the glass even if it stayed on the exact same spot between tests. Knowing that this complete randomization is sometimes impossible in industrial experiments, due to higher costs and longer time, there are statistical design methods for dealing with it.

Next, replication is performing an independent experimental run again, performing the full experiment matrix from start to finish; a simple repetition of measurements during a single, same run would not be categorized as replicates, but only as repeated measurements. Correct replication allows the estimation of the experimental error, determining whether observed differences in the data are really statistically different. Also, if the sample mean is used to estimate the true mean response for one of the factor levels in the experiment, replication permits the experimenter to obtain a more precise estimate of this parameter.

Finally, blocking is a technique used to improve the precision with which comparisons among the factors of interest are made, reducing the impact of nuisance factors, factors that may influence the experimental response but in which there's no direct interest. This includes noise variables such as ambient temperature and humidity in a non-controlled environment.

Knowing those techniques, to start a design of experiments, usually all the factors that impact the system are structured into two main labels: potential design factors and nuisance factors. The first category are the factors which are important for the experiment: the design factors themselves, which are the variables of the system the experimenter wants to evaluate and that will change levels according to the test matrix; the held-constant factors, variables that may have some effect on the response but are maintained the same during the experiment; and the allowed-to-vary factors, which the effect is expected to be relatively small so won't be controlled. For the nuisance ones, there are often controllable, uncontrollable and noise factors, all of them not of any interest to the experiment, so will be adjusted into a certain level or have their variations blocked during the result analysis.

2.6.2 Factorial Designs

Many experiments involve the study of the effects of two or more factors. In general, factorial designs are most efficient for this type of experiment. By a factorial design, we mean that in each complete trial or replicate of the experiment all possible combinations of the levels of the factors are investigated. For example, if there are a levels of factor A and b levels of factor B, each replicate contains all ab treatment combinations (MONTGOMERY, 2006).

The simplest and most used type of factorial design is a 2-level design (2^k). This means that among the k analyzed factors of the DOE, all of them have only two levels, a high and a low; these can be either quantitative or qualitative (binary), as exemplified on the subsection before. A full-factorial 2-level design with k factors requires 2^k runs for a single replicate. That means that a two level experiment with three factors would require eight complete runs.

Considering a complete randomized experiment, when levels are changed, the main effect of a factor is defined as the difference in the response produced by this change. This is given by the averages of responses:

$$\text{Effect} = \frac{\sum Y_+}{n_+} - \frac{\sum Y_-}{n_-} \tag{8}$$

where Y is either the average in which the factor level is high or low and n is the sample size.

One of the advantages in the use of the DOE is the analysis of factor interactions, besides their individual impact. This is done by multiplying the parent terms. For example, in a experiment which x_1 and x_2 are the main factors, the response of a run with x_{1-} and x_{2-} produces $x_1 x_{2+}$, following the sign multiplication rules. After that, Equation 8 is used to calculate the effect of each interaction. A first-order model can be constructed with these

Figure 22 – Impact of the choice of factor levels in an unreplicated design

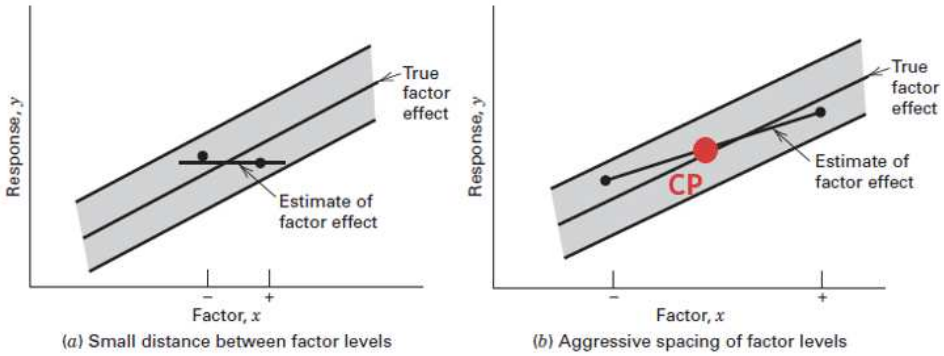

Source: Montgomery (2006) (modified)

interactions, representing the curvature in the response function:

$$y = \beta_0 + \sum_{j=1}^{k} \beta_j x_j + \sum \sum_{i<j} \beta_{ij} x_i x_j + \epsilon \tag{9}$$

Because resources are usually limited, the number of replicates that the experimenter can employ may be restricted, since a single experiment with six different factors, for example, would demand 64 runs total. For this reason, unreplicated designs may be conducted. In this case, the most reliable way to define the levels of each variable is taking an aggressive spacing between the high and the low, screening any noise that can interfere with the response, as noticed in Figure 22.

The assumption of linearity in the factor effects is a potential concern in the use of two-level factorial designs. In the case quadratic effects are noticed, where a certain factor doesn't have a linear behavior, a new second-order model for the response would develop from Equation 9:

$$y = \beta_0 + \sum_{j=1}^{k} \beta_j x_j + \sum \sum_{i<j} \beta_{ij} x_i x_j + \sum_{j=1}^{k} \beta_{jj} x_j^2 + \epsilon \tag{10}$$

As Figure 22 shows, a method can provide protection against curvature from second-order effects as well as allow an independent estimate of error to be obtained, especially useful in unreplicated designs: the addition of center points (CP). CPs are values set halfway between the low and high settings (when the factor is quantitative) and ran preferably at the start and at the end of the experiment, to ensure the factors remained stable through it.

2.6.3 Experiment Matrix and Statistical Analysis

In order to not only structure the experiment test order and analyse the factor effects, but also compare the effects between each other, several softwares can be used. Minitab, in particular, is a statistics application useful for several types of DOE, building and randomizing the experiment matrix according to the type of design, number of factors, levels, center point runs and others. It also completely calculates all the important statistical data and charts once

the responses of the experiment are given, and this section will briefly explain how they are done.

The construction of factorial experiment matrices with the Minitab is simple. First of all, the number of analyzed factors, their name, type (quantitative or qualitative) and high/low levels have to be chosen, which will then display all the possible designs for that size. On all experiments stages of this project, a full factorial run was executed for a complete understanding of the variables involved, meaning that every combination of the 2^k runs was tested. Fractional factorials are also available when there are more than three factors in the design, where a matrix size is reduced at the cost of result resolution. The number of center points per replicate and the total number of replicates are also inputted by the user and then the experiment matrix is finally created, with its runs randomized. The constructed matrices will be displayed on Chapter 3.

After all the experiments are done and the response values are entered into the worksheet, several types of data analysis are available. In order to assess the effects of each factor and their interactions, some theoretical background has to be presented. Not all the statistical values from the Minitab analysis were used, so only the main ones will be presented.

2.6.3.1 Factor effects assessment

To analyze the results of a statistical process, an hypothesis about the data has to be made. A statistical hypothesis is a statement either about the parameters of a probability distribution or the parameters of a model, reflecting some conjecture about the problem situation. The statement $H_0 : \mu_1 = \mu_2$ is called the null hypothesis, while $H_1 : \mu_1 \neq \mu_2$ is called the alternative hypothesis. In the case of the experiments on this project, the null hypothesis would mean that the change of levels on the factor in question has no effect on the response; for example, that taking off the waist sealing has no impact on the variance of system stiffness.

Two kinds of errors may be committed when testing hypotheses. If the null hypothesis is rejected when it is true, a type I error has occurred. If the null hypothesis is not rejected when it is false, a type II error has been made. The general procedure in hypothesis testing is to specify a value of the probability of type I error α, often called the significance level of the test, and then design the test procedure so that the probability of type II error β has a suitably small value (MONTGOMERY, 2006).

One of the main tools used for hypothesis testing in statistics is the Student's t-test. Its objective is to evaluate how significant the differences between factors/groups are, showing if those differences (in averages) could have happened by chance or not. This is done using a one or two-tail t-distribution, which is a normal distribution when the scaling term is unknown and is replaced by an estimate based on the input data.

In order to test if a certain factor has a significant impact on the analyzed response via a t-test, P-values are calculated for each of them via numeric methods (in this project,

Figure 23 – Factor's p-value inside a t-distribution

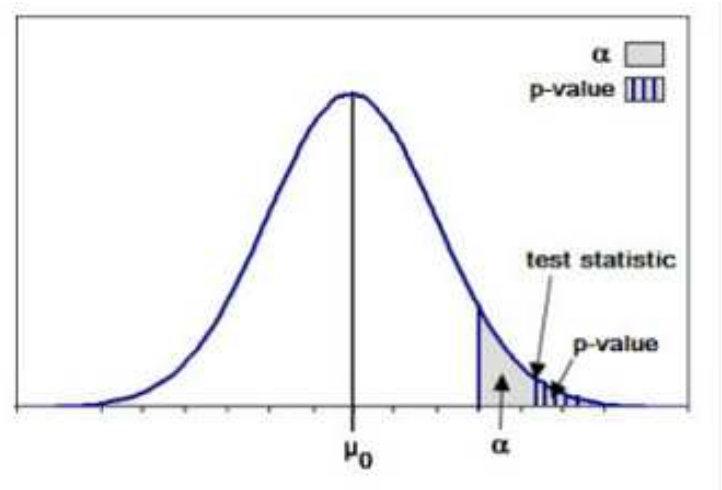

Source: <http://www.sigmapedia.com/includes/term.cfm?&word_id=2185&lang=ENG>

done via Minitab). P-value is the probability that the test statistic will take on a value that is at least as extreme as the observed value of the statistic when the null hypothesis H_0 is true, as Figure 23 illustrates. It is customary to call the test statistic (and the data) significant when the null hypothesis H0 is rejected; therefore, we may think of the P-value as the smallest level α at which the data are significant (MONTGOMERY, 2006). In other words, when a P-value calculated from a factor's effect is below the level of significance α chosen for the experiment, the null hypothesis H_0 is rejected and thus the effect is statistically significant.

When an experiment has multiple different factors, two types of charts are used to better illustrate which of their effects are statistically significant or not. The first one is a

Figure 24 – Example of Pareto chart of effects

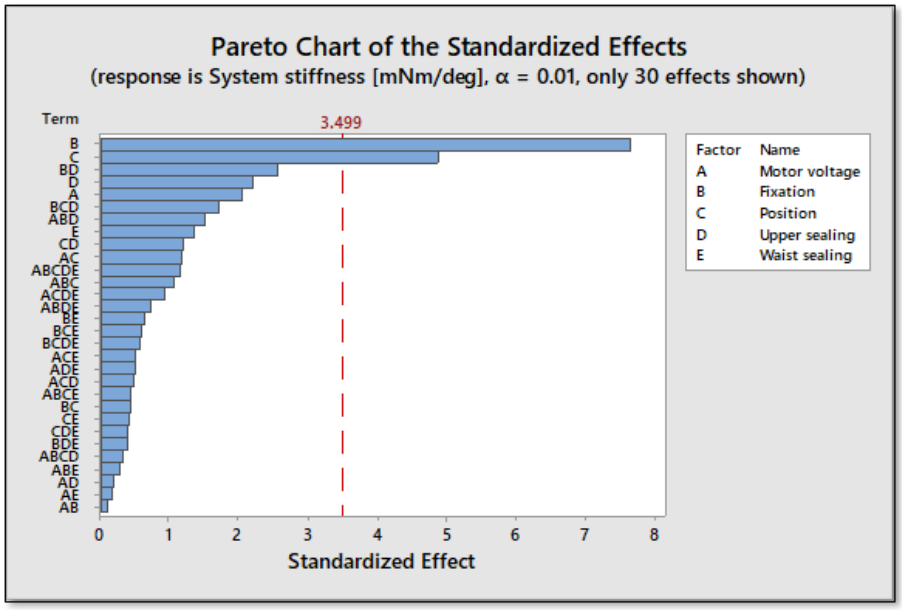

Source: Own elaboration

Pareto chart (Figure 24), which shows the absolute values of the standardized effects[1] from the largest effect to the smallest effect. The chart also plots a reference line to indicate which effects are statistically significant, based on the significance level α chosen for the experiment. If the error term has one or more degrees of freedom, the red line on the Pareto chart is drawn at t, where t is the $(1 - \frac{\alpha}{2})$ quantile of a t-distribution with degrees of freedom equal to the degrees of freedom for the error term. This value is taken from numeric methods or directly from a t-table.

The other chart is a half-normal plot of effects (Figure 25). This is a plot of the absolute value of the standardized effect estimates against their cumulative normal probabilities. The straight line that passes through the origin indicates the normal distribution, so data points above or near it represent effects not statistically significant. On the other hand, individual or interaction of effects that are further from the line and that have a P-value lower than α are labeled statistically significant on the graph.

Finally, it is also possible to visualize the individual and interaction of effects from each factor on the system responses. These graphs show how the outputs behave according to the change of levels on each input, by using the average response on each of the levels. The interaction plots are constructed the same way, but instead with the response varying according to the switch of two factor levels at the same time. They will be presented on the results chapter further on.

Figure 25 – Example of half-normal plot of effects

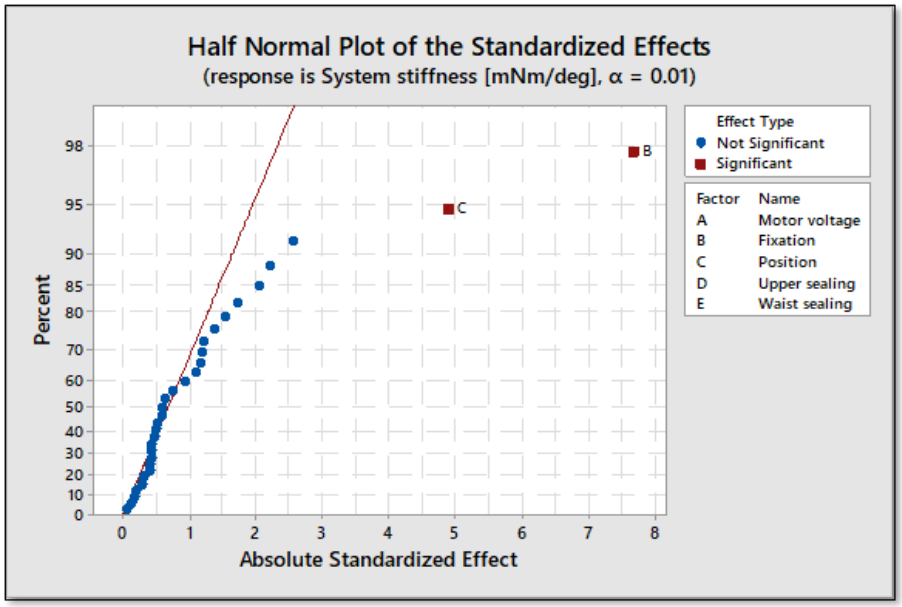

Source: Own elaboration

[1] Standardized values, or z-scores, are data points scaled by population/data size that test the null hypothesis that the effect is 0.

2.6.3.2 Linear Regression

Linear regression is an equation for estimating the conditional or expected value of a variable y, given the values of some other variable x and aiming to address a value that cannot be estimated initially. In linear regression, the relationships are modeled using linear predictor functions whose unknown model parameters are estimated from the data. Such models are called linear models (SEAL, 1967).

This type of regression most often uses the least squares estimation method that derives the equation by minimizing the sum of the squared residuals, or squared distances between the sample's data points and the values predicted by the equation. The resulting regression follows the linear model:

$$y = a + bx \tag{11}$$

where a and b are taken from the data:

$$a = \frac{(\sum y)(\sum x^2) - (\sum x)(\sum xy)}{n(\sum x^2) - (\sum x)^2} \quad \text{and} \quad b = \frac{n(\sum xy) - (\sum x)(\sum x)}{n(\sum x^2) - (\sum x)^2} \tag{12}$$

The two main metrics for model evaluation are the R-squared, coefficient of determination, and again the p-value. The R^2 is the proportion of the variance in the dependent variable that is predictable from the independent variable. In the above example's case, how much variance of y can be predicted from x. The R-squared value can be determined by:

$$R^2 = 1 - \frac{SS_{res}}{SS_{tot}} \tag{13}$$

where SS_{res} is the sum of squares of residuals and SS_{tot} the total sum of squares proportional to the variance of the data in relation to the mean. While what coefficient of determination is considered acceptable for a certain regression analysis varies between applications, for this project, considering all countless different variables that affect a WR system, including inherent differences between different samples (like two motors), a R^2 value limit of 0,5 will be adopted.

In the case of the P-value, it works similarly to the effect analysis. While a low P-value, below α, rejects the null hypothesis and indicates that the predictor value is related to the response, a high P-value means that changes in independent variable are not associated with changes in the dependent variable. All of this analysis is also done automatically via Minitab.

3 METHODOLOGY

Using the background explained by Chapter 2, this chapter aims to describe how the experiments analyzing the glass tilting were planned and executed throughout the project's timeline. Starting from the equipment setup, all sensors had to be calibrated and assembled onto the door systems analyzed. Then, three different DOE test matrices were constructed, each with a different objective, and the responses were registered into measurement files. Finally, all the required data was mined through scripts and then statistically analyzed via Minitab, generating the results that will be later shown on Chapter 4. All the algorithms, images and tables that were developed but are not vital for the conclusions and understanding of the project will be later presented at the end of the document, on the appendix and annex sections.

3.1 RESPONSE AND SIGNAL DEFINITION

In order to analyze the effects of the glass tilting generated by all the system factors, the comparison between measurement signals after the tests is the simplest way, plotting them against each other on the CANape screen. However, this method is only feasible for two or three signals each time because of the amount of different sensor data in them, making it best for individual cases and not to analyze an entire experiment matrix. Knowing this, it was necessary to define responses able to be compared between runs and experiments in a quantifiable way.

The first and most obvious way to analyze the tilting is measuring the glass displacement throughout the WR movement. While the optimal way would be measuring directly the rotational angle created on the slider, a simpler and more practical way was checking the window movement on the X-axis. For this, a potentiometric displacement sensor 8712-25, detailed at subsection 2.5.3, was fixed on the glass edge near the B-column of the front doors and measured the distance in millimeters [mm].

Since the motor is the most important component on the window regulator, its behavior during the tilting was an interesting place to continue the analysis. On preliminary experiments, when the glass started moving on the X-axis, besides its rotational speed a change on the rise of the blocking current was noticeable, meaning that its torque was also not increasing in a linear way (as already displayed on Figure 17, Chapter 2). Because of that, a torque sensor 5413-1200/20-S (see subsection 2.5.1) was chosen to be placed between the actuator and the window regulator, registering its mechanical effort through all window movement.

However, one problem arose: depending on the door setup, such as different supplying voltages, the glass traveled and blocked at different speeds. Because the torque of the motor was also affected by that, it was not possible to simply compare the difference in the blocking torque from different measurements, one to one, and a different approach was necessary. The

Figure 26 – Full stroke showing trapping event and area of interest

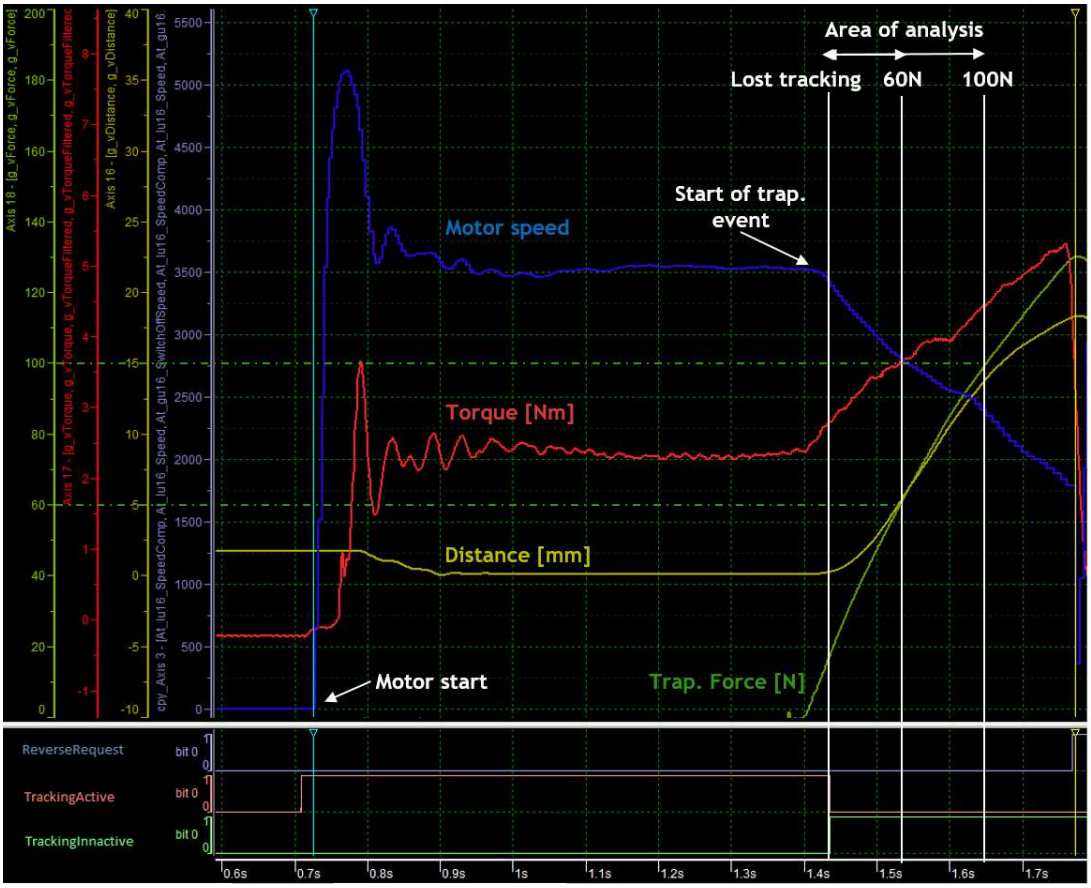

Source: Own elaboration

solution was using the position signal given by the WR electronic, normalizing the torque with the external gear rotation in a certain time range, thus creating the transmission or system stiffness seen by the motor, in millinewton-meter per degree [mN m/°]. This is akin to its rotational stiffness, in which the applied torque is proportional to the angular displacement of one side/end with respect to the other, and is calculated by:

$$u = \frac{\Delta M}{\frac{\Delta Pos \times 1{,}125°}{4}} \tag{14}$$

where M is the torque and Pos the position signal value. The value in degrees varies depending on the motor gear ratio, 1:80 in the case of the actuators studied in this project.

To define which regions of the stroke range should be measured, previous knowledge of the problem was critical. On most doors, the glass tilting occurs mainly from the start of the trapping event until the trapping force reaches a region between 40 N to 60 N. The start of the trapping was defined as the time the diff. speed signal crosses the tracking threshold and the switch-off signal freezes, as shown by the Figure 26. To normalize the responses, all the runs of a experiment take the same range of analysis for the system stiffness and the X-axis displacement. Also, the linear distance when the force gauge has a bigger value, around 80 N to 100 N, was also measured to check if the WR behaves the same through all the trapping event.

Summarizing, the responses outlined for analysis in this project are:

- System stiffness seen by the motor in [mN m/°]
- Glass tilting on the X-axis, between 40 N to 60 N, in [mm]
- Glass tilting on the X-axis, between 80 N to 100 N, in [mm]

3.2 SENSOR SETUP

In order to get the required responses with precision, the optimal placement and calibration of all sensors was fundamental. Not only mechanical and electronic adaptor for multiple sensors had to be developed, but their signals also had to be correctly transformed into physical units through mathematical conversions and offsets. The complete diagram with the hardware used on this project is displayed on Figure 27 and will be detailed on this section.

Starting with the displacement sensor, after clipping it to the window with a small metal adaptor, a rail at the door's B-column was necessary to guide the sensor tip through the movement. As shown on Figure 28a, a metal piece with the length of the window movement was placed and screwed on the door frame and aligned parallel with the WR direction, ensuring that the distance signal remained almost constant until the tilting. Besides measuring the position of the rail with a ruler, the signal was evaluated in multiple regions to get the maximum straightness through the course. However, since the doors fundamentally have different areas of friction, especially on the side rails and because of the inherent horizontal movement caused by the inverted pendulum dynamic, the window never travels exactly on a straight line. For this reason, the sensor was effectively normalized on the region right before the window starts the trapping event, so the displacement caused by the tilting is correctly taken.

For the torque sensor, several actions had to be taken. First off, a mechanical cage to

Figure 27 – Sensor diagram

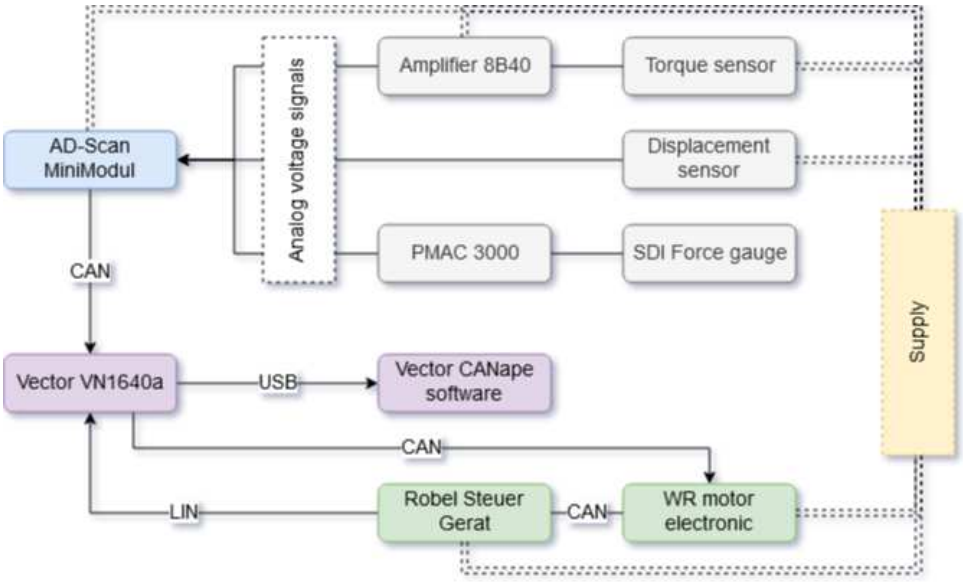

Source: Own elaboration

Figure 28 – Displacement and torque sensors set up

(a) Displacement sensor guided by a rail

(b) Torque sensor inside metal cage

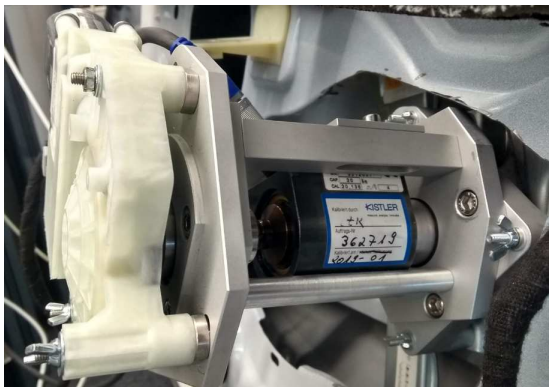

Source: Own elaboration

fix it between the motor, a BM2010 (also produced by Brose), and the WR cable-drum house was constructed by Brose's Test Department. It placed the sensor on the same axis of the gear and prevented it from rotating, as presented by Figure 28b; movement on the Y-axis was also prevented by making it tight and with little "game" for it to vibrate. Couplings were also used for the connections and fit the evaluated motor, also trying to minimize any gaps between the coupling internal gaps and the gear teeth.

Additionally, an amplifier had to be used, since the torque sensor has an output on the $10^{-3}V$ range and a bigger input was required for the AD converter. In this case, the 8B40 amplifier module was used, as it was available at the company during that time. The device amplified the signal by a 100 times and protected it from noise by isolating and filtering it with a low-pass band of 1 kHz. A connection adapter LEMO was used to access the signal wires for the amplifier, as well as a metal box was constructed to keep it protected. After checking some noise around 300 Hz on preliminary tests, this time a software low-pass filter was constructed via a CANape script, which will be presented further on this chapter.

The SDI force gauge, also connected to the PMAC 3000 processing device, at first was set up on the same way as the regular anti-trapping experiments are performed. With a clamping mechanism attached to the gauge, it was placed on the glass edge with its arm lever in perpendicular to the direction of movement and to the door frame. However, since one of the objectives of the project was also to analyze the differences on the placement of the SDI at the door frame instead, a new solution had to be developed. Even though one could hold the gauge directly at the frame by hand, a mechanical device was preferable to minimize vibrations and other human interference on the test results. A prototype, shown at Figure 29, was constructed with a replacement clamping mechanism: its lower part would get inside the frame sealing, preventing it from moving in the Y-axis, while the lever pushed against the frame at the top, effectively fixing the SDI. While improvements could be made to the

Figure 29 – SDI fixed on the door frame

Source: Own elaboration

attachment, inhibiting even more movement of the sensor, the prototype was reliable enough for the purposes of this project, having little to minimal interference on the responses.

After the sensors were set up, it was imperative to adjust configuration of the AD-Scan module, designed to convert all analog voltages into CAN signals that could be after interpreted by the Vector box. To establish the CAN connection, a bitrate of 100 kBit/s and message frame of 11-Bit (standard CAN) was preferred. For the sensor signals, the following conversions were used, according to their respective sensitivity factors:

- Torque: $Phys[Nm] = 2[Nm/V] \cdot Signal[V]$; excitation of ± 5 V.
- Trapping force: $Phys[N] = 10[N/V] \cdot Signal[V]$; excitation off (supplied by PMAC).
- Distance: $Phys[mm] = 6[mm/V] \cdot Signal[V] + Offset$, where the offset was calculated at the start of each experiment in order to zero the sensor's signal; excitation of ± 5 V.

For the analysis of the signals from the motor electronic Brose uses its own device, Robel Steuer Gerat, to interpret them. Its function is basically to adapt the bitrate of the received signals so they can be then interpreted by the LIN network set up by the CANape software.

Finally, all signals are received by the Vector VN1640a box through its CAN and LIN channels and sent for the CANape application via an USB cable. The box also has an individual CAN connection to the electronic so it's possible to change its parameters and calibration.

3.3 PLANNING AND PERFORMING THE DESIGN OF EXPERIMENTS

Once all the required responses were defined and the hardware for data collection set up, the experiment matrix was constructed according to factorial design of experiments structures. Three different stages of experimentation were established, according to the project objectives: factor screening, optimization and confirmation. Each phase will be detailed on the subsections below on how they were planned and performed. At the end, a final subsection describes how the regression analysis between the DOE responses was conducted.

3.3.1 Factor Screening

The factor screening is the phase to consider all the main aspects of the window regulator system that create or influence on the glass tilting phenomenon, finding the most statistically important ones. For easier and simpler classification of the factors, three groups were established: design factors, which will be changed between levels and analyzed; held-constant factors, which will be maintained the same throughout the experiment; nuisance factors, which can not be fully controlled in the setup and will be checked at the start and at the end to ensure their stability.

Table 1 – Factor screening factors

			Design factors			Held-constant factors		Nuisance factors	
Experiment stage	**Center point runs**	**N. of runs (2^k)+CP**	**Factor**	**Low**	**High**	**Factor**	**Value**	**Factor**	**Predicted range**
FACTOR SCREENING	8	40	Motor voltage	10V	16V	Glass position	≥50mm	Door temperature	20°C-25°C
			Gauge fixation	Glass	Frame	Time between measurements	≥5s	Motor temperature	20°C-30°C
			Gauge position	5cm	15cm	Electronic parameters	Adjusted		
			Upper sealing	without	with	Measuring equipment	SDI		
			Waist sealing	without	with	Door system	Renault Kadjar		
						WR design	Single-guided		
						Operator	Anderson		
						Door stability	Leveled		
						Motor profile	0.1Ω pre-resistance		

Using previous knowledge on the window tilting dynamic, five different factors were chosen as the ones that have the most impact overall (Table 1). First of all, the supply voltage changes the electric current and consequently the rotational speed of the motor gear, which can have an effect on how the speed signal re-accelerates during the glass displacement. Since most customer projects require that the WR behaves according to the specification on the 10 V to 16 V range, those were chosen as the high and low levels to be switched between.

According to Feyh (2019) and Petkun (2018), the placement of the SDI gauge is one of the main variables responsible for the rotation of the glass during trapping events. Through the study of the WR dynamics on several doors, Feyh established a critical zone in which the closer the sensor was to the A-column, the bigger the tilting. Also, when experimenting an alternative method, holding the sensor upside-down against the frame, instead of the fixing it on the window, the displacement of the glass lowered substantially. This is explained by two main reasons:

1. Like explained in the subsection 2.4.3, the friction between the SDI arm and the sealing rubber causes the trapping movement to create a second point of rotation in the system. When positioning the SDI against the frame, the metal arm now has contact with the glass instead, creating less friction and avoiding or lowering the rotation.
2. The weight of the SDI now does not have any impact on the window's center of mass. When fixed on the window, it dislocated the center of mass closer to the A-column,

contributing with the rotational momentum.

Under this pretext, the two variables were established as design factors of the DOE. Gauge position represents the distance of the SDI arm from the door's A-column; fixation means if it is placed against the glass or the door frame. Precautions were made so that the contact during the trapping would stay on the same geometrical point on either way of fixation: a straight line was drawn from the slider rotation spot to the measurement positions (5 and 15cm).

The two last factors to be analyzed were the upper and the waist sealing of the door. The first one interacts directly with the gauge, creating friction between it and the metal frame of the door. When the upper sealing is detached, the collision happens with the frame instead, which has significantly less resistance. The waist sealing, on the other hand, creates friction on the base of the glass, affecting the closing speed, which could also impact on the tilting.

Table 2 – Factor screening experiment matrix

StdOrder	RunOrder	CenterPt	Blocks	Motor voltage	Fixation	Position	Upper sealing	Waist sealing
36	1	0	1	13	Frame	10	With	Without
38	2	0	1	13	Frame	10	Without	With
13	3	1	1	10	Glass	15	With	Without
29	4	1	1	10	Glass	15	With	With
12	5	1	1	16	Frame	5	With	Without
14	6	1	1	16	Glass	15	With	Without
18	7	1	1	16	Glass	5	Without	With
32	8	1	1	16	Frame	15	With	With
34	9	0	1	13	Frame	10	Without	Without
37	10	0	1	13	Glass	10	Without	With
7	11	1	1	10	Frame	15	Without	Without
2	12	1	1	16	Glass	5	Without	Without
11	13	1	1	10	Frame	5	With	Without
28	14	1	1	16	Frame	5	With	With
23	15	1	1	10	Frame	15	Without	With
3	16	1	1	10	Frame	5	Without	Without
30	17	1	1	16	Glass	15	With	With
5	18	1	1	10	Glass	15	Without	Without
19	19	1	1	10	Frame	5	Without	With
27	20	1	1	10	Frame	5	With	With
6	21	1	1	16	Glass	15	Without	Without
21	22	1	1	10	Glass	15	Without	With
22	23	1	1	16	Glass	15	Without	With
4	24	1	1	16	Frame	5	Without	Without
9	25	1	1	10	Glass	5	With	Without
20	26	1	1	16	Frame	5	Without	With
25	27	1	1	10	Glass	5	With	With
26	28	1	1	16	Glass	5	With	With
17	29	1	1	10	Glass	5	Without	With
39	30	0	1	13	Glass	10	With	With
24	31	1	1	16	Frame	15	Without	With
16	32	1	1	16	Frame	15	With	Without
8	33	1	1	16	Frame	15	Without	Without
31	34	1	1	10	Frame	15	With	With
33	35	0	1	13	Glass	10	Without	Without
10	36	1	1	16	Glass	5	With	Without
1	37	1	1	10	Glass	5	Without	Without
15	38	1	1	10	Frame	15	With	Without
40	39	0	1	13	Frame	10	With	With
35	40	0	1	13	Glass	10	With	Without

Since a two-level full factorial design was applied for this DOE, the number of runs for a single replicate would be two to the power of five, resulting in 32 runs. Among the design factors, two of them are quantitative: motor voltage and gauge position. That is why a center point was established for both, halfway their ranges (10 cm and 13 V). As it was desired to

experiment the CPs also with the full range of the other three qualitative factors, eight (two to the power of three) more runs were added to the factor screening, totalling 40. Those CP runs were spread at the start, middle and end of the matrix after the randomization, as showed by Table 2. Also, each run was repeated three times on each measurement to lower the effects of any noise that may affect them.

To guarantee the stability of the tests, some other factors had to be held constant. In order to eliminate the effect of the acceleration phase of the motor when the window starts closing (which also generates speed oscillations), a minimum distance of 5 cm was established. This ensured the motor to be with an almost constant speed when the trapping of the SDI started.

One problem that could impact the results is the temperature of the motor. As the tests start being performed, the friction of the internal brushes would start heating the system up, changing the motor performance curve and its profile. Hence, a rest time of at least 5 s between the three measurements of each run was established (time between runs would already take longer because of the change on the setup caused by the randomization). Also, a small electric fan was placed right next to the motor armature through all the procedures.

So the window would reverse only after 100 N on all situations, allowing an analysis of all the area of operation, the electronic parameters of the WR were adjusted from the release version accordingly. Other functions, such as different compensations that could affect the tests and create differences between runs, were also turned off.

Other factors that were held consistent: the SDI as the measuring device, the Renault Kadjar driver's door, the single-guided WR, the author as the only operator, the stability of the doors and setup and finally the cable pre-resistance for the motor, at $0{,}1\,\Omega$. While the test environment was controlled by the building's air conditioning system, an ideal and stable temperature was not guaranteed and, because of that, it was checked throughout the experiment. During this and the next stages, however, the temperature remained on the 23 °C to 24 °C range, not generating any adverse effects on the results.

With the matrix constructed, the individuals runs were randomized with the Minitab DOE tool and conducted on the order displayed by Table 2. Each test began with the window resting in a middle position, with the sensors all set up and with the CANape software recording. Then, the motor switch was pressed on automatic mode and the window started closing, until the gauge hit the sealing or the glass, creating the glass tilting. After reaching a force beyond 100 N, the window reversed and went down to the starting position. As mentioned before, this was repeated three times, back-to-back, at each setup on the same measurement file, which was saved on .mdf format. Finally, the setup was renormalized before the following run: quantitative factors were switched to their CPs and qualitative factors were reset (i.e. even between two runs with the gauge on the glass and on the same position, it would be reattached anyway), guaranteeing the principle of independence between tests.

3.3.2 Optimization

After conducting the factor screening tests and checking the results, which will be discussed on the next chapter, the optimization stage was planned to examine alternatives to reduce the glass tilting dynamic, considering all the system variables effects (Table 3). Since they were the main inputs after the factor screening, the gauge position and fixation will be analyzed again, in a new DOE matrix.

Table 3 – Optimization factors

			Design factors			Held-constant factors		Nuisance factors	
Experiment stage	**Center point runs**	**N. of runs (2^k)+CP**	**Factor**	**Low**	**High**	**Factor**	**Value**	**Factor**	**Predicted range**
OPTIMIZATION	6	22	Gauge fixation	Glass	Frame	Glass position	≥50mm	Door temperature	20°C-25°C
			Gauge position	5cm	15cm	Time between measurements	≥5s	Motor temperature	20°C-30°C
			Tape on SDI arm	Without	With	Electronic parameters	Adjusted for project		
			SDI Roller	Wihtout	With	Measuring equipment	SDI		
						Door system	Renault Kadjar		
						WR design	Single-guided		
						Operator	Anderson		
						Door stability	Leveled		
						Motor voltage	13V		
						Waist sealing	with		
						Upper sealing	with		
						Motor profile	0.1Ω pre-resistance		

While the SDI on the door frame setup was shown as a viable option to optimize the trapping force measurements and approximate them to real-life conditions, the collision of its metal arm on the glass raised concerns about the damage it could do to after continuous runs. Thinking of way to envelop the arm on a different material to reduce the risk of any break, a polyester cloth tape from Cloroplast, model 838X, was chosen (Figure 30a).

Figure 30 – Attachments to the SDI arm

(a) SDI arm with tape on contact point

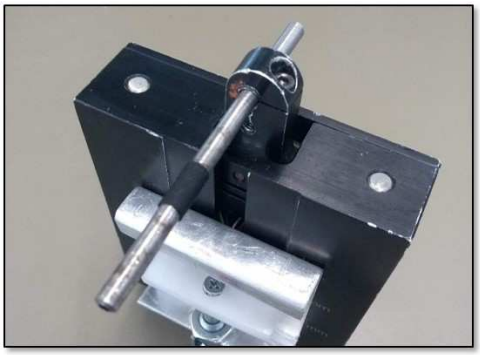

(b) SDI with roller

Source: Own elaboration

Originally, the tape was designed for automotive application of wire harnesses binding, presenting increased abrasion resistance and a expansive temperature range of $-40\,^{\circ}\mathrm{C}$ to $150\,^{\circ}\mathrm{C}$. This was specifically important in order to be resistant to the climate chamber conditions it

Table 4 – Optimization experiment matrix

StdOrder	RunOrder	CenterPt	Blocks	Fixation	Position	Tape	Roller
24	1	0	1	Frame	10	With	With
23	2	0	1	Glass	10	With	With
15	3	1	1	Glass	15	With	With
10	4	1	1	Frame	5	Without	With
13	5	1	1	Glass	5	With	With
1	6	1	1	Glass	5	Without	Without
12	7	1	1	Frame	15	Without	With
17	8	0	1	Glass	10	Without	Without
4	9	1	1	Frame	15	Without	Without
7	10	1	1	Glass	15	With	Without
9	11	1	1	Glass	5	Without	With
2	12	1	1	Frame	5	Without	Without
11	13	1	1	Glass	15	Without	With
20	14	0	1	Frame	10	With	Without
5	15	1	1	Glass	5	With	Without
14	16	1	1	Frame	5	With	With
16	17	1	1	Frame	15	With	With
6	18	1	1	Frame	5	With	Without
3	19	1	1	Glass	15	Without	Without
8	20	1	1	Frame	15	With	Without
18	21	0	1	Frame	10	Without	Without
19	22	0	1	Glass	10	With	Without

could go through during future product development. The tape was then included on this stage to check if it has any significant impact on changing the friction of contact, especially when the gauge is placed on the frame.

Also, a roller device was available for attachment on the SDI arm (Figure 30b). It functions as a way to avoid the locking that happens when the sensor pushes into the rubber, lowering the friction on the point of contact and allowing the gauge to slide through the upper seal. In order to again avoid the impact on the glass during frame fixation setups, there were runs with both the roller and the tape covering it.

Similarly to the factor screening phase, the optimization matrix was also randomized to avoid the propagation of errors (Table 4). All the procedures were done as before, especially the renormalization between runs. Also, the held-constant factors remained the same, including now the voltage, fixed at 13 V and the presence of the upper and waist seal, as they were not statistically significant on the results.

3.3.3 Confirmation

All the tests so far were conducted on a single system, the Kadjar's driver door. While the results were satisfying and confirmed the initial thesis that the change of placement of the trapping force gauge was a reliable way to reduce the glass tilting effect, those results still do not mean they can be generally accepted for other different projects. Under this pretext,

a different door, with a different geometry and window regulator, was chosen to confirm the conclusions taken for the Renault Kadjar: a new project development, under the codename Renault LJL.

This door, also on the driver's side, had already gone through initial tests and presented too a glass tilting behaviour, even though it was smaller than the Kadjar's. The actuator used on this project, a WR19 family motor from Mitsuba Corporation, was similar to the BM2010 regarding its gearwheel ratio and fixation points, so the cage adaptor for the torque sensor could still be used. With some mechanical adaptions on the door, the displacement sensor, with its guiding rail, and the frame fixation device for the SDI could also be applied on the experiments. Since the electronic was different from the one already tested, the parameters had to be analyzed again and adjusted for the good performance of the tests.

Table 5 – Confirmation factors

			Design factors			Held-constant factors		Nuisance factors	
Experiment stage	**Center point runs**	**N. of runs (2^k)+CP**	**Factor**	**Low**	**High**	**Factor**	**Value**	**Factor**	**Predicted range**
CONFIRMATION	8	40	Motor voltage	10V	16V	Glass position	≥50mm	Door temperature	20°C-25°C
			Gauge fixation	Glass	Frame	Time between measurements	≥5s	Motor temperature	20°C-30°C
			Gauge position	5cm	15cm	Electronic parameters	Adjusted		
			Upper sealing	without	with	Measuring equipment	SDI		
			Waist sealing	without	with	Door system	Renault LJL		
						WR design	Single-guided		
						Operator	Anderson		
						Door stability	Leveled		
						Motor profile	0.1Ω pre-resistance		

Every factor remained the same from the first DOE stage, ensuring that the results from one door could be translated and compared with the other (Table 5). All the general procedures from the past experiments were followed again. The experiment matrix for this phase will be available as an appendix at the end of this document.

The only difference came in the form of how the resulting signals were analyzed. The LJL door was difficult system to get really high trapping forces (above 100 N) on all setups for the analysis of the whole spectrum, especially because of its lower tilting effect. Also, when the tilting occurred, it ended earlier that the Kadjar door, restricting the area of interest. For this reason, the limits to calculate the system stiffness and distance were switched from 60 N and 100 N to 40 N and 80 N on the confirmation stage.

Finally, because of time constraints, only a brief check of the alternatives tested on the optimization stage were repeated for the Renault LJL, mainly with the roller attachment.

3.3.4 Regression Analysis

An investigation on the correlation between the system responses, stiffness seen by the motor and glass tilting distance, was also planned for the project. This could provide some basis to understand more of the glass tilting problem, showing what type of direct effect the

rotation of the glass has on the energy transferred to the motor and, consequently, how the electronic will behave while monitoring its rotational speed.

On account of that, a regression model was performed on the results after the effect analysis from the DOE factors of each stage. The Minitab was again used for that, showing which model would fit the responses better statistically.

3.4 SIMULATION AND DATA ANALYSIS

Once all three DOE stages were done, the result was a total of 102 measurement files, with three recorded window strokes each. With this amount of data, evaluating them individually and gathering the required responses for the statistical analysis would consume too much time and be susceptible to errors. For this reason, an automated way to run all the measurement signals was desired.

While the main objective of the CANape software is setting up the communication with automotive devices through CAN and LIN networks, sending and receiving messages, it offers a programming language, CASL (Calculation and Scripting Language), and its own editor for writing cross-device scripts and functions. The CASL shares a lot of similarities with the C programming language, like syntactical structures and variable types, making it easier to use to it. The main support material for writing the code blocks was the user manual from Vector Informatik GmbH (2015), which present definitions and also usage examples for all the different features on the CANape environment. While the most important parts of the code will be displayed on this section, others will be added at the end of the document as appendix.

First off, Brose has already been using some scripts to help on the electronic development process, not only for WRs but also other devices. When measurements are done on climate chambers and on the test field of customers, usually the time is too short to analyze the signals, adjust all the parameters that operate the actuator and check the results of the changes. A simulation tool was then developed to recalculate the measurement signals under the different parameters, taking into account how the system performed on the environment and at the time of the experiment. This is especially done for checking and altering the limiting offsets that achieve the correct point of window reversal on all situations. Using this tool as basis, functions were developed to cut the data and calculate the required responses for this project. A GIT repository was also used with version control, for a more secure development and easier switch between CANape configurations of different vehicles (Kadjar and LJL), since the configurations used when measuring the trapping events were different from the ones that are used for the simulation.

A special panel was created on the CANape environment, Figure 31, in order to control all the simulation process, and had several inputs: a text file in which the user specifies the path of all the measurement files to be simulated, the parameter set for the electronic to be used, the destiny folder for all the simulated files and the report, and finally a counter to switch between multiple types of reports, useful for future applications. At the bottom, a

Figure 31 – Panel for simulating multiple files

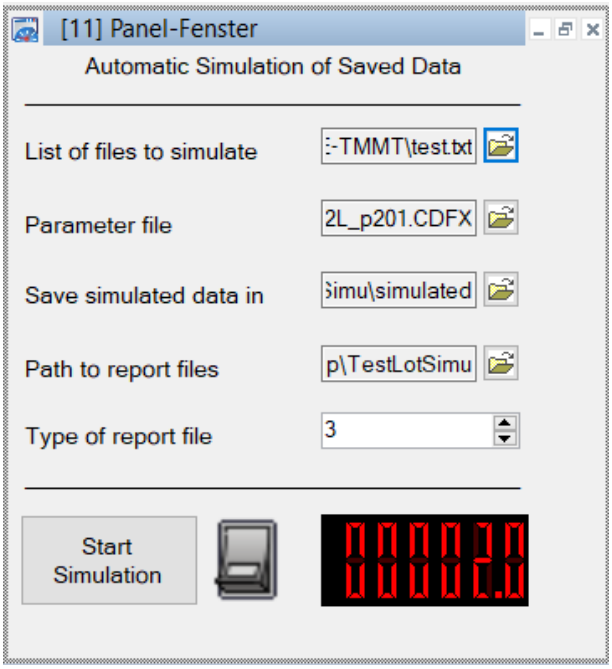

Source: Own elaboration

switch controls the start of the simulation while the counter shows which file is currently being reproduced.

At the start of the simulation, while the process of recreating the WR signals on the simulation was already implemented, the sensor signals used a different sample rate. Because of that, the samples of each signal needed to be synchronized, so the points in which the responses were calculated were at the same time. This was done calling a Main function at every clock of the electronic and calculating all the sensor values at that time through an interpolation. The following code, Listing 1, shows a part of the script that treated the torque signal, using some functions already implemented on the CANape environment and the position signal from the WR electronic as reference. This was also done for the distance and force signals.

```
1  int l_iteratorMode = 1; // Iterator Modus, 0 -> index synchron., 1 -> time synchron.
2
3  //Getting the torque signal from its name if the file contains a torque signal
4  SIMAPE_STIM.GetVariableByName(l_signal_Torque, l_signalNameTorque);
5
6  // Creation of the interpolation for the torque measurement
7  l_interp_handle = SignalValueIteratorOpen(l_iteratorMode)
8
9  if (l_interp_handle == 0){
10             // The inerpolation failed
11             l_bool_itFailure = 1;
12
13             Write("The interpolation of the torque measurement failed, check the
                ↪  iterator modus.");
14     }
15 else{
16     l_bool_itFailure = SignalValueIteratorAdd(l_interp_handlel_signal_Torque)
17
18     if (l_bool_itFailure != 0){
19         // The interpolation failed
20         l_bool_itFailure = 1;
21
```

```
22          Write("The interpolation of the torque measurement failed. Check the function
             ↪  SignalValueIteratorAdd.");
23      }
24
25  l_posTimeBuffer = time(); // Interpolation using the last time information(actual one
     ↪  because the position signal should be simulated before the execution of this
     ↪  function)
26
27  l_bool_itFailure = SignalValueIteratorSeek(l_interp_handle, l_posTimeBuffer);
```

Listing 1 – Snip of the interpolation code for the torque signal

The acquired torque signal, however, showed a significant noise at the 300 Hz range, passing through the amplifier's filter, and could potentially interfere in data acquisition for the system stiffness. Under this pretext, a low-pass filter of first order was built after the interpolation of the signal, using a nested function. Knowing that the transfer function of this type of filter is:

$$\frac{Y(s)}{U(s)} = \frac{w_c}{s + w_c} \tag{15}$$

yielding, for a T_s sampling period,

$$y[k] = \frac{w_c T_s}{1 + w_c T_s} u[k] + \frac{1}{1 + w_c T_s} y[k-1]$$

or

$$y[k] = \alpha u[k] + (1 - \alpha) y[k-1] \tag{16}$$

where w_c is the cutoff angular frequency in [rad/s]. It was then adapted for the application and successfully eliminated the noise from the data. To avoid delaying the filtered torque signal from the others, an offset corrected it before the data acquisition process.

With the data properly synchronized, first was necessary to extract the three strokes from each recorded file. One of the signals sent by electronic on every message is the MotorState, a binary value informing the current polarity of the actuator. Using this as reference, one reversal cycle was defined as:

Motor Stopped → Up Direction → Down Direction (without transition) → Motor Stopped

at the beginning of each cycle, a global counter *g_SimuLotData_ReversalCycle* was updated. The script checked it on each iteration, saving on a timestamp array the moment it increased; this would be used later to snip the files.

Timestamps were also used to identify where the system stiffness and distance measure points were to be taken. After the start of reversal cycle was acknowledged by the simulation, the script continuously checked the speed and force signals to acquire the responses: the start of the range from when the TrackingInnactive flag went to high, meaning that the trapping event was starting, until the force reached 60 N and 100 N. With those three, it meant five important timestamps/moments for each stroke:

Figure 32 – Example of a report file generated by the script

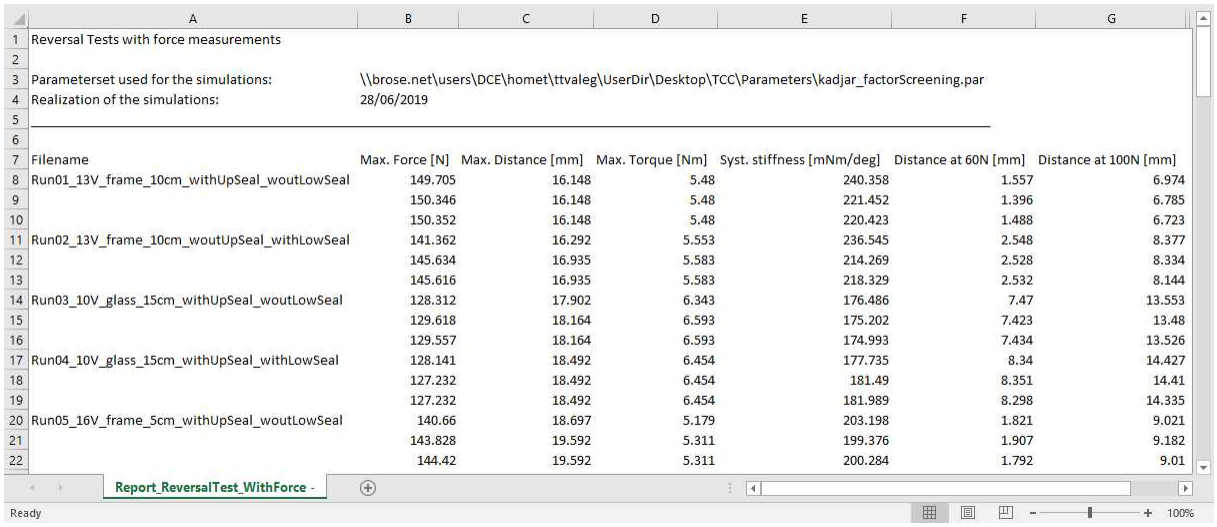

	A	B	C	D	E	F	G
1	Reversal Tests with force measurements						
2							
3	Parameterset used for the simulations:	\\brose.net\users\DCE\homet\ttvaleg\UserDir\Desktop\TCC\Parameters\kadjar_factorScreening.par					
4	Realization of the simulations:	28/06/2019					
5							
6							
7	Filename	Max. Force [N]	Max. Distance [mm]	Max. Torque [Nm]	Syst. stiffness [mNm/deg]	Distance at 60N [mm]	Distance at 100N [mm]
8	Run01_13V_frame_10cm_withUpSeal_woutLowSeal	149.705	16.148	5.48	240.358	1.557	6.974
9		150.346	16.148	5.48	221.452	1.396	6.785
10		150.352	16.148	5.48	220.423	1.488	6.723
11	Run02_13V_frame_10cm_woutUpSeal_withLowSeal	141.362	16.292	5.553	236.545	2.548	8.377
12		145.634	16.935	5.583	214.269	2.528	8.334
13		145.616	16.935	5.583	218.329	2.532	8.144
14	Run03_10V_glass_15cm_withUpSeal_woutLowSeal	128.312	17.902	6.343	176.486	7.47	13.553
15		129.618	18.164	6.593	175.202	7.423	13.48
16		129.557	18.164	6.593	174.993	7.434	13.526
17	Run04_10V_glass_15cm_withUpSeal_withLowSeal	128.141	18.492	6.454	177.735	8.34	14.427
18		127.232	18.492	6.454	181.49	8.351	14.41
19		127.232	18.492	6.454	181.989	8.298	14.335
20	Run05_16V_frame_5cm_withUpSeal_woutLowSeal	140.66	18.697	5.179	203.198	1.821	9.021
21		143.828	19.592	5.311	199.376	1.907	9.182
22		144.42	19.592	5.311	200.284	1.792	9.01

Source: Own elaboration

1. Reversal cycle starting point
2. TrackingInnactive flag switch from LOW to HIGH
3. SDI force value of 60 N
4. SDI force value of 100 N
5. Reversal cycle ending point

Using the saved torque and position values, the system stiffness was calculated via the Equation 14, while the total displacement was taken by the difference between the start and finish distance values. Also, the program snipped the files on those same ranges and saved only the Position and Speed signals, which would be used on an acceleration analysis later on the project.

When each file finished simulating, the responses were saved on a CSV report file taht could be opened on Excel, as exemplified by Figure 32. After taking the average values for the three responses on each run, the values were then exported to the Minitab spreadsheet, for the DOE analysis. The process on the Minitab software was pretty straightforward: once all the DOE responses were in place, the application calculated all the required factor effects, their p-values and other statistical data, plotting all the corresponding graphs for each response, which will be presented on the next chapter. The linear regression was also done via the software, selecting the response columns and choosing the desired level of confidence.

3.4.1 ATP Tool Analysis

Instead of using the CANape analysis window as usual, an easier approach to compare multiple measurement files at the same time is using the ATP Tool, an application developed by Brose for the parameter development of WR electronics. First, the tool needs a ASCII file with two data arrays, one containing the motor glass position and the other the motor speed

during a test run. Using other information inputted by the user, such as the motor gear ratio, it plots the maximum speed modulation (in rpm) of a certain region of the glass course against angle widths of the motor gear rotation. Among other functions, this one is mostly used to check for the presence of speed modulations caused by motor gear deformations, changes on the friction of the glass and others that can lead the electronic to interpret a false trapping event.

In the context of this project, the tool can graphically show which measurements do not have a constant speed drop, from when the SDI is trapped by the window until the end of the defined area of analysis (60 N and 100 N for the Kadjar; 40 N and 80 N for the LJL). For this reason, as mentioned on the section above, all files were also snipped between the chosen timestamps and converted into ASCII files containing only the Position and Speed signals. The ones of interest were then loaded on the ATP Tool for analysis.

4 RESULTS

Reviewing back the problem being studied, the glass tilting effect has a significant impact on the WR behaviour, especially on the transmission of torque from the actuator to the rest of the device. While the glass moves on the x-axis, a shift on the system stiffness seem by the motor translates into a direct change of its rotational acceleration and a consequent increase of total anti-trap forces. The two main responses derived from this situation, system stiffness and glass tilting in 60 and 100 N, are the main results shown in this chapter.

After collecting the data for each DOE through the processes explained on Chapter 3, all the measurements were simulated and snipped on CANape by the developed scripts, at the end generating a report value with all the required and other reference responses.

The three phases of the DOE plan will be presented in the proper order, initiating with the Factor Screening (4.1), followed by Optimization (4.2) and finally Confirmation (4.3). In each section, first an analysis of the main factors and the interactions between them will be done by plotting the standardized values on Pareto charts and half-normal plots, displaying which of them are statistically significant or not in the context of the experiment. Right after, the factors will be evaluated on their solo effects and also the interaction between each of them on a 2-way basis, taking their absolute values for easier comparison. Finally, a study on the correlation between the system stiffness and the glass tilting throughout the DOE will be displayed on by the response regression (4.4).

4.1 FACTOR SCREENING RESULTS

Figure 33 – Effects significance associated with system stiffness on the Renault Kadjar

(a) Statistical significance through Pareto chart (b) Statistical significance through half-normal plot

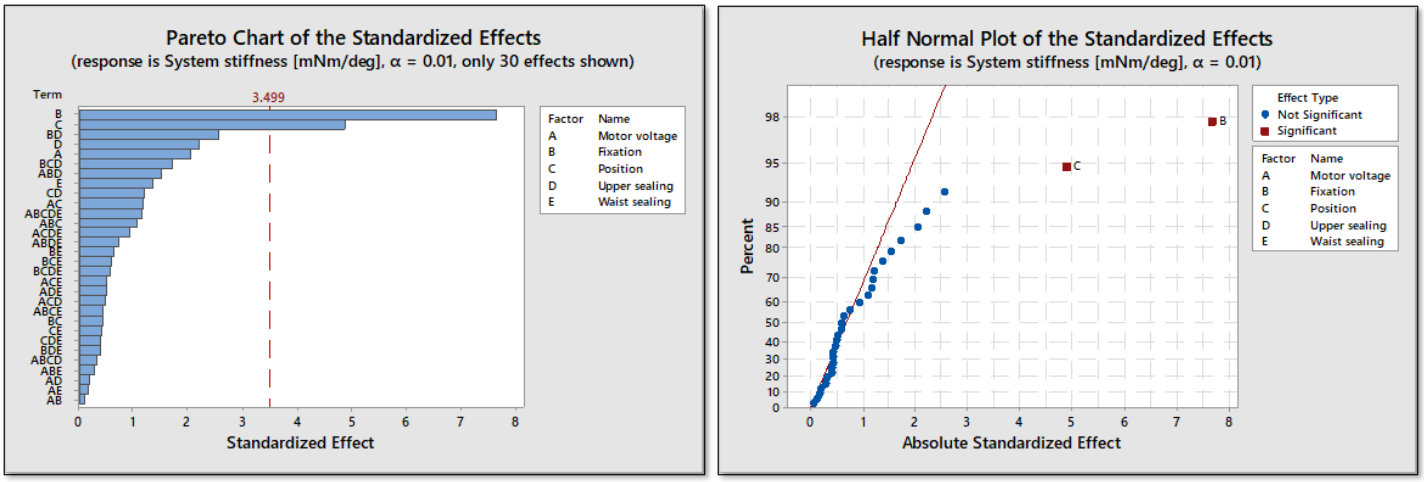

Source: Own elaboration

The aim of this first stage is to study all the factors that compose the window regulator operation on the Renault Kadjar driver door. Based on knowledge from past projects and preliminary studies, five main factors were identified and tested. Both for this stage and the following ones, the hour and ambient temperature from the start to the end of the tests were recorded, ensuring as less system variability as possible.

Figure 34 – Plotted effects regarding system stiffness on the Renault Kadjar

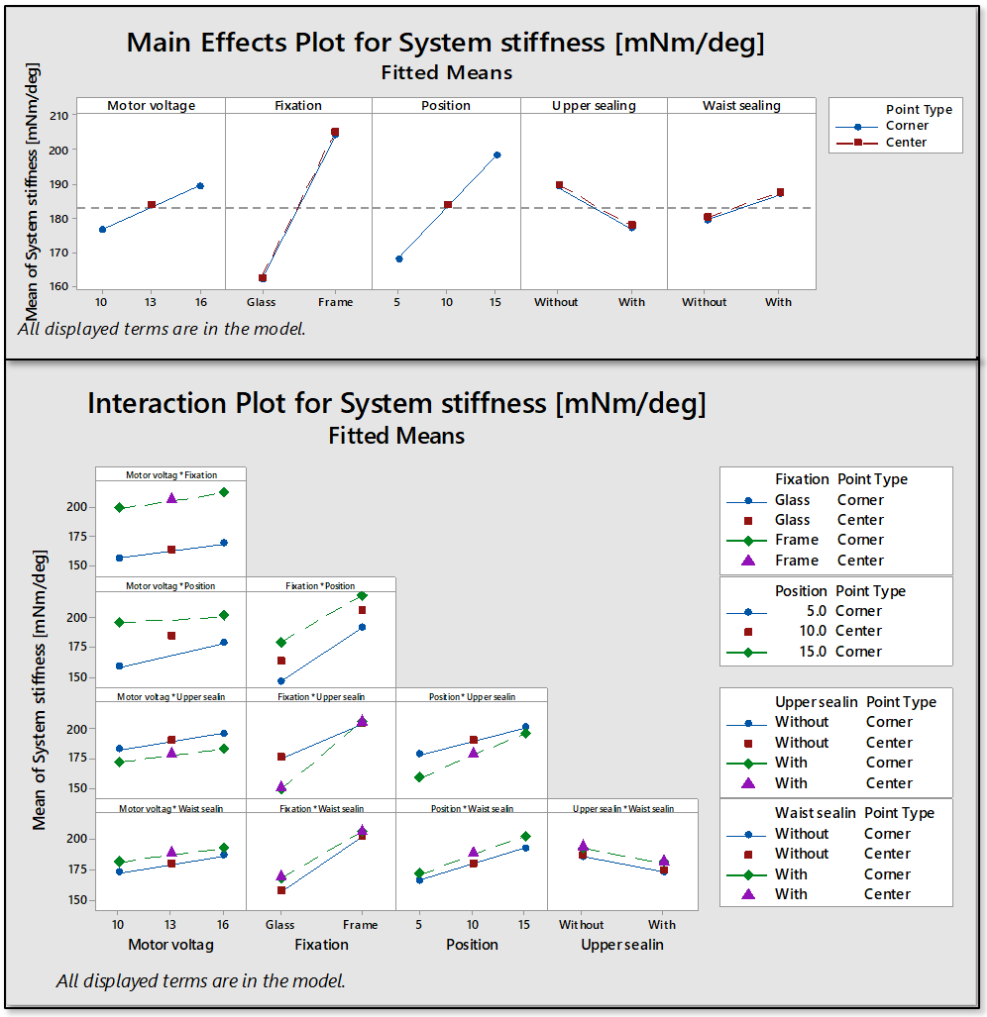

Source: Own elaboration

Figure 33 show how all the factors tested have an impact on the system stiffness worked by the motor during an AT event. Both representations confirm that the statistically significant elements, under a confidence level of 0.01, are, in order: fixation place of the SDI (p-value < 0.001), either on the frame or the glass, and its position in relation to the door's A-column (p-value of 0.002). Other effects, below the limit line of 3.499 on the Pareto chart and away from the normal distribution on the half-normal plot, aren't statistically significant for this response. While this outcome was expected, from the early studies done on the glass tilting subject, it's now possible to properly compare how big is the impact in relation to the other system factors.

Shown on Figure 34 are the individual and interaction effects of each variable. The center points depicted for discrete/text factors are from runs in which the continuous ones (motor voltage and position of SDI) were at their respective middle point; since they have bigger sample sizes, throughout all sections, the corner point means will be considered.

One of the main takeaways comes from the fixation plot, where the system stiffness has the biggest variation between levels, raising from a mean of 161,76 mN m/° to 204,95 mN m/°. It means that, maintaining all the other evaluated factors constant, changing the fixation of the SDI from the glass to the frame raises the stiffness seem by the motor on an average of 43,19 mN m/°, a 26.7% increase.

Figure 35 – Comparison between fixation levels during Factor Screening

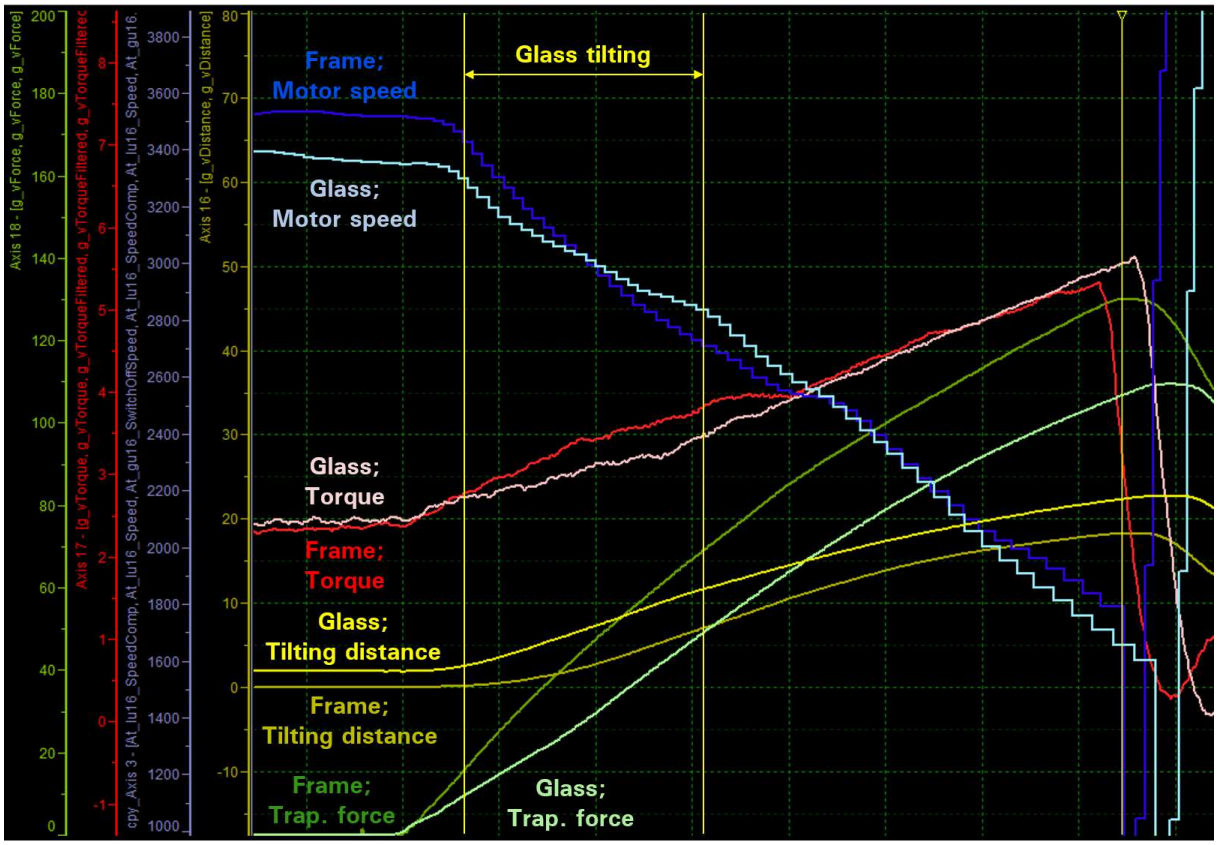

Source: Own elaboration

Figure 35 shows a detailed signal analysis from two configurations, A and B, in which the only different factor level is the fixation point: A with the SDI on the glass, represented by the lighter colors, and B with the SDI on the frame, represented by the darker colors. At the start of the image, there's already a difference between the speed signals, A having bigger values since the window is travelling without the gauge attached and with less total weight. From the point the obstacle starts blocking the movement, there are two different behaviors. Configuration A's speed starts decreasing in a steep way, maintaining this deceleration almost linear until the force reaches around 100 N; configuration B's speed, however, starts with a smaller deceleration until the force reaches around 50 N, that's where the glass tilting effect

mainly occurs.

As explained on chapter 2, when in contact with the rubber from the sealing, the friction makes the SDI lever arm "lock in place", generating the window movement on the X-axis. With the gauge attached to the frame, the friction at the start of the trapping is much lower, between metal and glass, making them slide among each other. Impact of this friction element can also be seen on the upper sealing analysis, presented on Appendix C as Figure 55. The absence of additional weight near the front column, changing the center of gravity of the window, also helps at minimizing its movement.

While the glass is rotating around the slider, the trapping force is not being directly transferred to the WRD, decreasing its rotational speed, but the pressure on the contact point continues increasing steadily. This can also be seen on the torque given by the actuator: in this region, the stiffness seem by B is lower, so the motor generates less mechanical power/torque to the system. The distance sensor also shows the bigger displacement occurring on the B setup, with a movement of 12 mm at the end of the main section of the glass tilting. This effect will be better shown in Figure 36. By the time the main tilting movement ends on B, the trapping force is high enough to overcome the static friction between gauge and sealing, allowing them to start sliding and decreasing the window rotation rate, also increasing the stiffness seem by the motor.

Looking at the force sensors, it could be interpreted that the maximum force generated by B is lower than A, but it's important to remember that the switch-off values for the experiment are set intentionally higher, in order to evaluate all the spectrum permitted by the legislation (i.a. until 100 N) in every measurement run. If the electronic parameters were set to limit these forces, the A setup would reverse much earlier than B because of the bigger motor deceleration, thus having a lower trapping force overall.

Regarding the other factors from Figure 34, approaching the gauge from 15 cm to 5 cm lowers the stiffness by 30,25 mN m/°, 18% less than originally. This change moves the rotation point around the SDI arm away from the WR's direction of movement, allowing the glass to move more horizontally. Motor voltage, upper and waist sealing follow with absolute effects of 12,69 mN m/°, 12,22 mN m/° and 7,58 mN m/° respectively. The center point measurements aligned right in the middle show that the behavior of the factors in this region of the window is linear. This also means the configuration was consistent throughout the experiments.

On the interaction plot, most factors combined with the fixation point have little effect compared to the main chart, except for one. When combined with the presence of the upper sealing, the difference is noticeable: if the gauge is on the frame, the sealing has no effect, as expected. Other combinations are mostly shown as parallel lines as they don't have a big statistical significance (all p-values above 0.01).

Next, Figure 36 represents all the factors in regards to the glass tilting until 60 N. Once again, the biggest outcomes are related to the arrangement of the measuring gauge, its fixation and position, with both p-values below 0.001. However, this time the presence of the

Figure 36 – Effects significance associated with glass tilting at 60N on the Renault Kadjar

(a) Statistical significance through Pareto chart (b) Statistical significance through half-normal plot

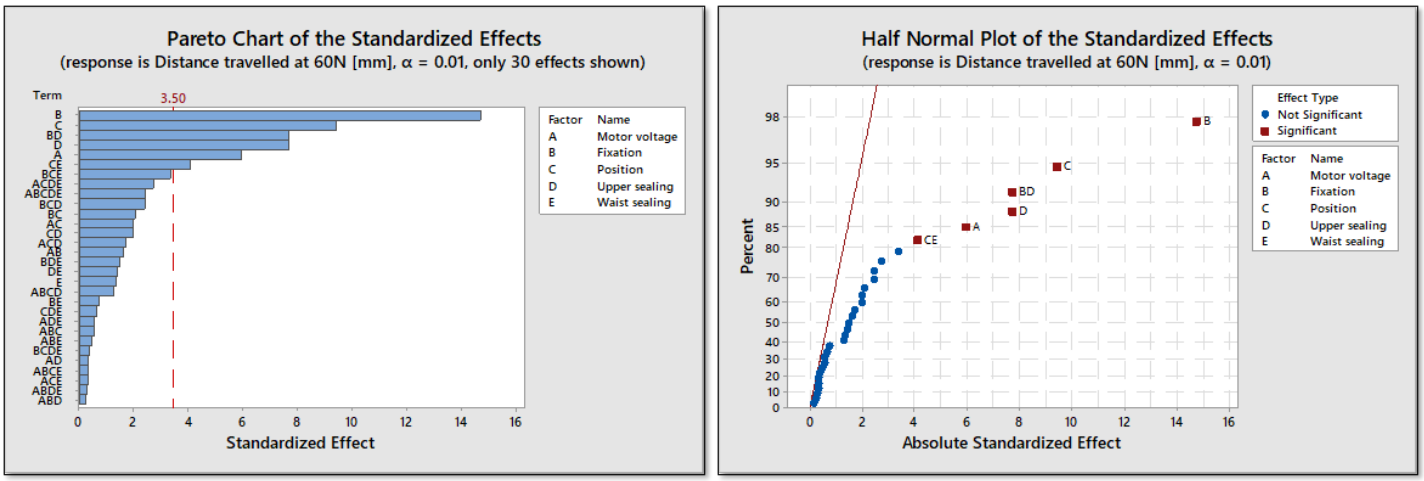

Source: Own elaboration

Figure 37 – Plotted effects regarding glass tilting at 60N on the Renault Kadjar

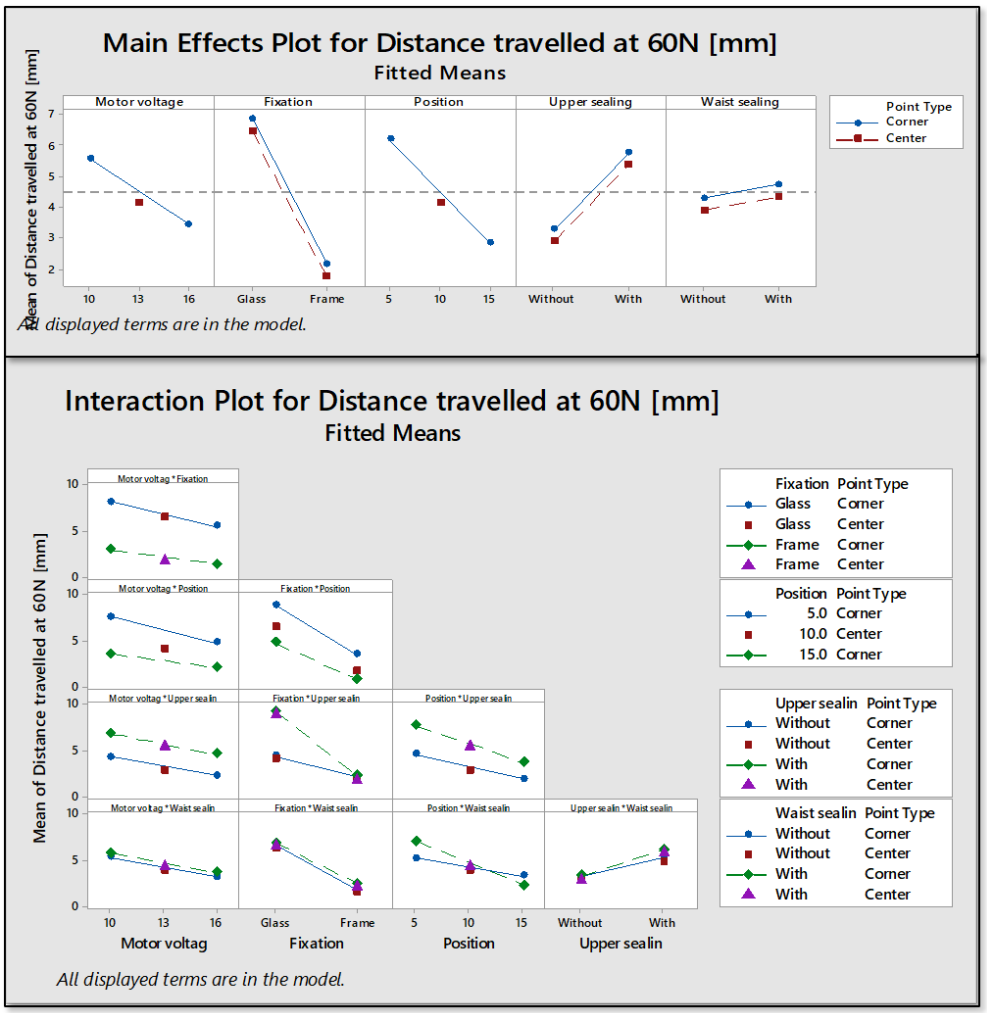

Source: Own elaboration

upper sealing also has a significant repercussion, both by itself and also in combination with the B factor [1], and also the motor voltage (p-values below or equal to 0.001).

When looking at the B factor on Figure 37, just making the measurement from the frame reference instead from the window reduces the glass tilting on an average of 4,69 mm, the most considerable difference. While increasing the motor voltage and distancing the SDI from the A-column also decrease the movement in 2,13 mm and 3,36 mm, the presence of the sealing is detrimental to the system in about 2,46 mm. Again, the impact of the gauge placement is clearly seem.

One particular interaction is between the gauge position and the waist sealing of the door. Having the rubber as means to increase friction on the up-movement while measuring close to the window limit raises the tilting, but keeping it on a 15 cm run can lower the effect. Regarding the most statistically significant effects, the best combination to keep the tilting minimum is conducting the run on the door frame and farthest from the A-column, with an average value of 0,85 mm.

Finally, Figures 38 and 39 show the analysis done from the point the speed leaves the tracking threshold until the trapping force reaches 100 N. Between the factors, this time the SDI position appears as the most statistically significant, accompanied by the fixation point. The former has an impact average of 6,92 mm, while the latter generates a difference of 5,22 mm. This happens because, as the range analyzed is longer this time, the effect of the bigger rate of tilting during the start of the movement, caused by the friction between gauge and sealing, is surpassed by the longer overall rotation the 5 cm allows.

Onto the other factors, motor voltage and upper sealing have very similar effects, 3,03 mm and 3,02 mm respectively, and like the previous situations, the presence of the waist sealing has the least impact of all, with an effect of only 0,02 mm. Most interactions don't have a high relevance, as noticed again by the parallel lines between levels.

Overall, the results of this DOE stage support the argument that the measuring equipment is the main responsible for the glass tilting and its consequent effects. Both the difference in stiffness and in tilting distance until 60 N and 100 N show that changing the measuring method has the best impact on the anti-trap algorithm for the Renault Kadjar driver's door.

[1] Again, D and BD have a similar effect because the presence or not of the sealing while fixing the SDI on the frame is irrelevant.

Figure 38 – Effects significance associated with glass tilting at 100N on the Renault Kadjar

(a) Statistical significance through Pareto chart (b) Statistical significance through half-normal plot

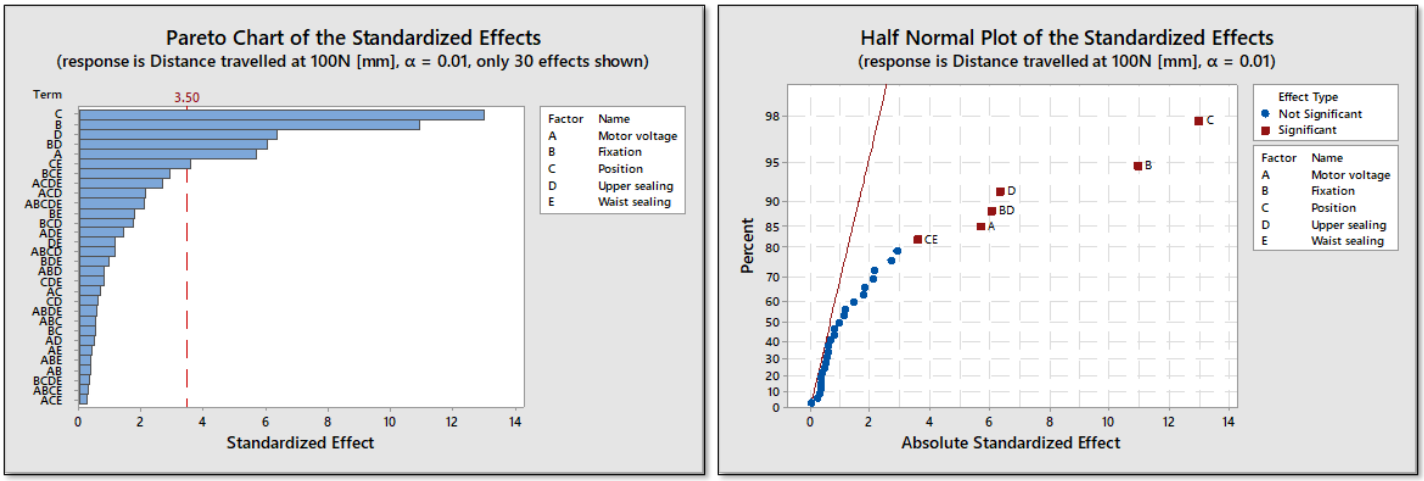

Source: Own elaboration

Figure 39 – Plotted effects regarding glass tilting at 100N on the Renault Kadjar

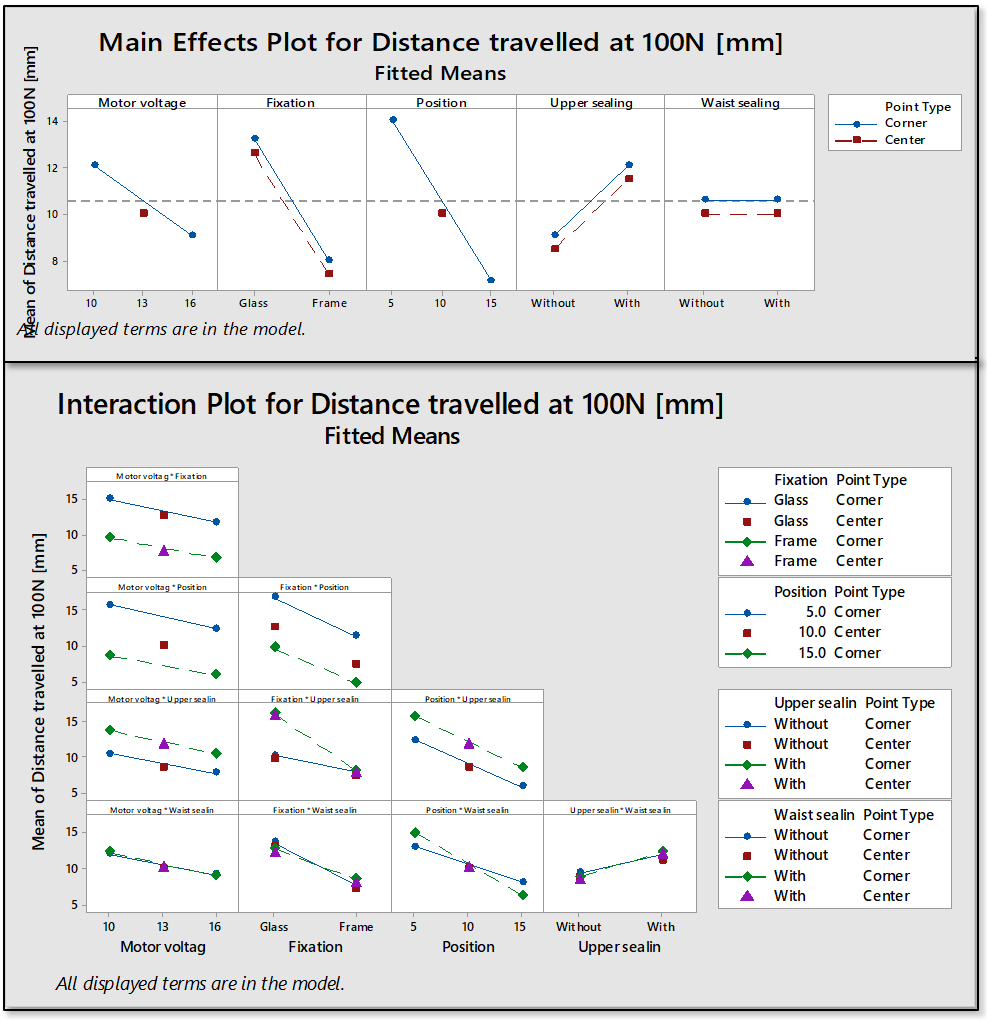

Source: Own elaboration

4.2 OPTIMIZATION RESULTS

After the system has been characterized and it is reasonably certain that the important factors have been identified, the next objective is optimization: introducing new ways to achieve the response targets that were established. In the case of this work, a higher system stiffness transmitted to the motor, with minimum glass tilting, would be the optimal situation. The most important factors identified on the Factor Screening, both the position and place of fixation of the SDI, are analyzed again, but with the inclusion of a tape covering the point of contact and also the using of a SDI roller. In this experiment, the limits used for the snipping of measurements were 60 and 80 N, as explained on Chapter 3.

Figure 40 presents the data collected with four factors evaluated regarding the system stiffness. Three individual variables stood out: gauge fixation (p-value < 0.001), gauge position (p-value: 0.003) and the presence of the roller (p-value: 0.004). Other factors and interactions are considered not-significant.

As shown on Figure 41, the biggest individual effect on the transmitted stiffness is from the placement of the SDI on the frame or glass, with the absolute value of 44,16 mN m/°, followed by the distance from A-column (27,71 mN m/°), presence of the roller (21,98 mN m/°) and attachment of the tape (7,25 mN m/°).

Looking at the interactions, the effect of the tape makes little difference when the measurement device is on the glass, but raises to 14,46 mN m/° when it changes to the door structure. Also, while the interference of the tape directly on the lever arm is minimal (2,61 mN m/°), when attached to the roller it's more significant (11,88 mN m/°). Finally, adding the roller to the gauge both on the glass or on the frame creates a big reaction on the stiffness values (28,15 mN m/° and 15,81 mN m/° difference).

When checking the glass tilting until 60 N on Figures 42 and 43, the order of the main effects change. Now the roller has the biggest statistical impact (p-value < 0.001), with an absolute value of 4,73 mm, followed by the gauge fixation (p-value < 0.001) with 4,39 mm. Other important ones are the position (p-value < 0.001) with 3,30 mm and the interaction between roller and fixation (p-value < 0.001) with 2,38 mm.

In this stage, the interaction AD stands out from the others: while the roller on the frame only lowers the tilting in 2,59 mm, on the glass it gets to 7,11 mm. The addition of the tape has little interference, 0,60 mm on average. The comparison of factors on the glass tilting at 80 N is pretty similar to the ones at 60 N, with changes only on the magnitude of the effects and don't bring anything more to the analysis. For this reason, the resulting charts will be displayed in the Appendix D.

Overall, the results with the roller were positive. While the best results were still from simply switching the fixation place of the gauge, the rolling of its arm through the upper seal lowers the friction enough that the tilting effect is minimized. Also, the use of the tape for the glass protection had no substantial impact on the tilting dynamic, so it could be a viable alternative in case the SDI-on-frame setup turns into the standard experimental method.

Figure 40 – Effects significance associated with system stiffness on the Kadjar optimization

(a) Statistical significance through Pareto chart (b) Statistical significance through half-normal plot

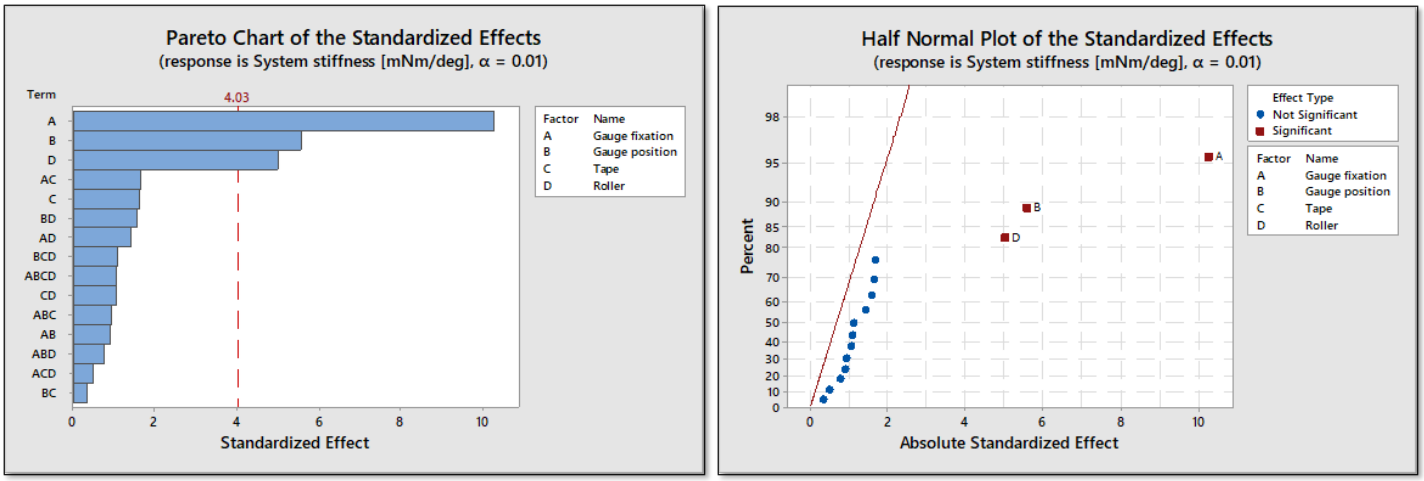

Source: Own elaboration

Figure 41 – Plotted effects regarding system stiffness on the Kadjar optimization

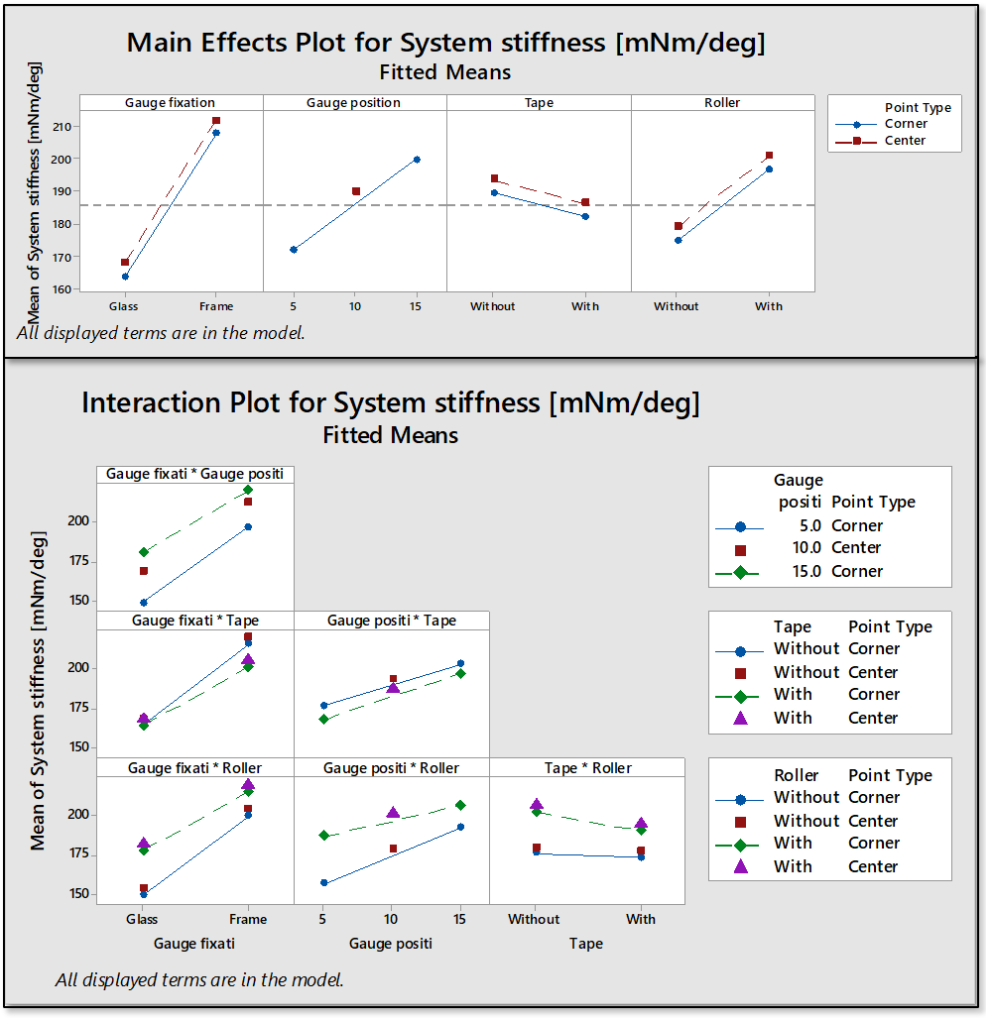

Source: Own elaboration

Figure 42 – Effects significance associated with glass tilting at 60N on the Kadjar optimization

(a) Statistical significance through Pareto chart (b) Statistical significance through half-normal plot

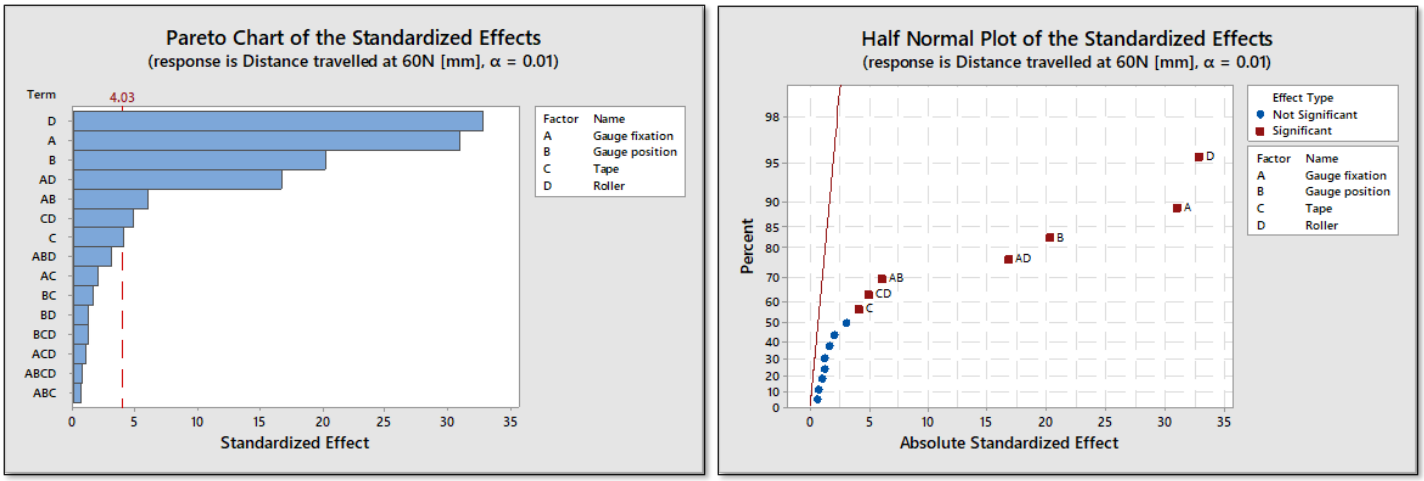

Source: Own elaboration

Figure 43 – Plotted effects regarding glass tilting at 60N on the Kadjar optimization

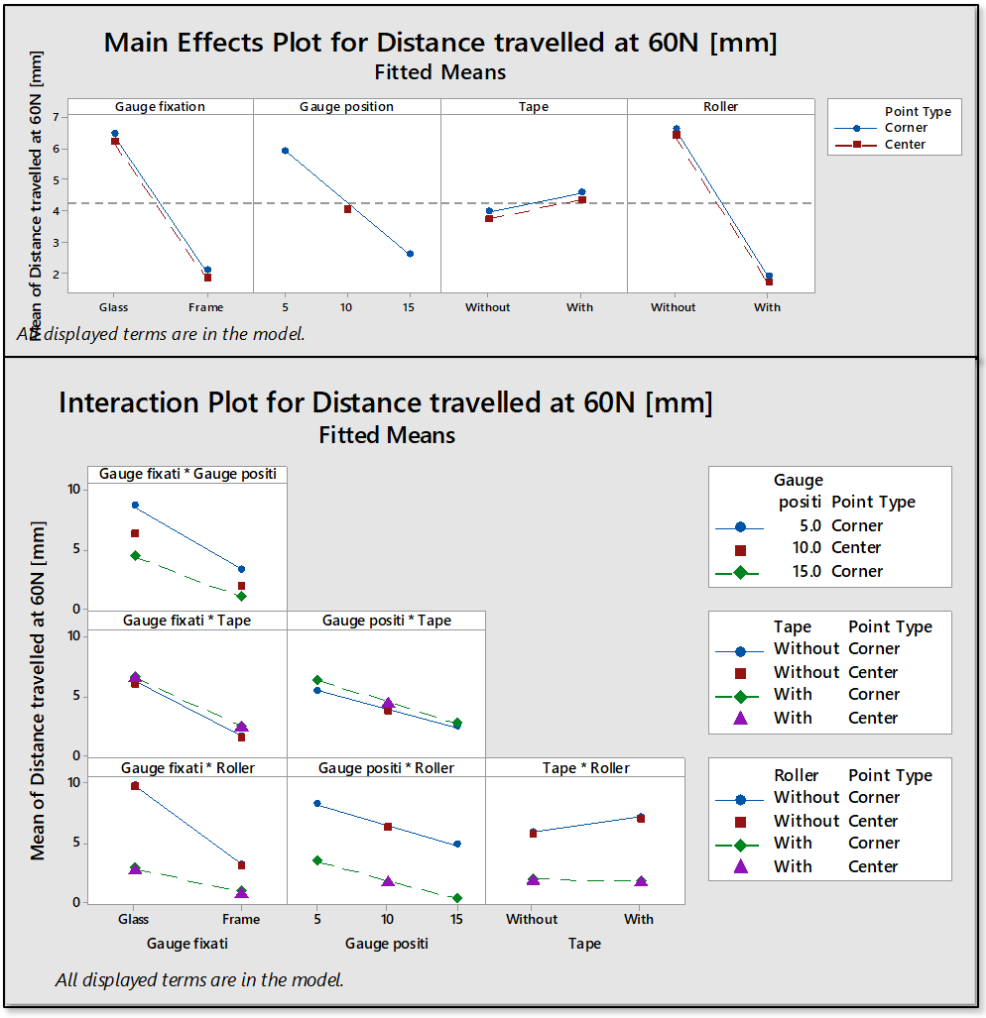

Source: Own elaboration

4.3 CONFIRMATION RESULTS

To assure that the results collected on the first two steps weren't exclusive to the Renault Kadjar's door architecture and environment, both DOEs were planned to be repeated on the Renault LJL project. Although the factor screening was completed entirely, because of time constraints the experiments with the SDI roller were done in a simple comparative basis, with the only two factors being the presence of the bearing and the fixation of the gauge.

Figures 44 and 45 show that the main factors responsible for the difference on the system stiffness seem by the motor remain nearly the same, lead by three individual effects with p-values below 0.001. Even though the position variable (30,78 mN m/°) has a bigger individual effect than the fixation of the SDI 29,08 mN m/°, it remains in second place because of the latter's higher t-value and its variance between corner and center points. Presence of the sealing comes third with an impact of 26,85 mN m/° and then voltage with 17,51 mN m/°.

Two particular interactions appear between the factors BC and CD. In the first correlation, the difference in stiffness between 5 and 15 cm with the gauge on the window is only 15,66 mN m/°; if it changes to the frame, the delta increases to 45,91 mN m/°. The interaction CD then shows that moving the gauge closer to the A-column significantly increases the impact of the upper sealing from 10,68 mN m/° to 43,01 mN m/°.

Moving on to the tilting movement until 40 N on Figures 46 and 47, the impact of the upper sealing on this door is highlighted. While many other effects are statistically relevant, the main ones, with p-values below 0.001, are the fixation of the SDI once again, with 2,66 mm, the interaction BD, with 2,38 mm, and the upper sealing of the system, with 2,33 mm. Through the interaction plot, the significance of the position is minimal with the gauge on the frame

Figure 44 – Effects significance associated with system stiffness on the Renault LJL

(a) Statistical significance through Pareto chart

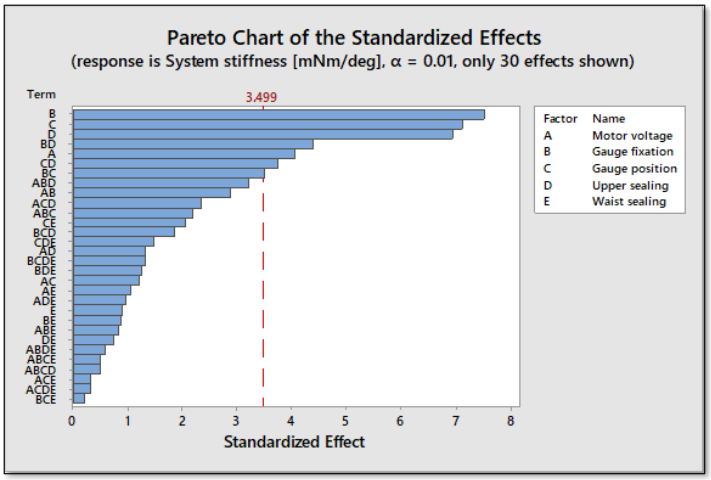

(b) Statistical significance through half-normal plot

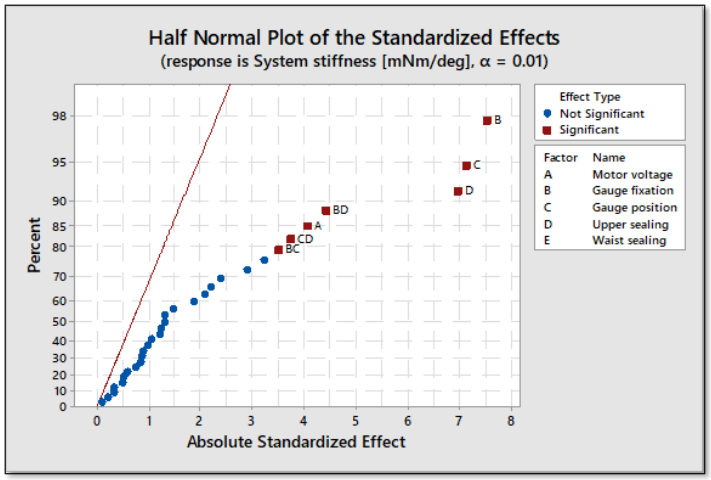

Source: Own elaboration

Figure 45 – Plotted effects regarding system stiffness on the Renault LJL

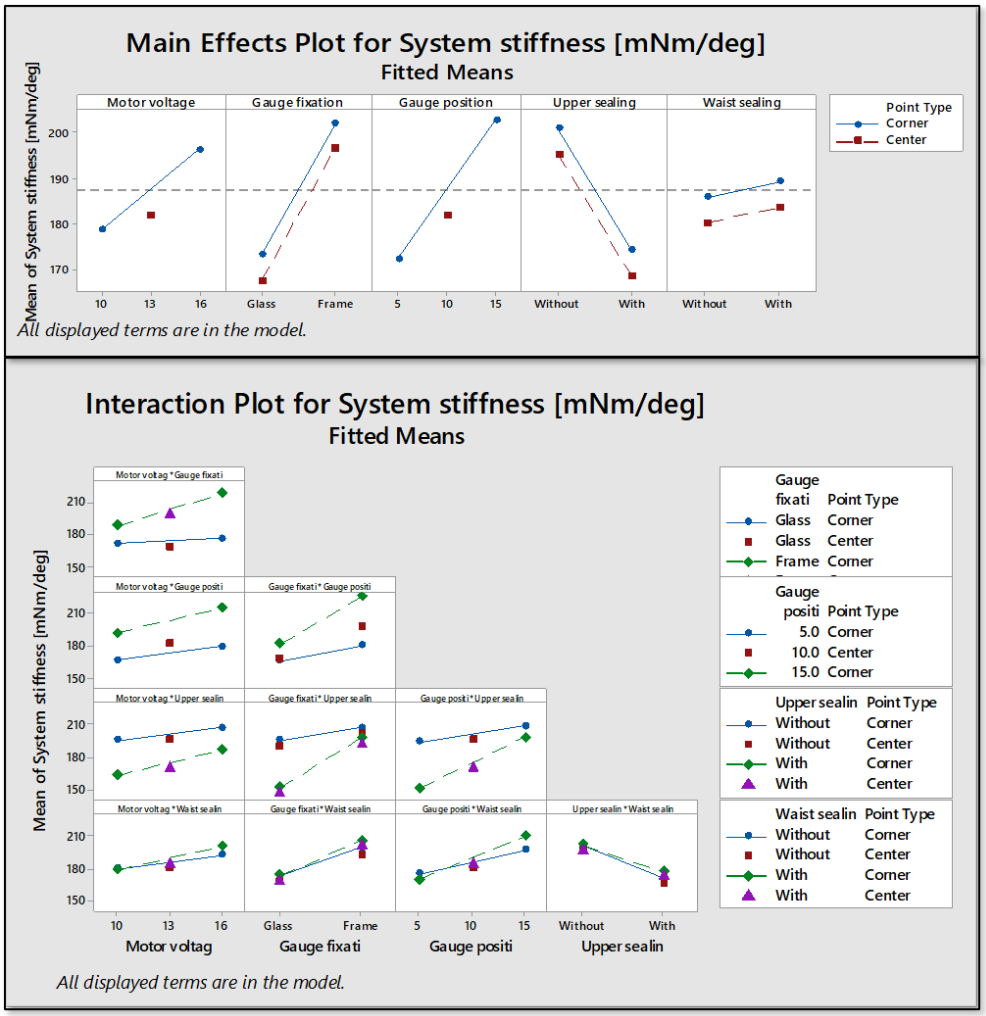

Source: Own elaboration

Figure 46 – Effects significance associated with glass tilting at 40N on the Renault LJL

(a) Statistical significance through Pareto chart (b) Statistical significance through half-normal plot

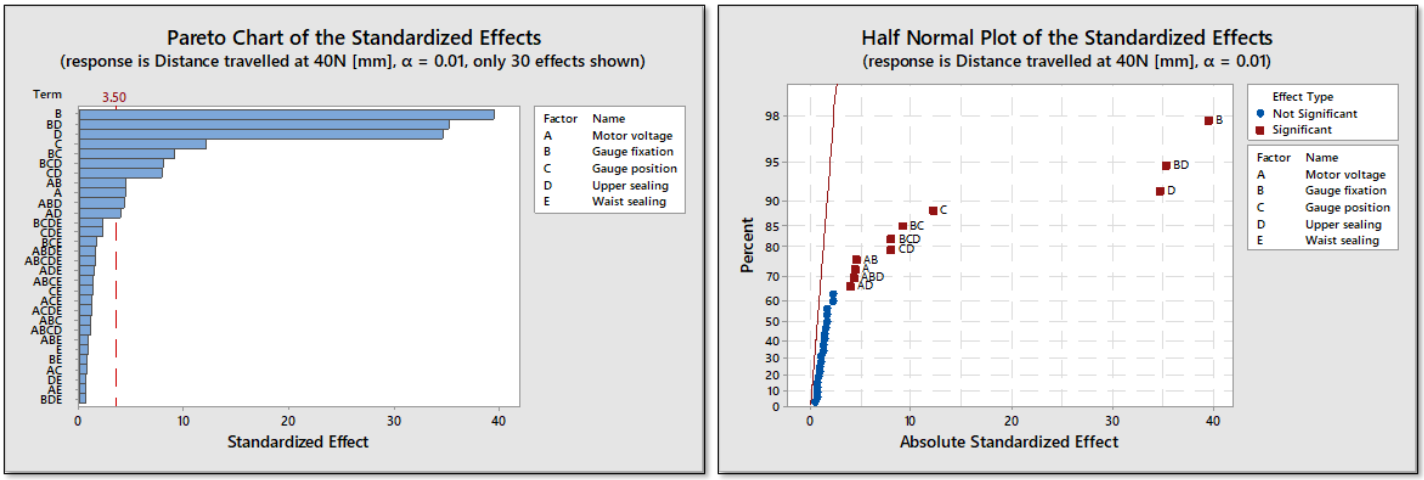

Source: Own elaboration

Figure 47 – Plotted effects regarding glass tilting at 40N on the Renault LJL

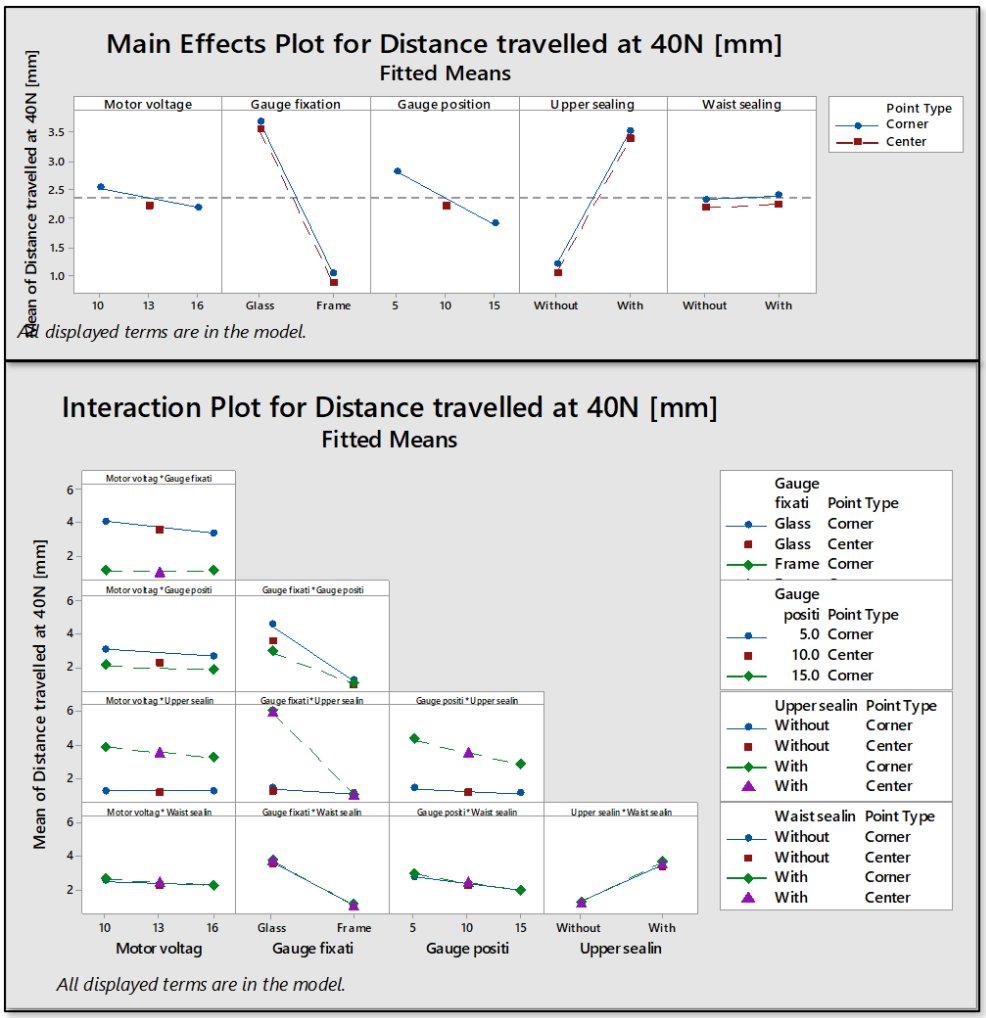

Source: Own elaboration

reference, while it grows to 1,62 mm when on the glass. The waist sealing presents itself once again as an almost irrelevant factor.

The analysis for the glass tilting until 80 N has the same significance order on the main factors, varying only their impact and reinforcing the linearity of the continuous variables. The results will be presented only as reference on Appendix E.

During the individual analysis of experiments on the LJL door, a new and different behaviour was noticed that could have had a significant impact on the results. The architecture of the upper seal, when fixed to the frame, still had an air gap inside, therefore presenting a variable stiffness when pressed by the sensor. This ensued the dynamic that can be seen especially when checking the influence of the roller attachment on the LJL system, in Figure 48.

Figure 48 – Sealing effect of the LJL door

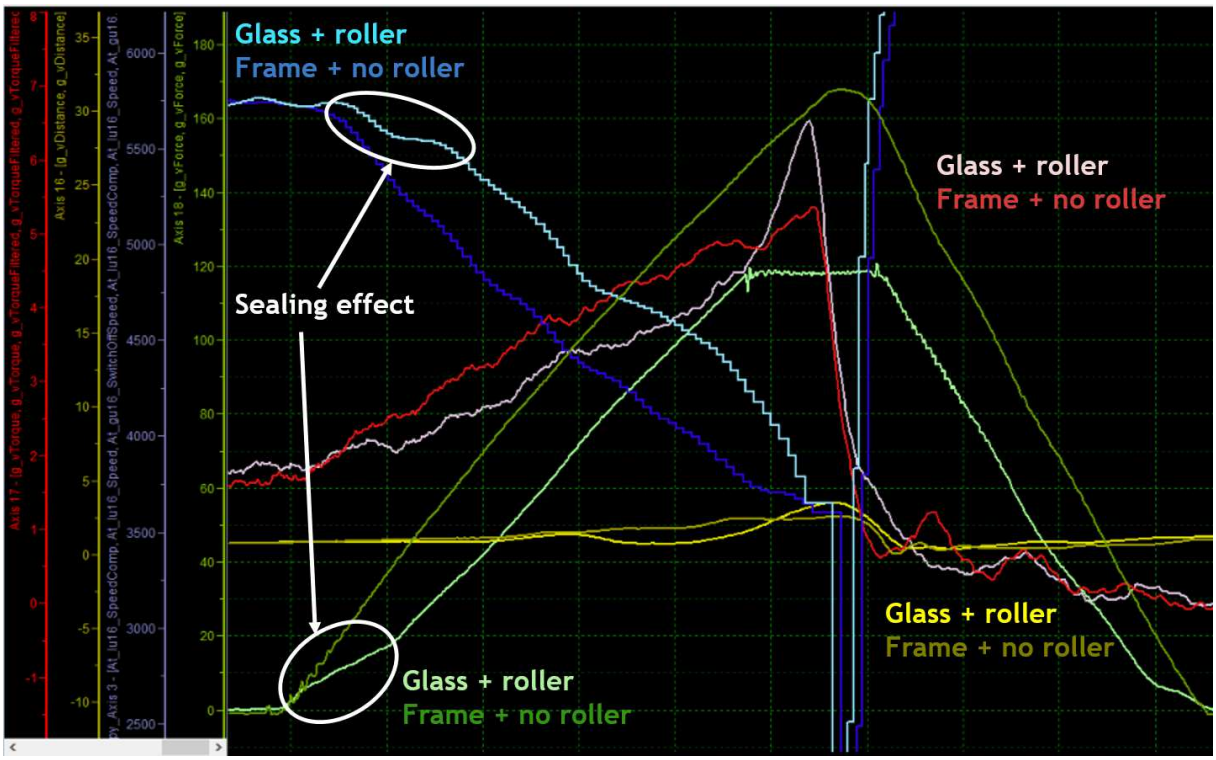

Source: Own elaboration

On the speed curve from the setup with the SDI on the glass and with the roller, the start of the movement shows an early re-acceleration right after the the collision with the upper seal, because of the mentioned air gap that lowers the stiffness. When the speed starts dropping again (and has again to surpass the tracking limit, since the electronic was updated because of the re-acceleration), almost 20 N is already accumulated on the sensor without real transference of energy to the motor, creating a much higher peak force than desired before the window would reverse.[2] This behaviour was also seen without the roller, throughout the confirmation stage. After this initial region, both speed curves then behave similarly inside the area of interest and create almost to no glass tilting, as seen by the distance sensor values.

The inherent characteristic of this sealing and door system is another detail that could be avoided in other projects by changing the fixation of the force gauge. The results of the design of experiments, as well as the comparison with the roller device, show that this is indeed the most viable option to reduce the glass tilting effects and approximate the development test procedures to real-life situations.

[2]Reminding that the switch-off parameters were adjusted for experiment, designed to indeed push the forces above 100 N if possible for the analysis of the whole spectrum. The peak trapping force of the "glass + roller" configuration being lower does not matter in this case.

4.4 RESPONSE REGRESSION

After collecting all the responses, an additional analysis was done to identify a possible correlation between the system stiffness transmitted to the WR actuator and the glass tilting movement. In order to get more narrow boundaries on the prediction plots, an α level of 0.1 was used for all the analysis. The measurements from the boundaries of each graph, with the highest and lowest glass tilting values, were then evaluated on the ATP Tool.

4.4.1 Factor Screening Response Regression

Figure 49 presents the regression analysis on the factor screening DOE stage. The responses of the forty runs were plotted against each other, creating a regression line between the points and generating the model:

$$Y = 214.9 - 7.181X \tag{17}$$

where Y is the system stiffness in [mN m/°] and X the movement on the X-axis in [mm].

The resulting plot has an r-square (coefficient of determination) of 76.03% (75.40% adjusted), which is the proportion of the variability in the data "explained" by the model, while

Figure 49 – Factor screening: response regression fit

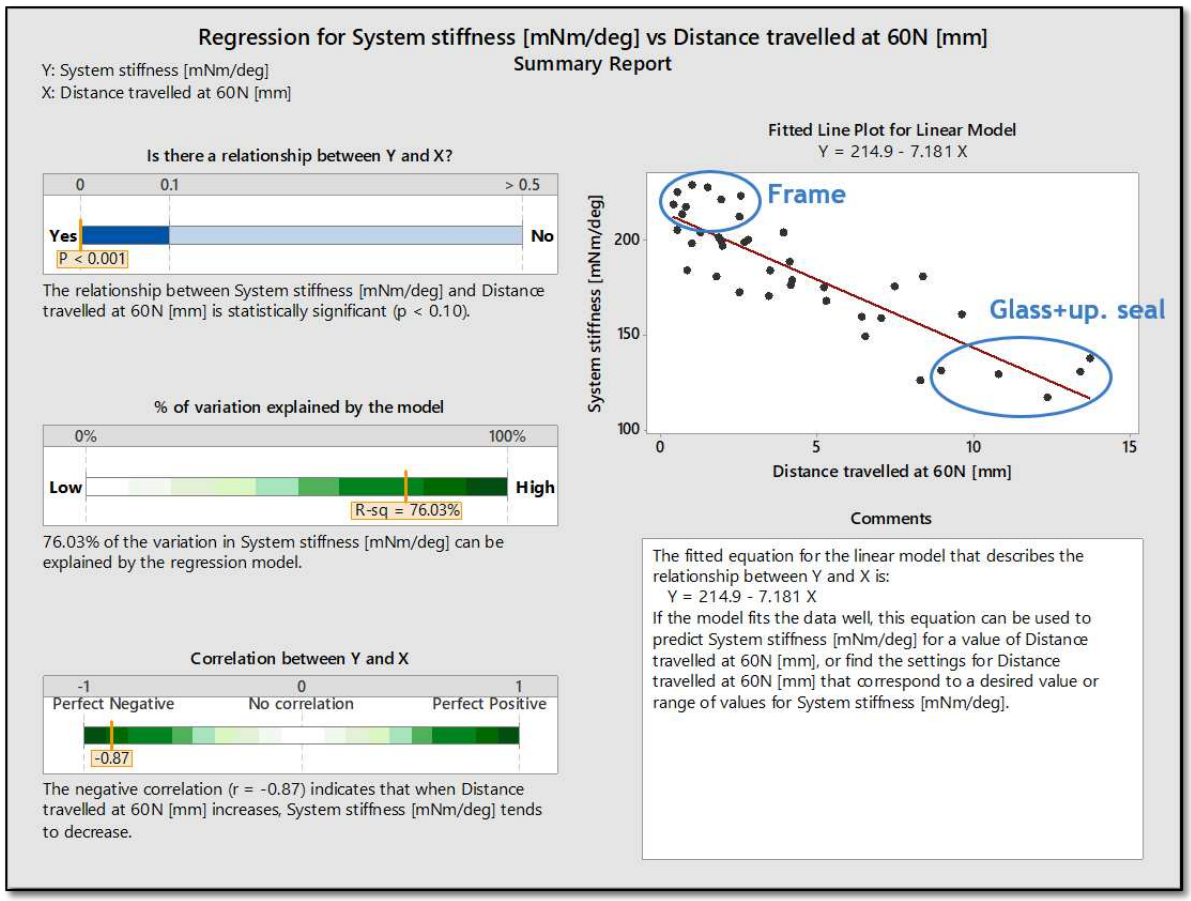

Source: Own elaboration

Figure 50 – Speed modulation comparison between factor screening runs using ATP Tool

(a) Factor screening runs with high stiffness

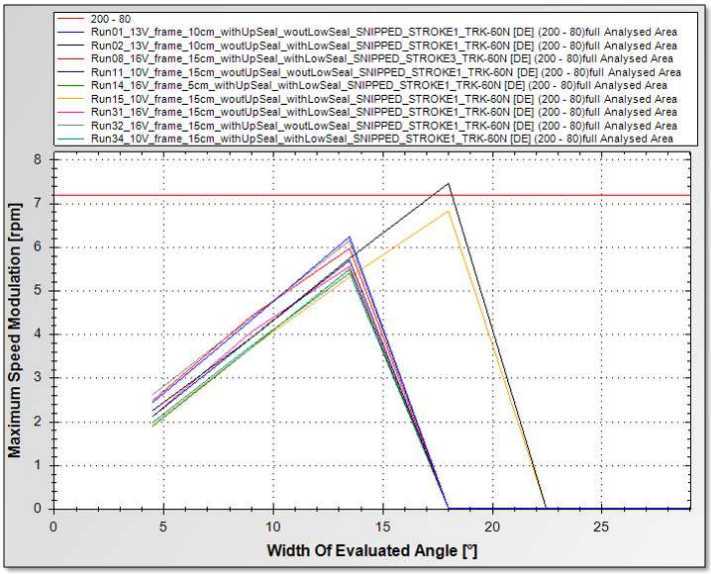

(b) Factor screening runs with low stiffness

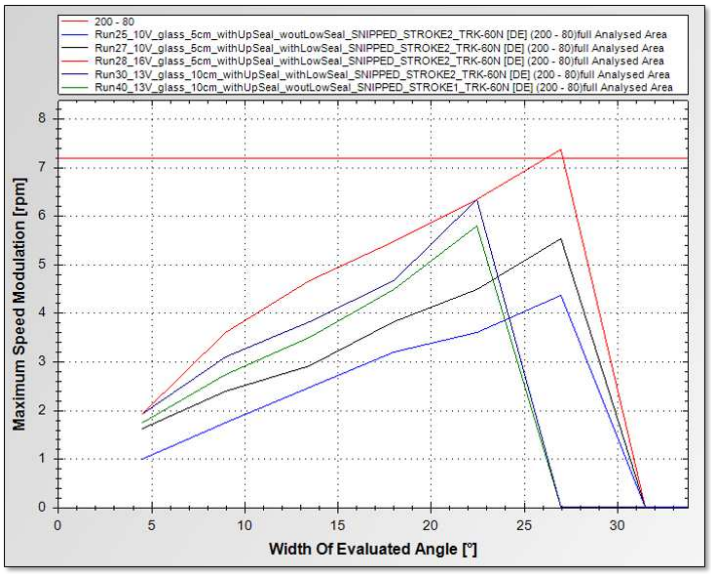

Source: Own elaboration

the adjusted value also takes into account the sample size and number of variables, turning it less biased. In this case it means that more than 3/4 of the observed values can be predicted from the resulting model. The standard deviation σ of the residual points is 15,36 mN m/° from the fitted line. Since the p-value of the regression is below 0.001, the correlation between the responses is statistically significant.

On the upper left part of the regression graph, the nine circulated runs presented the highest stiffness among them and low glass tilting. All have a single factor level in common: with different motor voltages, presence or not of the upper and waist sealing and even on different distances from the door's A-column, all of them were measured with the SDI fixed on the glass. On the other hand, among the runs that had the lowest system stiffness and high glass tilting, the factors in common between them were the SDI fixed on the glass together with the upper sealing.

In order to analyze the speed signals of these boundaries, they were converted and loaded into the ATP Tool. All of them are snipped from the established range between the TrackingInnactive flag until 60 N of trapping force.

Figure 50a shows the circulated runs with the SDI placed on the door frame, while Figure 50b shows the ones with the gauge on the glass and touching the sealing. While the first group has an almost linear increase on the speed modulation, as the width of the evaluated angle on the WRD gear rotation increases, the second visually presents a lesser constant increase over time. Another difference is how much rotation it takes for each group to achieve a certain value of speed modulation: most signals from 50a achieve 5 rpm on between 10° to

13°, while most curves at 50b only dropped the rotational speed by that amount after 15°.

This explains not only how a higher transmission stiffness results in a higher and more constant speed drop on trapping events, but also how measurements with the force gauge placed on the door frame help achieve this effect on the Renault Kadjar. The traditional measuring method, on the other hand, creates more glass tilting overall, which in turn decreases the stiffness seem by the motor and finally has a slower and inconsistent speed decrease.

4.4.2 Optimization Response Regression

On the optimization stage, the results were similar to the factor screening, as shown by Figure 51. After 22 runs, the resulting regression line follows the model:

$$Y = 214.3 - 6.582X \tag{18}$$

With a standard deviation of 14,15 mN m/° and an r-square value of 77.79% (76.76% adjusted), the pattern also explains more than 3/4 of the observed responses on this DOE. The p-value is again less than 0.001, so the relationship is statistically significant for this confidence level. Again, the runs with the highest stiffness and lowest glass tilting responses are the ones when measuring the force from the frame reference, while measuring from the glass and having

Figure 51 – Optimization: response regression fit

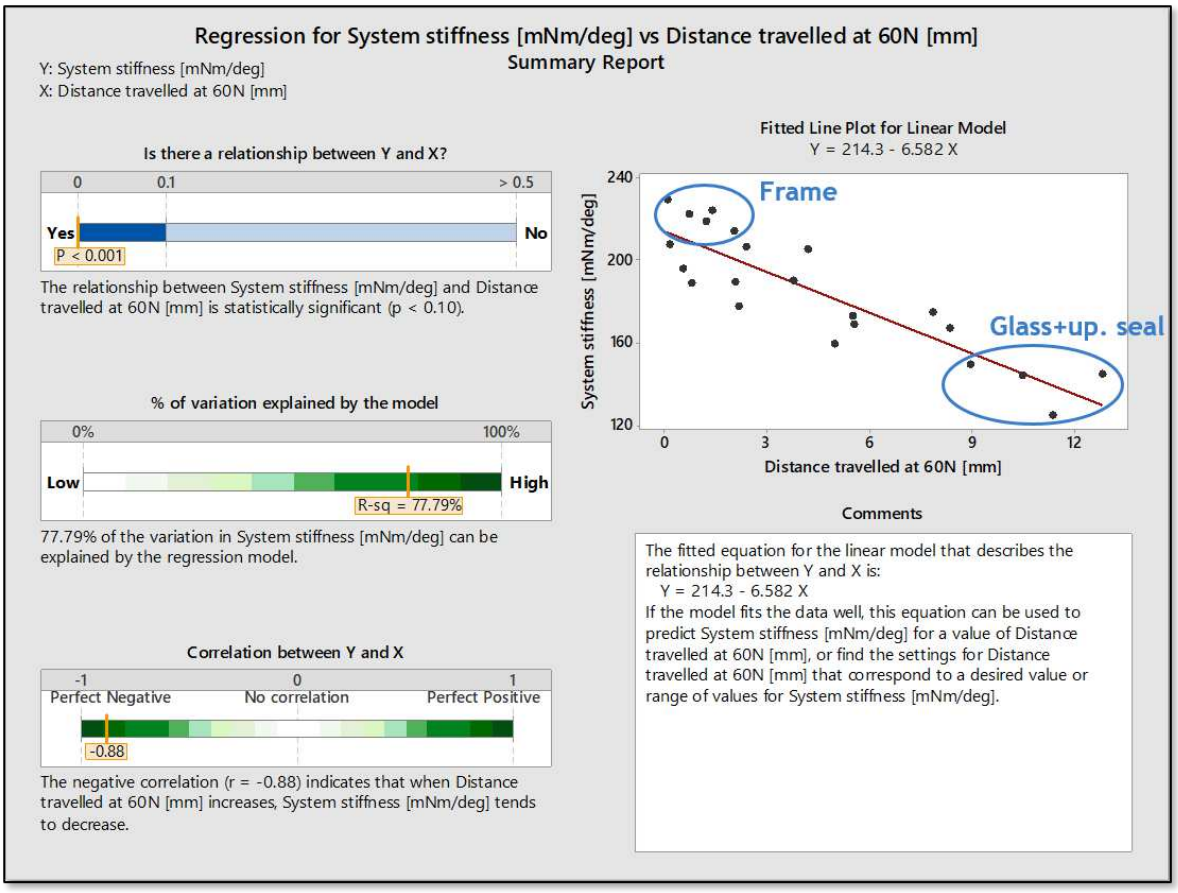

Source: Own elaboration

Figure 52 – Speed modulation comparison between optimization runs using ATP Tool

(a) Optimization runs with high stiffness

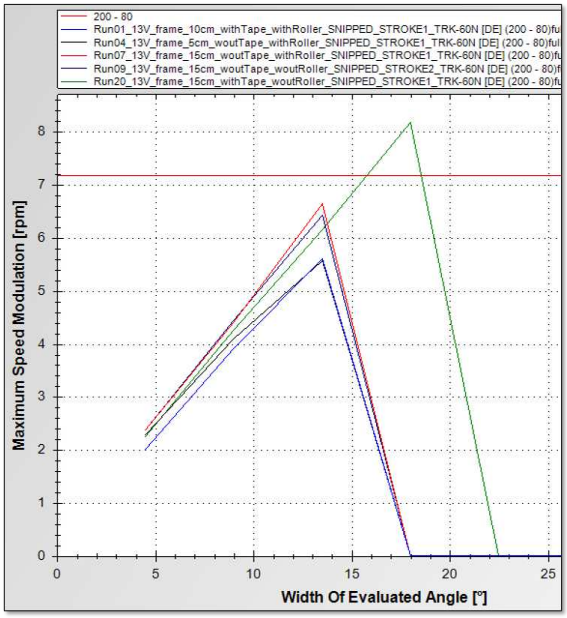

(b) Optimization runs with low stiffness

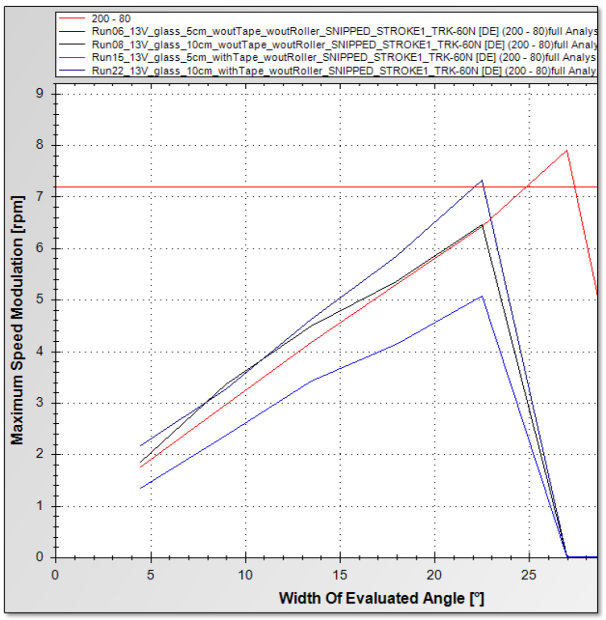

Source: Own elaboration

the upper seal attached once again creates lower stiffness and higher displacement of the window. The last group also did not have the roller attached in any of the tests.

On the ATP Tool, even though the behaviour of the speed signals is not exactly the same, the overall pattern repeats itself. Figure 52a shows that the tests with less glass tilting are the ones with a more steep modulation, meaning earlier window reverses. Adversely, tests conducted with the SDI on the window colliding with the sealing, without the roller device and that created more glass tilting have a slower speed drop, although more consistent in this experiment.

One of the main takeaways from this subsection analysis is how the linear regression continues to fit the response correlation, even if the method of changing the glass tilting changed. In this case the position from the A-column stood the same on every run, its effect on the experiment matrix was essentially substituted by the presence roller. Even then, decreasing the movement of the glass meant a higher transmission stiffness for the motor, which in turn created steeper speed drops before the window reverses.

4.4.3 Confirmation Response Regression

Finally, Figure 53 shows that the LJL system has a different behavior regarding the tilting. The regression model is defined by:

$$Y = 210.5 - 10.27X \tag{19}$$

Figure 53 – Confirmation: response regression fit

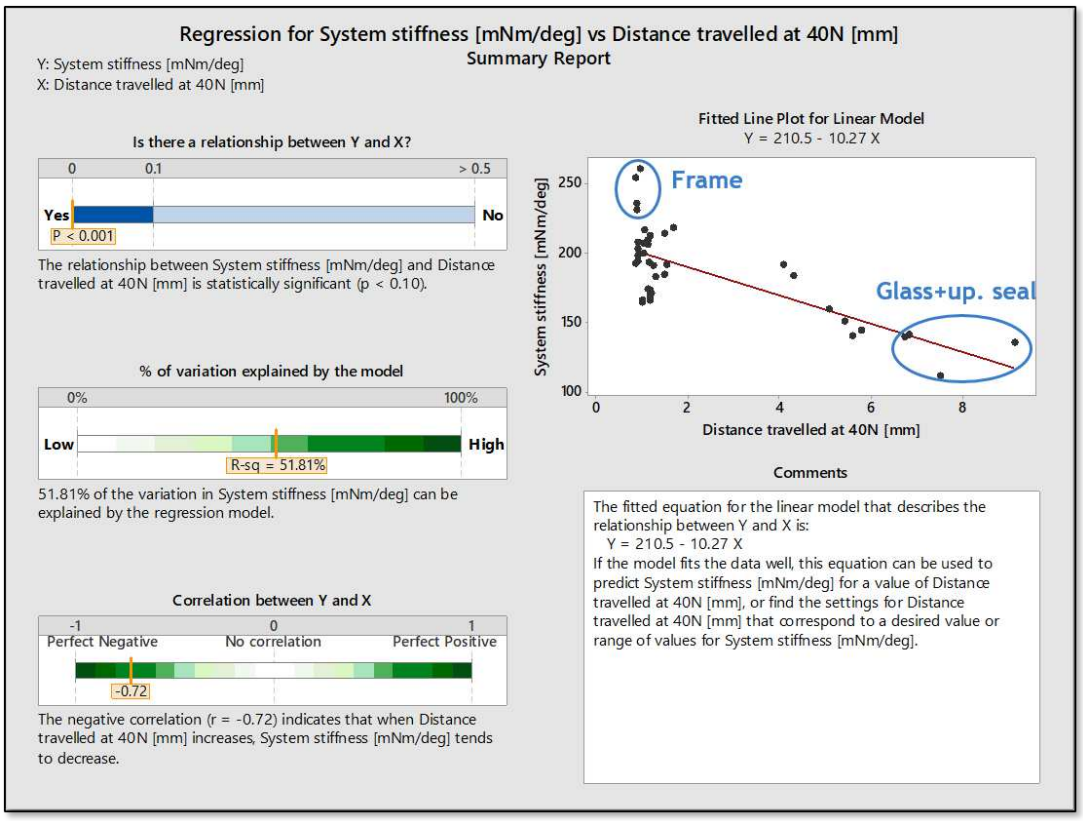

Source: Own elaboration

While the regression equation seems similar to the former situations, this door's architecture had less overall tilting during the experiments: only on ten runs the glass moved more than 2 mm until the trapping force reached 40 N. When it moved, however, the result was an overall reduction on the stiffness seen by the actuator. The standard deviation in this case increased to 22,92 mN m/° and the r-square lowered to 51.81% (50.55% adjusted). The p-value below 0.001, however, confirms that the linear correlation between system stiffness and glass tilting on the Renault LJL is still statistically significant.

After the Kadjar's results and observing the case of the LJL door, the overall linear correlation between system stiffness and glass tilting and the impact of the measuring method can be further confirmed. Once more, the runs that created less glass horizontal movement and higher transmission of energy to the WRD are all with the SDI clamped on the frame; the runs with more glass tilting and lower stiffness all with the SDI clamped on the glass.

The behaviour of these measurements on the ATP Tool also translates: Figure 54a has a steeper and more consistent speed modulation during obstacles collisions, while Figure 54b has a slower, more inconsistent decrease (with some help of the sealing effect saw on the section 4.3). It's important to notice that the area analyzed this time is smaller than on the Kadjar's, due to the force limit being only 40 N and the glass tilting occurring much earlier and briefly.

Overall, the regression analysis on the second door helped confirming that this linear

correlation between the responses may as well be consistent throughout different projects, and not only exclusive to the Renault Kadjar. Even with much lower effect from the glass tilting, the tendency is that this movement from the window lowers the transmission of energy to the motor and creates the re-acceleration problem on trapping events.

Figure 54 – Speed modulation comparison between confirmation runs using ATP Tool

(a) Confirmation runs with high stiffness

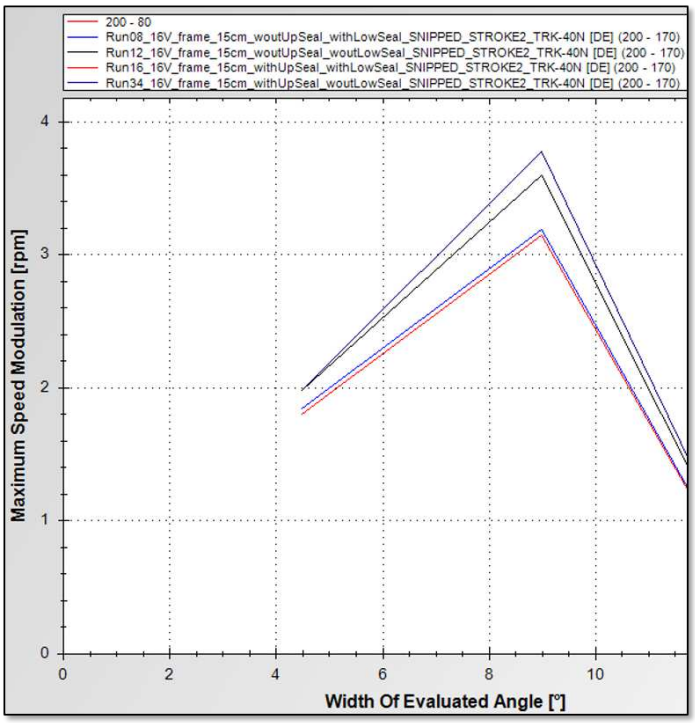

(b) Confirmation runs with low stiffness

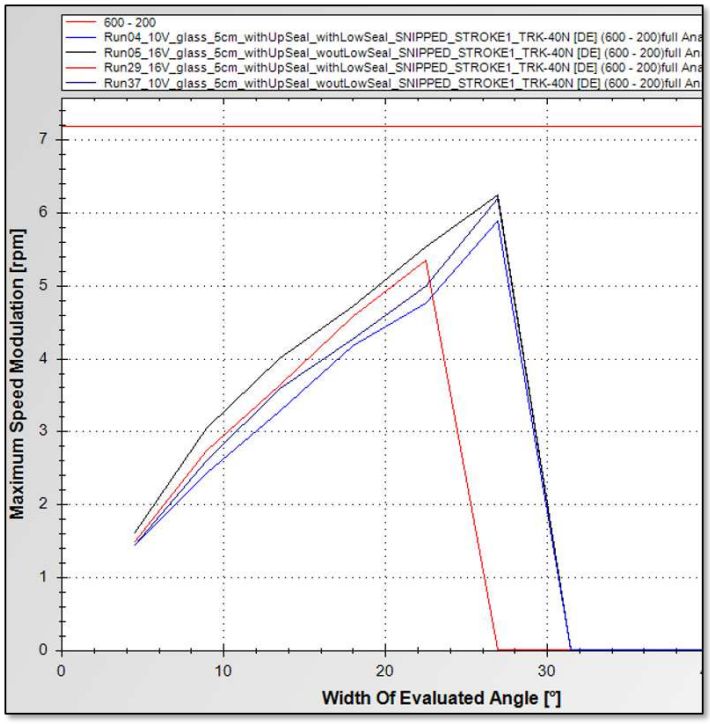

Source: Own elaboration

5 CONCLUSION

The aim of this work was to analyze the effect of the glass tilting on doors with single-guided window regulators, using a scientific and experimental method to evaluate what system factors help the most on the creation of this movement and how the trapping force measuring method, in specific, can be adjusted to minimize it. This was accomplished in several steps, as detailed throughout the thesis.

On the background study, mathematical and physical elements were gathered and explained, as well as related works as reference, in order to form a solid base knowledge. This allowed the design of an analysis setup, through the use of different sensors and software, and the construction of a experimental method using statistical data gathering, in the form of a factorial design of experiments. Also, the problem of the glass tilting was presented in detail, showing how it affects the development and validation of window regulator electronics and how should be minimized, since it does not translate to real-life situations, as explained by past works that were used as basis for this project.

After the setup assembly described on Chapter 3, the signals gathered by the torque, distance and force sensors, together with the electronic data from the WR motor, were enough to better understand the consequences of the glass tilting on the systems of interest. Using the system stiffness seem by the motor (transmission stiffness) and the displacement distance of the window during trapping events measured by the SDI gauge, it was possible to elaborate an analysis matrix capable of comparing all the different factors responsible for the tilting dynamic. Also, it was intended to check if the force measuring device itself had the most impact between the variables, as presumed by past works on the subject.

Starting with the factor screening analysis on the Renault Kadjar's driver door, five factor effects were compared: the motor voltage, the placement of the SDI in relation to the A-column, the fixation of the SDI on the glass or on the door frame, the upper and the waist sealing. Using the statistical methods available for the DOE analysis, it was possible to affirm that, given the Kadjar's door architecture and a confidence level of 0.01, the main factors, among the ones analyzed, that have the most statistically significant impact on glass tilting distance and system stiffness are, in order: the place of fixation of the SDI, either on the frame, raising the system stiffness, or on the glass, lowering the system stiffness; the SDI position, raising the tilting movement the closer it is to the A-column.

This was also confirmed through the individual comparison of two measurements, one using the gauge on the frame and other with it on the glass. With the decrease on the stiffness using the glass reference, at the start of the collision the trapping force is not being as directly transferred to the actuator, creating a re-acceleration that overall would delay the reversal of the window, creating higher forces as result. Changing the fixation to the frame would greatly reduce the tilting, 4,69 mm on average, and increase the stiffness, 43,19 mN m/°, resulting in

more reliable measurements.

Comparing the responses of this first stage, given the same sample size and conditions of the experiment, there is a 99,9% probability that the glass tilting and the Kadjar's WR system stiffness have a linear correlation greater than or equal to the one observed on this case; in other words, there is less than a 0,1% chance that this correlation is purely random or derived from system noise. In both evaluated distances (with the force at 60N and 100N), 76,03% of the variation on system stiffness can be explained by the regression models presented. For future and similar projects, this would help evaluate how the system would behave according to the door's architecture, where an overall reduction on the stiffness worked by the motor, through several possible means, can create more rotation of the glass. Also, through the ATP Tool analysis, it was possible to see how the runs in which the measured system stiffness was the lowest (the ones with the SDI on the glass) the tilting effect can be seen directly on the speed signal, which had a smaller and more inconsistent deceleration.

After the system was characterized, other factors were included to build a new DOE. Again, given the Kadjar's door system and a confidence level of 0.01, the main factors, among the ones analyzed, that have the most statistically significant impact on glass tilting distance and system stiffness are the place of fixation of the SDI followed by the addition of the roller device. It means that, on this door at first, the presence of the roller on the measurement of forces using the SDI sensor can be viewed as advantageous in relation to the glass tilting effect, since it significantly lowers the movement of the window on the X-axis, the total system stiffness seen by the motor increases and we have a steeper and more linear speed drop during AT events. Also, the addition of the tape to cover the SDI arm, in an effort to minimize the impact and protect the glass of mechanical damages, is a valid alternative as it has no significant influence on the glass tilting.

Through the regression analysis, again the linear correlation between the responses was confirmed, even if some of the means of affecting the stiffness were different from the first experiment. Again, given this factor setup, there's a 99,9% probability that the glass tilting and the Kadjar's WR system stiffness have a linear correlation greater than or equal to the one observed on this experiment. At the same time, the speed signals still show how the lower displacement of the glass on trapping events creates a more steep and constant deceleration.

Finally, as means to confirm the result breakdown of the Kadjar door, the same DOE structure was applied to the Renault LJL. This time, given the different structure and the lower tilting overall, the impact of the upper seal was bigger, but behind the fixation of the gauge, which was once again the most statistically significant. Another phenomenon that was present on the experiment measurements and that could also be helped by the change to the frame reference is the sealing effect, in which its construction creates a variable stiffness on the contact point between door and SDI, also resulting in higher anti-trapping forces. For this reason, the addition of the roller was not as advantageous as believed initially.

The regression and ATP Tool evaluations also confirmed the results of the first two

stages. Even with lower tilting, its correlation with the stiffness worked by the WRD is still linear. A bigger sample size in this case could improve the R-squared value so more of the data could be explained by the model. And once again, the breakdown of the speed signals show how less glass tilting, with the SDI on the frame, creates better deceleration curves for the anti-trapping detection.

In summary, the results of this project showed how a change on the measuring method of trapping forces can greatly improve the tests on window regulator projects. The fixation of the SDI gauge on the frame reference creates a more optimal dynamic for the anti-trapping detection algorithm, creating less glass tilting and resembling more the real-life situations.

5.1 FUTURE WORK

Although all the experiments were performed using only the SDI as the force measuring device, which is the industry standard, other sensors with similar application could also be tested. The results presented by the regression analysis indicate that, even if the method itself is different, the tendency is that the ones that have a lower effect on the transmission of energy to the motor consequently rotate the glass less, having an overall better behavior for anti-trapping measurements.

Another improvement for this subject study is conducting experiments on the extreme environmental conditions the WRs go through the validation process, inside climate chambers. Different humidity levels and extreme temperatures, either low or high, can have a big impact on some of the factors analyzed on the DOE, especially on all the door sealing and on how the motor performs.

Finally, a bigger sample size, either on the same or different door, would always increase the reliability of the results acquired. One interesting target would be studying the behavior of the SDI on the frame while measuring doors with double-guided window regulators. Since their dynamics are completely different, relying on two support points for the glass instead of one, which in turn already reduce the glass tilting effect, it would be necessary to check if the new method has any adverse effects in that case.

Bibliography

BURSTER PRAEZISIONSMESSTECHNIK GMBH & CO KG. **Potentiometric Displacement Sensors - Models 8712, 8713**. [S.l.], 2018. Available at: <https://www.burster.com/fileadmin/user_upload/redaktion/Documents/Products/Data-Sheets/Section_8/8712_EN.pdf>. Mentioned on page 35.

CSM GMBH. **ADMM classic**. [S.l.], 2018. Available at: <https://www.csm.de/en/component/jdownloads/send/16-datasheets-can-minimodule/85-admm-classic-datasheet>. Mentioned on page 36.

DATAFORTH CORPORATION. **8B40/41 Voltage Input Modules, 1kHz Bandwidth**. [S.l.], 2017. Available at: <https://www.dataforth.com/catalog/pdf/8b40_41.pdf>. Mentioned on page 35.

DATAFORTH CORPORATION. **8BPWR-2 Power Supply Module**. [S.l.], 2017. Available at: <https://www.dataforth.com/catalog/pdf/8baccs.pdf>. Mentioned on page 35.

ESTRADAS.COM.BR. **Renault faz recall depois que menino morreu estrangulado na janela de carro**. 2005. Available at: <https://estradas.com.br/renault-faz-recall-depois-que-menino-morreu-estrangulado-na-janela-de-carro/>. Accessed on: 29th of March of 2019. Mentioned on page 16.

FEYH, C. **Validierung und Optimierung eines Modells zur Simulation eines invertierten bistabilen Pendels im Einklemmfall**. Master's Thesis (Master's Thesis) — OTH Regensburg - Ostbayrische Technische Hochschule, Regensburg, Germany, 3 2019. Mentioned 3 times on pages 15, 33, and 50.

FINK, D.; BEATY, H. **Standard Handbook for Electrical Engineers**. [S.l.]: Mcgraw-hill, 2006. (Electrical engineering). ISBN 9780071441469. Mentioned on page 23.

KISTLER INSTRUMENTE GMBH. **Torque sensor with rotating measuring shaft - Type - 1200/...** [S.l.], 2017. Available at: <https://www.kistler.com/?type=669&fid=93438&model=document>. Mentioned on page 34.

MONTGOMERY, D. C. **Design and Analysis of Experiments**. USA: John Wiley; Sons, Inc., 2006. ISBN 0470088109. Mentioned 6 times on pages 37, 38, 39, 40, 41, and 42.

NATIONAL HIGHWAY TRAFFIC SAFETY ADMINISTRATION. **Federal Motor Vehicle Safety Standards; Power-operated window partition, and roof panel systems**. 2008. Available at: <https://www.govinfo.goapp/details/CFR-2011-title49-vol6/CFR-2011-title49-vol6-sec571-118>. Accessed on: 29th of March of 2019. Mentioned on page 17.

NATIONAL HIGHWAY TRAFFIC SAFETY ADMINISTRATION. **Not-in-Traffic Surveillance – Non-Crash Fatalities and Injuries**. 2015. Available at: <https://crashstats.nhtsa.dot.gov/Api/Public/ViewPublication/812120>. Accessed on: 29th of March of 2019. Mentioned on page 16.

NATIONAL TRAFFIC COUNCIL. **Contran Resolution No. 468/2013**. 2013. Available at: <https://www.legisweb.com.br/legislacao/?id=262925>. Accessed on: 29th of March of 2019. Mentioned on page 17.

PETKUN, S. Dynamic behaviour of power window regulator system. In: **24th Symposium Simulationstechnik - ASIM 2018**. Hamburg, Germany: [s.n.], 2018. Mentioned 3 times on pages 15, 32, and 50.

SCHAKOWSKY, J. D. R. **Cameron Gulbransen Kids Transportation Safety Act of 2007**. Washington D.C., 2008. Available at: <https://www.congres.gv/bill/110th-congress/house-bill/1216>. Accessed on: 29th of March of 2019. Mentioned on page 17.

SEAL, H. L. Studies in the History of Probability and Statistics. XV The historical development of the Gauss linear model. **Biometrika**, v. 54, n. 1-2, p. 1–24, 06 1967. ISSN 0006-3444. Available at: <https://doi.org/10.1093/biomet/54.1-2.1>. Mentioned on page 44.

VECTOR INFORMATIK GMBH. **CANape CASL User Manual**. [S.l.], 2015. Available at: <https://assets.vector.com/cms/content/products/canape/Docs/CANape_CASL_Manual_EN.pdf>. Mentioned on page 56.

APPENDIX A – Anti-trapping legislation worldwide

Table 6 – Anti-trapping regulations

Anti Trap Legislation Comparison Table						
Legislation name:	74/60/EEC; ECE R-21	FMVSS 118	TSD No. 118, Rev.0	ADR 42/03	762/92	468/13
Valid in:	European Union	USA	Canada	Australia	Brazil (until 31.12.2016)	Brazil (up 01.01.2017)
Window may close without anti-trap when:						
• Ignition key in position ON, START or ACC	yes	yes	yes	yes	yes	yes
• after ignition OFF or removing ignition key and before opening one of front doors	yes	yes	yes	45 sec + 45 sec	1 min	yes
• after ignition OFF or removing ignition key and after opening one of front doors	no	no	no	45 sec + 45 sec	no	no
• at least one front door already open when ignition OFF or removing ignition key	not described	not described	not described	not described	during the time the door is open	not described
Opening width permitted for frameless doors w/o Anti-Trap after door closing (Short drop):	12 mm	4 mm	4 mm	12 mm	not defined	12 mm
The door window may close in one touch mode (WR switch) without Anti-Trap when:	while ignition key in position ON, only driver's door	In all conditions above, all doors	In all conditions above, all doors	In all conditions above, only driver's door	In all conditions above, all doors	no
Safety area	4 mm - 200 mm	4 mm - 200 mm	4 mm - 200 mm	4 mm - 200 mm	4 mm - 200 mm	4 mm - 200 mm
Spring ratio of the test equipment	10 N/mm	<25 mm: 65 N/mm >25 mm: 20 N/mm	<25 mm: 65 N/mm >25 mm: 20 N/mm	10 N/mm	10 N/mm	74/60/EEC or ECE R-21 or FMVSS 118
Safety reversing until:						
• Min. reversing stroke or	50 mm	125mm	125mm	50 mm	25 mm	50 mm
• Window opening or	200 mm	200 mm	200 mm	200 mm	n. A.	200 mm
• Return to starting point of movement	yes	yes	yes	yes	n. A.	yes
Window operated by remote control w/o Anti-Trap:						
• with visibility	11 m	11m	11m	11 m	No	No
• without visibility	6 m	6m	6m	11 m	No	No
Rear windows switch function can be disabled by driver	yes	not described	not described	yes	yes	yes

APPENDIX B – Confirmation Renault LJL run order

Table 7 – Confirmation run order

StdOrder	RunOrder	CenterPt	Blocks	Motor voltage	Fixation	Position	Upper sealing	Waist sealing
36	1	0	1	13	Frame	10	With	Without
33	2	0	1	13	Glass	10	Without	Without
1	3	1	1	10	Glass	5	Without	Without
25	4	1	1	10	Glass	5	With	With
10	5	1	1	16	Glass	5	With	Without
27	6	1	1	10	Frame	5	With	With
20	7	1	1	16	Frame	5	Without	With
24	8	1	1	16	Frame	15	Without	With
3	9	1	1	10	Frame	5	Without	Without
29	10	1	1	10	Glass	15	With	With
7	11	1	1	10	Frame	15	Without	Without
8	12	1	1	16	Frame	15	Without	Without
39	13	0	1	13	Glass	10	With	With
12	14	1	1	16	Frame	5	With	Without
28	15	1	1	16	Frame	5	With	With
32	16	1	1	16	Frame	15	With	With
31	17	1	1	10	Frame	15	With	With
22	18	1	1	16	Glass	15	Without	With
18	19	1	1	16	Glass	5	Without	With
35	20	0	1	13	Glass	10	With	Without
13	21	1	1	10	Glass	15	With	Without
21	22	1	1	10	Glass	15	Without	With
14	23	1	1	16	Glass	15	With	Without
38	24	0	1	13	Frame	10	Without	With
17	25	1	1	10	Glass	5	Without	With
30	26	1	1	16	Glass	15	With	With
34	27	0	1	13	Frame	10	Without	Without
23	28	1	1	10	Frame	15	Without	With
26	29	1	1	16	Glass	5	With	With
15	30	1	1	10	Frame	15	With	Without
2	31	1	1	16	Glass	5	Without	Without
4	32	1	1	16	Frame	5	Without	Without
11	33	1	1	10	Frame	5	With	Without
16	34	1	1	16	Frame	15	With	Without
19	35	1	1	10	Frame	5	Without	With
5	36	1	1	10	Glass	15	Without	Without
9	37	1	1	10	Glass	5	With	Without
6	38	1	1	16	Glass	15	Without	Without
37	39	0	1	13	Glass	10	Without	With
40	40	0	1	13	Frame	10	With	With

Source: Own elaboration

APPENDIX C – Upper sealing comparison on the Renault Kadjar

Figure 55 – Signal analysis with and without upper sealing

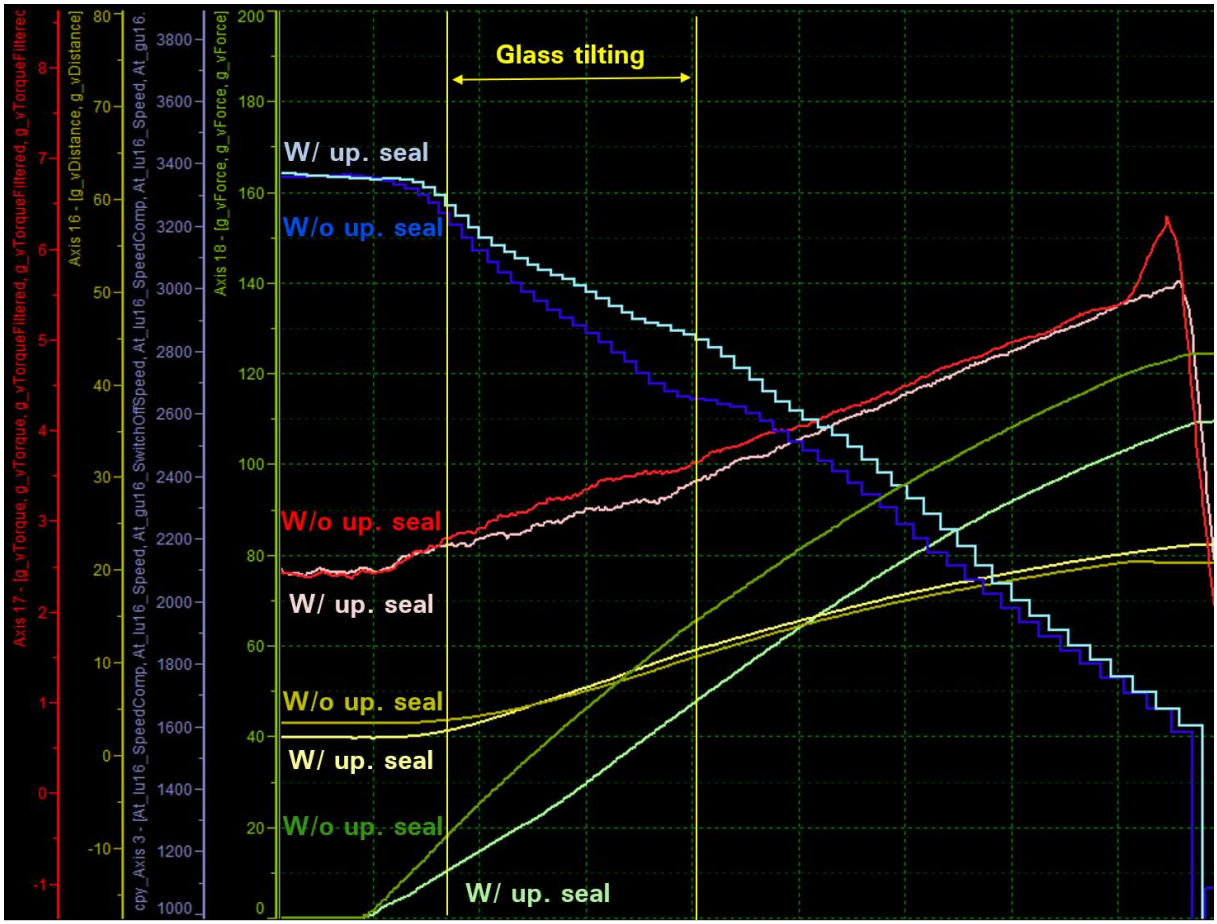

Source: Own elaboration

APPENDIX D – Glass tilting at 80N on the Renault Kadjar optimization

Figure 56 – Pareto chart - Glass tilting at 80N on the Kadjar optimization

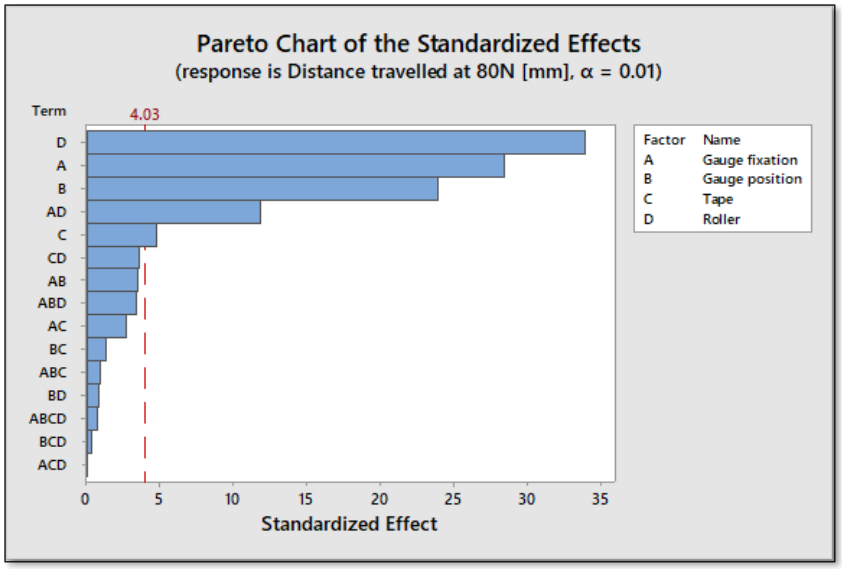

Source: Own elaboration

Figure 57 – Half-normal plot - Glass tilting at 80N on the Kadjar optimization

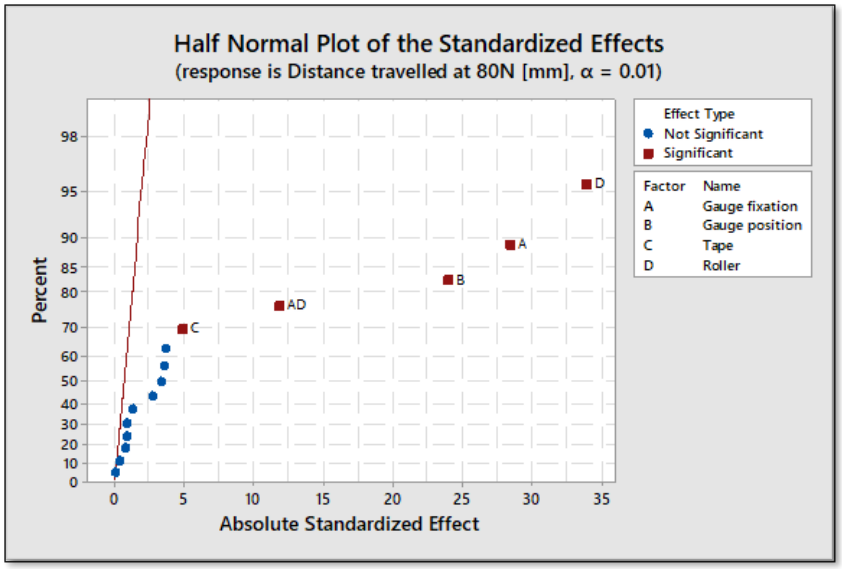

Source: Own elaboration

Figure 58 – Plotted effects regarding glass tilting at 80N on the Kadjar optimization

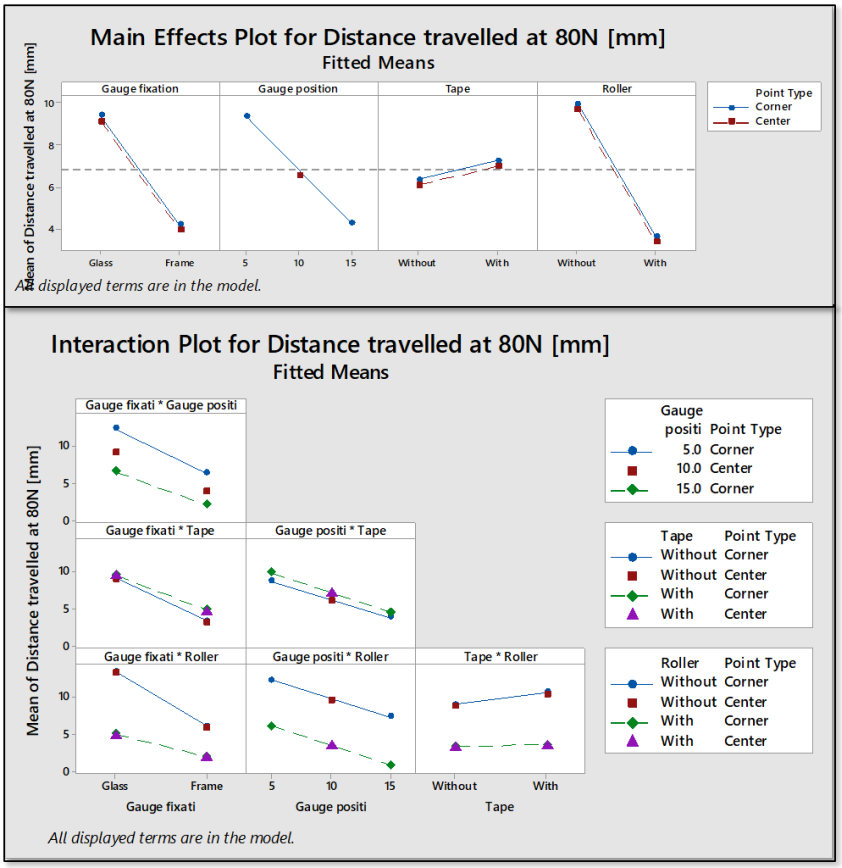

Source: Own elaboration

APPENDIX E – Glass tilting at 80N on the Renault LJL

Figure 59 – Pareto chart - Glass tilting at 80N on the LJL

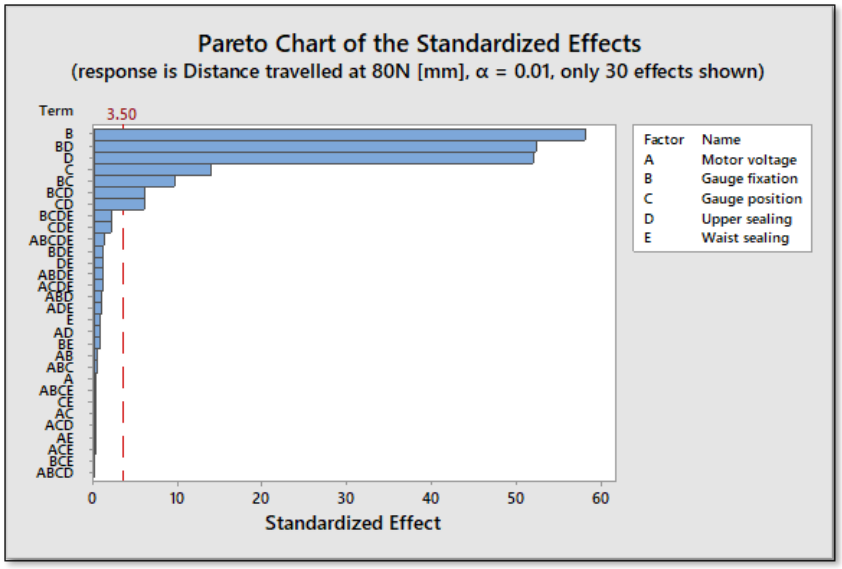

Source: Own elaboration

Figure 60 – Half-normal plot - Glass tilting at 80N on the LJL

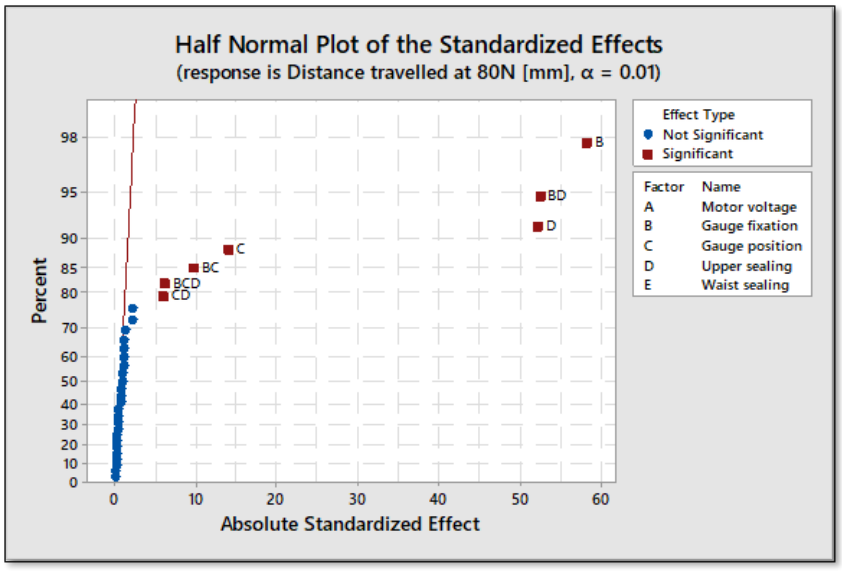

Source: Own elaboration

Figure 61 – Plotted effects regarding glass tilting at 80N on the LJL

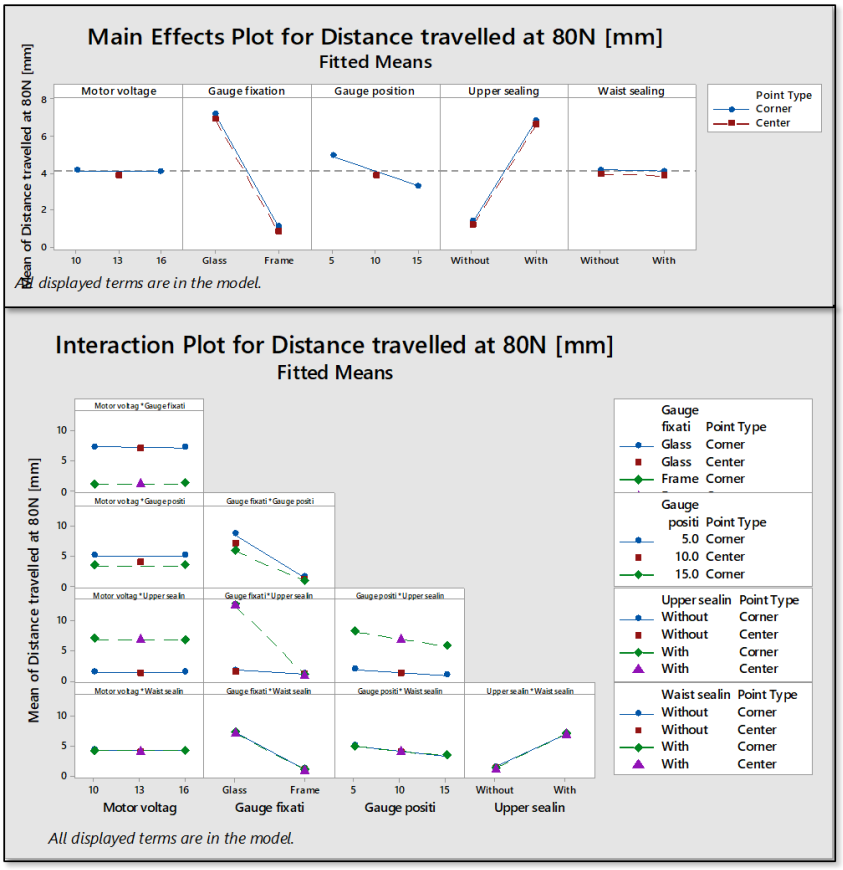

Source: Own elaboration

ANNEX A – VEHICLE COORDINATE SYSTEM

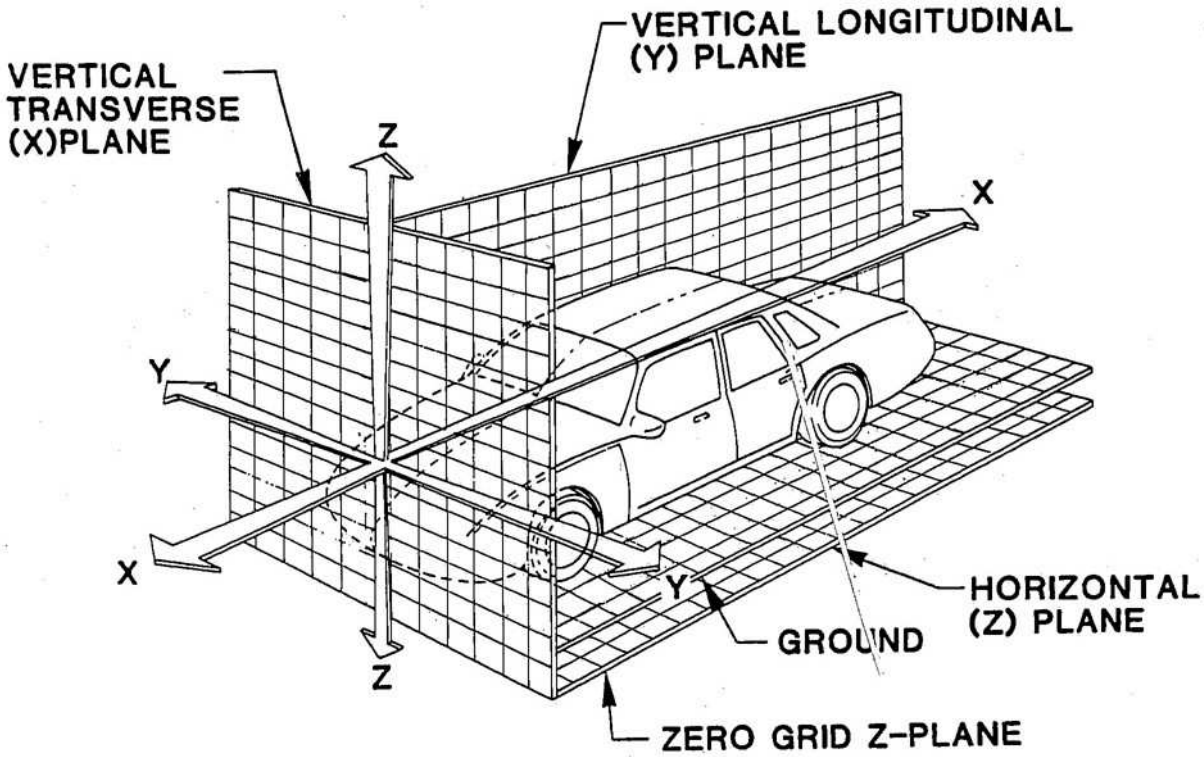

Figure 62 – Vehicle coordinates system
Source: <https://law.resource.org/pub/us/cfr/ibr/005/sae.j1100.2001.html>